LIÈGE université
Faculty of Applied Sciences
PEPs CHEMICAL ENGINEERING
Department of Chemical Engineering – Products, Environment, and Processes (PEPs)

Recovery of Phosphorus from High Phosphorus Content Sources in Southern Vietnam

A dissertation submitted to obtain the academic degree of Doctor of Philosophy (PhD) in Chemical Engineering

by

Vu Dinh Khang

Supervisor: Prof. Dr.-Ing. Andreas Pfennig

Doctoral College in Chemistry Engineering

Liège, January 2025

Vu Dinh Khang, MSc.

Recovery of Phosphorus from High Phosphorus Content Sources in Southern Vietnam

Dissertation

to obtain the academic degree of

Doctor of Philosophy

in

Chemical Engineering

submitted to

Université de Liège

supervisor:

Prof. Dr.-Ing. Andreas Pfennig

PEPs - Products, Environment, and Processes

Department of Chemical Engineering

Liège, January 2025

Acknowledgments

First, I would like to express my deepest gratitude to my supervisor, Prof. Andreas Pfennig, for his valuable guidance, continuous support, and encouragement throughout my PhD journey. His expertise and dedication have been instrumental in shaping my research and helping me overcome challenges.

I would like to sincerely thank thesis committee members, Prof. Angélique Leonard from Liège University and Prof. Le Hung Anh from the Industrial University of Ho Chi Minh City, Vietnam, for their insightful feedback and constructive suggestions, which have greatly improved the quality of my work.

I would also like to thank Prof. Angélique Leonard, Prof. Eppe Gauthier from Liège University, Mr. Hubert Halleux from Prayon n.v., and Prof. Le Hung Anh. They are important parts of the jury for my thesis defense. I appreciate the time and energy you put into reviewing my work.

I am deeply grateful for the financial support from the cooperation project between Wallonie-Bruxelles International and the Vietnamese Government, which has enabled me to pursue my stay in beautiful Liège City. I would like to thank Prof. Célia Joaquim-Justo, for her enthusiastic attention and support for my PhD journey.

I would like to extend my appreciation to the Industrial University of Ho Chi Minh City, where I am currently employed, for providing me with the best possible conditions and support during my PhD studies. I would like to thank Dong Nai Rubber Corporation for their cooperation and for providing the necessary samples to complete my thesis.

I am extremely grateful to Mr. Shariff Zaheer Ahmed for his dedicated support during my work. I am very grateful to Mr. Philippart de Foy Marc and Ms. Uslu Ezgi for your support and help. I would like to thank Mrs. Lovato Martin for your support.

Finally, I am profoundly grateful to my wife, my daughter, and my entire family for their love, patience, and immeasurable support. Their encouragement has been my greatest motivation to complete this dissertation.

Vu Dinh Khang

Abstract

Phosphorus (P) recovery from waste sources in Southern Vietnam presents a promising opportunity for sustainable resource utilization. This study evaluates the potential for P recovery from P-rich waste from wastewater treatment plants (WWTPs), catfish, pig, and cattle farming in Southern Vietnam through specific criteria namely P-reserves, contamination levels, waste collection, and transportation accessibility.

The total P-reserves in these sources were estimated at approximately 50 kt in 2019. Most waste from waste sources has low heavy metal contents. Wastes from catfish farming, pig and cattle farming are often restricted from outside access due to concerns about the spread of disease. Dewatered sludges from rubber latex-processing and domestic wastewater treatment plants were identified as highly suitable wastes for P recovery in Southern Vietnam.

In this study, a P-recovery process was developed using sludges from rubber latex-processing WWTP (RWWTP). To fully design the process for real RWWTP sludges, the P-recovery process parameters are first to be evaluated in laboratory experiments. Then, simulations with the solid-liquid-liquid thermodynamic equilibrium tool are used to optimize the process parameters. Finally, the P-recovery process with the optimized parameters is then validated in a small-scale pilot plant.

P-recovery process was developed using H_2SO_4 for leaching at optimized conditions: 1.7M H_2SO_4 and a phase ratio of 5 L kg^{-1} for BIOS sludge, and 2.0M H_2SO_4 with phase ratio of 10 L kg^{-1} for CHES sludge. This method achieved P-leaching efficiencies exceeding 90%. The leached liquid underwent selective precipitation using NaOH at pH equilibrium from 5.2 to 5.6 for BIOS and 5.1 for CHES, resulting in over 95% P precipitation efficiency. In the following dissolution step, at pH > 9.2, over 90% of P from P-precipitates was dissolved. Unwanted impurities, such as insoluble Fe-precipitates, are removed after liquid-solid filtration. A final precipitation step using $Ca(OH)_2$ at pH 13 produced Ca-P salts, which are suitable for agricultural applications. The overall P recovery efficiency was 67% for BIOS and 65% for CHES. Additionally, dissolved Al from a by-product of the P-recovery process from CHES can be recovered for reuse in WWTPs.

The process fulfills the basic criteria in relation to the economic and technical conditions in Vietnam, which demand a simple yet effective and environmentally friendly process. Some of the output mass flows in the process can be reused to increase economic feasibility, such as the dissolved Al recovered for reuse in RWWTPs. Unfortunately, the total costs exceed the total revenues generated in the current process, primarily due to the high energy demand for dewatering the input sludge and the significant chemical consumption, especially for primary leaching. Improvements in sludge dewatering and taking advantage of Vietnam's high solar energy reserves for at least partial drying sludges could improve the cost-revenues ratio. The implementation of this P-recovery process could significantly reduce P imports, mitigate environmental pollution, and support circular economy initiatives in Vietnam.

Résumé

La récupération du phosphore (P) à partir des sources de déchets dans le sud du Vietnam représente une opportunité prometteuse pour une utilisation durable des ressources. Cette étude évalue le potentiel de récupération du P à partir de déchets riches en P provenant de stations de traitement d'eaux usées (WWTPs), ainsi que de l'élevage de poissons-chats, de porcs et de bovins dans le sud du Vietnam, en se basant sur des critères spécifiques, notamment les réserves de P, les niveaux de contamination, la collecte des déchets et l'accessibilité au transport.

Les réserves annuelles totales de P dans ces sources ont été estimées à environ 50 kt en 2019. La plupart des déchets issus de ces sources contiennent de faibles quantités de métaux lourds. Les déchets issus de l'élevage de poissons-chats, de porcs et de bovins sont souvent restreints d'accès en raison des préoccupations liées à la propagation des maladies. Les boues déshydratées provenant du traitement des eaux usées de la transformation du latex de caoutchouc et des stations de traitement des eaux usées domestiques ont été identifiées comme des déchets hautement adaptés à la récupération du phosphore dans le sud du Vietnam.

Un procédé de récupération du P a été développé en utilisant les boues des WWTPs de transformation du latex de caoutchouc (RWWTP). Afin de concevoir entièrement le procédé pour ces boues, les paramètres de récupération du P ont d'abord été évalués par des expériences en laboratoire. Ensuite, des simulations utilisant un outil d'équilibre thermodynamique solide-liquide-liquide ont permis d'optimiser ces paramètres. Enfin, le procédé de récupération du P avec les paramètres optimisés a été validé à l'échelle pilote.

Le procédé de récupération du P a été mis au point en utilisant H_2SO_4 pour la lixiviation dans des conditions optimisées: 1.7 M H_2SO_4 avec un rapport de phase de 5 L kg^{-1} pour les boues BIOS et 2.0 M H_2SO_4 avec un rapport de phase de 10 L kg^{-1} pour les boues CHES. Cette méthode a permis d'atteindre des rendements de lixiviation du P supérieurs à 90 %. Le liquide lixivié a subi une précipitation sélective avec du NaOH à un pH d'équilibre entre 5.2 et 5.6 pour BIOS et de 5.1 pour CHES, entraînant une efficacité de précipitation du P de plus de 95 %. Lors de l'étape de dissolution suivante, à un pH supérieur à 9.2, plus de 90 % du P précipité a été dissous. Les impuretés indésirables, telles que les précipités insolubles de Fe, ont été éliminées après filtration

liquide-solide. Une étape finale de précipitation avec $Ca(OH)_2$ à pH 13 a permis d'obtenir des sels de Ca-P adaptés aux applications agricoles. L'efficacité globale de récupération du P était de 67 % pour BIOS et de 65 % pour CHES. De plus, l'aluminium dissous, sous-produit du procédé de récupération du P à partir de CHES, peut être récupéré pour être réutilisé dans les WWTPs.

Le processus répond aux critères de base en relation avec les conditions économiques et techniques au Vietnam, qui exigent un processus simple mais efficace et respectueux de l'environnement. Certains des flux de masse produits dans le processus peuvent être réutilisés pour accroître la faisabilité économique, comme l'aluminium dissous récupéré pour réutilisation dans les stations de traitement des eaux usées domestiques (RWWTP). Malheureusement, les coûts totaux dépassent les revenus totaux générés par le processus actuel, principalement en raison de la forte demande en énergie pour le déshydratation des boues d'entrée et de la consommation chimique importante, notamment pour le lixiviation primaire. Des améliorations dans le déshydratation des boues et l'exploitation des réserves d'énergie solaire abondantes du Vietnam pour au moins un séchage partiel des boues pourraient améliorer le ratio coûts-revenus. La mise en œuvre de ce processus de récupération du phosphore pourrait réduire considérablement les importations de phosphore, atténuer la pollution environnementale et soutenir les initiatives d'économie circulaire au Vietnam.

Table of Content

List of Figures

Appendix Figures

List of Tables

Appendix Tables

1 Introduction

Phosphorus (P) plays an important role in the development of living organisms, also the growth of plants. Phosphorus is a fundamental chemical element and assumes a critical role in the structural composition of nucleic acids, namely deoxyribonucleic acid (DNA), ribonucleic acid (RNA), and adenosine triphosphate (ATP), the energy carrier in living cell (Butusov & Jernelöv, 2013). These biomolecules play a pivotal role in cellular division, biomass proliferation, and botanical maturation. Therefore, P is an essential element for crop growth. In the context of the world's ever-increasing population, the demand for P in fertilizers for food production is increasing globally.

Unfortunately, phosphorus is mainly obtained from phosphate rock, a finite resource geographically concentrated only in specific territories and countries, raising concerns regarding global food security due to its vulnerability to geopolitical disruptions and significant wastage. This makes the United Nations' sustainable development goal to reach "no hunger" by 2030 difficult to achieve. Because P supplies are not diversified, unstable and easily affected by geopolitical decisions, efficient exploitation and use of P resources are receiving more attention, including solutions to limit P loss and recovery from different waste sources. Also, the European Union considers elemental P to be a critical raw material (European Commission, 2023). Consequently, many P recovery and recycling research projects have been conducted in the European Union. The Phos4You project is a typical example. This project was implemented in the region of North-West Europe (Interreg North-West Europe, 2020). This project aimed to address the P challenge through the development of technological solutions to recover 113 kt of P per year from municipal wastewater treatment plants, potentially replacing 26% of the mineral demand for phosphorus.

In Vietnam, the demand for P in manufacturing sectors is also very large, especially in agriculture, livestock and industry. According to the FAOSTAT (2022), in 2022 the nutrient phosphate P_2O_5 quantity for agriculture use in Vietnam was 645.5 kt. In Southern Vietnam, agriculture, forestry, aquaculture and livestock production are important sectors. Therefore, P is also used a lot in Southern Vietnam, where the population is about 36 million people, accounting for about 36% of Vietnam's population (GSO, 2024).

Southern Vietnam includes the Mekong River Delta (MRD) and the Southeast (SE) region. Southern Vietnam has a very clear division of specific economic sectors according to localities. While the SE develops light industry, services, and forestry, the MRD has strengths in developing agriculture and food production, such as aquaculture and processing, wet rice cultivation, livestock and poultry farming. Due to its inherent strengths and varied developmental prospects, P demand for the activities of these sectors is very large in Southern Vietnam. At the same time, P-rich wastes from these sectors are numerous and diverse. Unfortunately, solutions to use that waste effectively and limit P loss from waste have not received adequate attention in Southern Vietnam, especially solutions to recover and recycle P. A small part of P-containing waste is used for composting. The rest is mainly buried or even discharged into the environment without going through any treatment stage, which causes loss of P resources and directly pollutes the environment, especially water (Jupp et al., 2021).

In view of this background, this study was conducted to evaluate the potential for P recovery from waste sources and to find solutions to use waste sources effectively by developing a P-recovery process that can be utilized in Vietnam. In addition, the results from this study are expected to further promote the interest of waste source owners, scientists, and state-management agencies in the recovery and recycling of P from waste sources in Southern Vietnam particularly, and in Vietnam in general. Two main objectives are implemented in this study:

1. to evaluate the potential for P-recovery from waste sources, and

2. to develop a technological process to recover P from the most potential waste source in Southern Vietnam. The expected product from the developed process is a P-rich precipitate such as Ca-P salt, which can be used directly on the fields as fertilizer or included in a commercial fertilizer formulation.

For the first objective, the potential wastes used in the study were taken from prominent manufacturing sectors in Southern Vietnam. Based on the results achieved from this waste-source evaluation, the most suitable waste source was used as input material to study a P-recovery process. The P-recovery process parameters were optimized based on the equilibrium simulations and lab experiments. Finally, the optimal process was validated in a pilot-scale P-recovery process.

2 Literature Reviews

Phosphorus recovery

Phosphorus is an essential element for living life. In agricultural production, P is an irreplaceable ingredient in fertilizers. Therefore, the exploitation and rational and sustainable use of this P resource is equivalent to ensuring food security and human survival. Nevertheless, the life cycle of the P, especially human exploitation is notably brief and remains unclosed. In fact, human intervention has disrupted the natural cycle of P (Jupp et al., 2021; Withers et al., 2015). The loss of phosphorus resources occurs through various avenues, notably significant in the form of waste from human activities. P from human waste sources quickly enters the water and soil environment, especially causing surface water pollution. P-rich water then ends up in the ocean from which it can only be recovered with costly methods. Furthermore, the continuous loss of P intensifies reliance on finite phosphate rock (PR) reserves. This increases the pressure on ensuring global food security.

Large phosphate rock reserves are concentrated in a few countries and regions such as Morocco, Western Sahara, the USA, China, and Russia. If PR reserves-rich countries are not ready to share PR or are affected by adverse political decisions such as armed conflict, economic war economic protectionism, it can have a strong impact on the global supply and price of phosphate rock. A shock in phosphate rock prices was recorded in 2008, when it increased from 50$ t^{-1} in the previous year to 430$ t^{-1}. This was caused by several interconnected factors, including export restrictions on phosphate fertilizers implemented by China, import subsidies for phosphate fertilizers in India, and rising costs of phosphate rock and phosphate fertilizers from Morocco, which all contributed to the phosphate price surge in 2008 (Mew et al., 2023).. Recently, when the Russian attack on Ukraine started, phosphate rock prices were recorded to reach more than 300$ t^{-1} (IndexMundi, 2024). Countries that depend heavily on imported phosphate rock were strongly affected by changes in phosphate rock and phosphate fertilizer policies and prices from supplying countries.

Such risks have become the driving forces for developing P recovery and recycling solutions in many countries and regions, especially in Europe. Countries like Switzerland and Germany have implemented stringent regulations promoting rapid

adoption of P recovery technologies since 2016 and 2017, respectively (Jupp et al., 2021). The P life cycle can only be extended and closed if P recovery and recycling are jointly implemented. However, some main barriers, such as legislation and value chains, still slow down the achievement of P recovery and reuse (Jupp et al., 2021). In addition, P recovery and recycling techniques are not the main barriers but are challenges. Europe and Japan have pioneered solutions to put P recovery and reuse into practice (Jupp et al., 2021). Initiatives such as the European Sustainable Phosphorus Platform (ESPP, 2024) and the Dutch Nutrient Platform (DNP, 2024) were created to address the barriers. Findings from Cordell et al.'s research (2011) underscore the imperative to construct a comprehensive decision-making framework for phosphorus recovery and reuse solutions. The 8-step framework developed by Cordell et al. is shown in Fig. 2-1. This framework is adaptive and flexible, providing guidance and support for research-driven decisions in the realm of phosphorus recovery. The first step is to identify key drivers for P recovery, which emphasizes understanding the local, regional, or global factors driving phosphorus recovery. These include pollution control, renewable fertilizer production, food security, and wastewater treatment efficiency. Defining system boundary is the second step in the framework, which ensures a consistent approach to analyzing phosphorus flows and identifying specific potential recovery points, e.g., household, city, or national level.

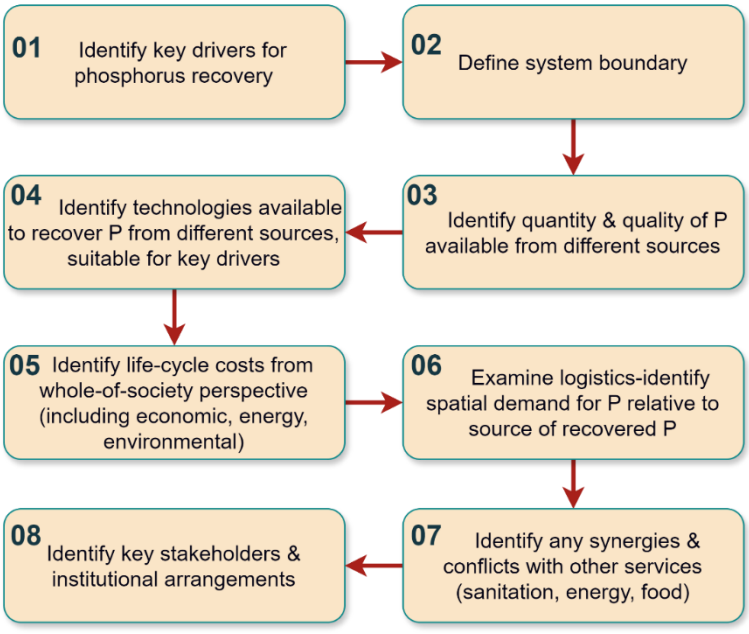

Fig. 2-1: The 8-step framework for decision-marking on P recovery research (Cordell et al., 2011)

The next step is to identify and quantify the phosphorus available from different sources. The most suitable P-rich waste sources will be prioritized for P recovery. The phosphorus recovery systems and techniques are the next evaluation. Appropriate technologies for P recovery depend on the nature and composition of the input materials. P recovery techniques are carefully considered in each context. For example, in Vietnam, P recovery techniques should meet at least the criteria of recovery efficiency and simplicity. In addition to the technical issues and P recovery efficiency, life cycle cost-benefit assessment and environmental impacts are essential. The framework developed by A also shows that the formation and operation of a P recovery project can only be stable and feasible when logistical issues such as collection, transportation, storage, and distribution of input materials and output products are ensured. In the last two steps, the opportunities for cooperation as well as conflicts of interest between stakeholders need to be assessed. Opportunities for cooperation that benefit all parties involved in P recovery projects should be promoted while minimizing conflicts through policy and institutional improvements to ensure consistency. In the context of P recovery in Vietnam, the consensus participation of stakeholders such as waste generators, policymakers, and supporting systems such as energy and water will promote the development of the P recovery industry.

Phosphorus recovery technologies

Over the years, more than thirty P-recovery technologies have been developed to recover phosphorus from various waste streams, including liquid such as wastewater and digested supernatant, sewage sludge, and sewage sludge ash (Bianchini & Rossi, 2020). The technology readiness levels (TRL) of developed P-recovery processes vary widely, ranging from laboratory experiments and pilot-scale trials to full-scale industrial applications. As of 2024, approximately 118 full-scale P recovery projects have been reported, with 71% of projects located in the United States, Japan and Europe, such as Germany and the Netherlands (Zhang et al., 2024). Fig. 2-2 shows a summary review of some published P-recovery processes. Fig. 2-2 provides a generalized overview of published processes, illustrating the relationships between input materials, extraction, leaching techniques, impurity removal technologies, and the final phosphorus products.

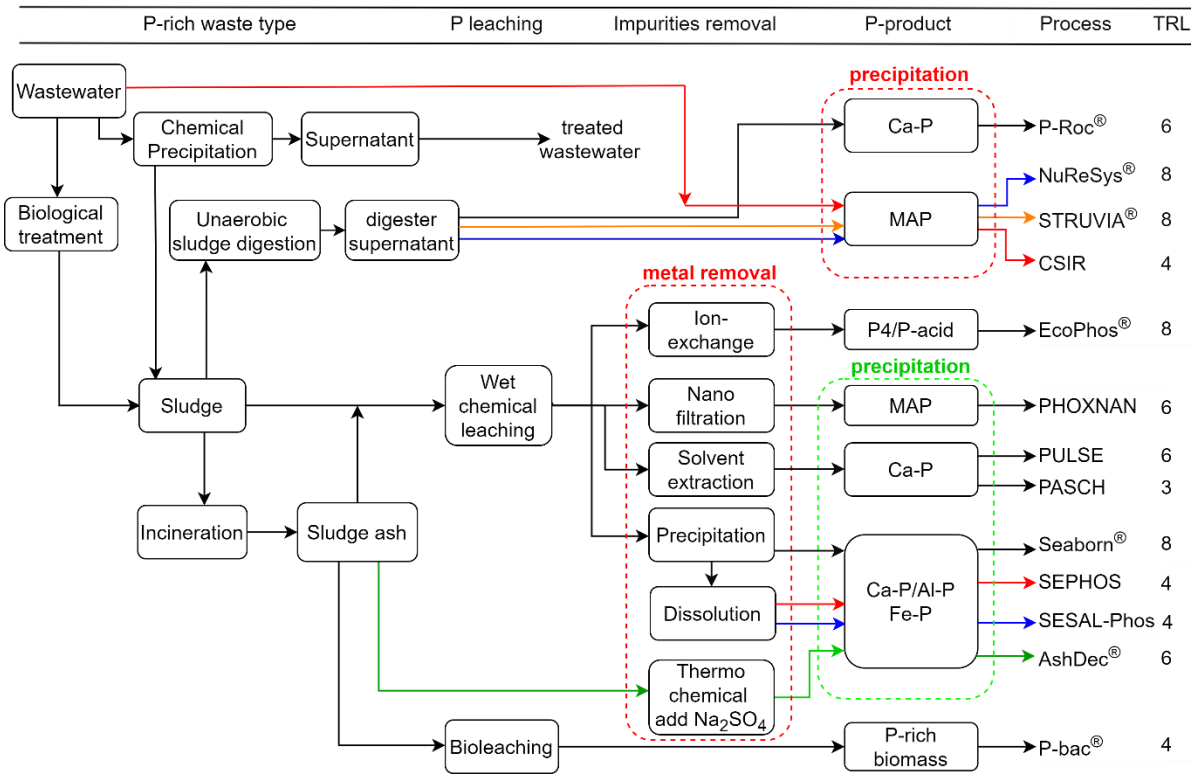

Fig. 2-2: Review of some published P-recovery processes

For liquid P-rich waste, such as wastewater and digested supernatant with low impurities such as metals, or heavy metals, direct precipitation techniques are commonly used. Processes applying direct precipitation techniques can avoid intermediate steps like leaching or thermochemical treatments. Common products obtained from direct precipitation techniques mainly include struvite (MAP) from CSIR process (Pinnekamp et al., 2007) and CaP salt from P-Roc® process (Berg et al., 2007). Two of such processes have already been commercialized like the Belgian NuReSys® process (Moerman et al., 2009) and the STRUVIA® process (Mêlé et al., 2014).

For input material pre-treatment, solid phosphorus-rich waste such as sewage sludge is often dried or incinerated to significantly reduce the waste volume before further steps, such as leaching, can occur. For P recovery from solid phosphorus-rich wastes, such as sewage sludge or sewage sludge ash, the techniques applied to recover P are much more complex than the direct precipitation techniques applied for liquid phosphorus-rich waste. Thermal technology combined with chemicals is used effectively to remove heavy metals in vapor form at high temperatures of up to 1050°C. The AshDec® process, which meets TRL 6, is a typical example. Thermal technologies are energy-intensive due to the high temperatures required. In addition, the exhaust gas

generated from incineration needs to be thoroughly treated due to the possibility of containing toxic organic and heavy metal vapors.

Wet chemical leaching technologies have been studied and applied quite commonly to leach P in input solid materials such as sewage sludge or sewage sludge ash (Egle et al., 2015; Jupp et al., 2021; Tarayre et al., 2016). Seaborn® (Günther et al., 2008) is a typical full-scale project using input sewage sludge to recover P by using H_2SO_4 for leaching. In addition, the PULSE (Shariff et al., 2023) and PHOXNAN (Blöcher et al., 2012) processes also use sewage sludge as input material to recover P at TRL 6 in the WWTP environment (PUSLE). Wet-chemical leaching method is also used for P leaching from sewage sludge ash as input material for EcoPhos® (De Ruiter, 2014), PASCH (Dittrich et al., 2009; Montag et al., 2011; Montag & Pinnekamp, 2009), SESAL-Phos (Petzet et al., 2011) and SEPHOS (Schaum et al., 2004) processes. Most P-recovery processes using wet-chemical leaching, especially using acid, have recorded P-leaching efficiencies of 90% or higher (Dittrich et al., 2009). There are currently few published studies and applications of bioleaching for P recovery, of which P-bac® (Inocre, 2013) is one of the few processes (Egle et al., 2015). Bioleaching is considered environmentally friendly when using specific microorganisms capable of producing acids to leach P, such as microorganisms that produce H_2SO_4 (Ehrlich, 2001; Sarlin et al., 2013; Zimmermann, 2010). According to Inocre® (2013), as much as 90% of the P may be recovered. One issue to note is that wet chemical leaching and bioleaching simultaneously leach P, metals and heavy metals from sewage sludge and sewage sludge ash to leach liquid (Chi et al., 2006; Petzet et al., 2011, 2012).

Impurity removal is a critical step in most P-recovery processes to ensure the final product meets quality standards for agricultural or industrial reuse. The composition and degree of contamination from input material can influence the decision to choose the impurity removal technique. The ion exchange method has been studied and shown to be very effective in removing impurities from leach liquid (Mendes & Martins, 2004). However, leach liquids obtained are often at very low or very high pH, which hinders the selective ion exchange process (Franz, 2008). Solvent extraction has been studied to remove feasible heavy metals as well as metals in leach liquid for P recovery from sludge, e.g. PASCH and PULSE (Shariff et al., 2023) processes. Extractant can be regenerated for reuse many times. Based on the different precipitation abilities of

metals and heavy metals species in liquid, these impurities are effectively removed in many P-recovery processes, such as the SESAL-Phos, Seaborn®, and SEPHOS processes. In the SEPHOS process, Al-rich ash was used. At pH range from 2 to 3, Al is precipitated as Al-P salt while Cu and Zn remain dissolved in the solution. Cu and Zn are then removed after filtration. Dissolution techniques can also be used to remove impurities based on different solubility of compounds. The dissolution method is often used with selective precipitation in P-recovery process to remove impurities further, as SEPHOS process. Removing metals and heavy metals from leach liquid by nanofiltration is rarely studied and applied in available P-recovery processes (Egle et al., 2015; Jupp et al., 2021). Two filter units and ultra-filtration followed by nanofiltration are used to separate Fe, Al and heavy metals from P in PHOXNAN process (Blöcher et al., 2012). The selectivity of the filtration steps is low and thus the P recovery potential with respect to the input sewage sludge is only 55% (Blöcher et al., 2009).

After the removal of impurities, the P-recovered products from available P-recovery processes are mainly P-precipitates, such as Ca-P, MAP, Al-P, or Fe-P salts. In addition, processes such as EcoPhos®, obtain liquid P products such as P4/P-acids.

The feed P-rich waste used influences the structure of the P-recovery process developed. In the available processes, the P recovery from liquid P-rich waste is much simpler than the process using input solid P-rich waste such as sewage sludge or sewage sludge ash. However, the P content from liquid waste is often dilute. Input material pre-treatment methods such as drying or incineration can be used to reduce the input material volume and enrich P. However, these pre-treatment methods also result in additional energy costs. The wet chemical leaching method is commonly used in available P-recovery processes due to its high leaching efficiency and suitability for all types solid P-rich waste. Techniques for removing impurities in P-recovery processes are diverse. Most of the techniques studied have shown high removal efficiencies. However, the appropriate technique to use depends on the specific type of impurity to be removed. Ca-P salt and MAP are finally recovered. The final P-product can be used directly as fertilizers in agriculture or as ingredients in fertilizers. In general, no single technology is universally optimal. And, the selection of an appropriate P-recovery process depends heavily on feed composition, impurity profile, and final product requirements.

3 Materials and Methods

This chapter presents the materials used, the methods and procedures applied to evaluate the potential for P recovery from P-rich waste sources in Southern Vietnam, as well as to develop the P-recovery process from the most suitable waste source.

3.1 Choice of Potential Feedstock

The input waste sources for this study are taken from Southern Vietnam. It includes 17 provinces and two municipalities in total, of which SE has five provinces and Ho Chi Minh City. In the SE region, Ferralsols, characterized by yellowish-red soil, and Acrisols, characterized by gray soil, occupy approximately 43% and 33% of the land area, respectively (Than Thi et al., 2020). These two soil types are suitable for growing perennial industrial crops, especially rubber trees. Therefore, the rubber-latex processing industry finds favorable conditions for development in SE.

The MRD is one of the delta plains with the largest area and lowest elevation in the world (Minderhoud et al., 2019, James et al., 2009). Water from the Mekong River flows through 6 different countries, including Vietnam, to the East Sea with a water flow of about 500 km^3 yr^{-1} (Vo Khac, 2012). This abundant surface-water reserve is a favorite resource for aquaculture in the MRD area, most notably intensive catfish farming (*Pangasius hypophthalmus*) and wet rice farming. However, about 40% of the aquaculture area is located in the acid-sulfate soils area, which requires pretreatment of surface water such as pH adjustment before it can be used for aquaculture (Guong & Hoa, 2012). In addition, livestock farming, such as cattle and pig farming, is also developed in Southern Vietnam. The large population and the development of the above sectors create a large amount of waste in the agricultural sector, including many P-rich wastes that need to be treated. The typical waste sources for evaluation are:

- sediment from catfish farming (CF);
- cattle manure from cattle farming (CTF);
- pig manure from pig farming (PF);
- sludges from rubber-latex processing wastewater treatment plants (RWWTPs);
- sludge from domestic wastewater treatment plants (DWWTPs).

Samples from these sources are collected to evaluate P recovery potential.

3.2 Materials

The chemicals used in this study meet quality standards for scientific research. Chemicals used for sample digestion, experiments and pilot trials, namely mineral acids HNO_3 65% (2989 BATCH 20227701), H_2SO_4 95-98% (0210 BATCH 20459011), and Ultrarace HCl 37% were obtained from Scharlab, Spain. The NaOH pellets 97-100% and $Ca(OH)_2$ 98% were purchased from the manufacturer Duksan, Korea. The bottled purified water used to mix the stock chemical concentrations is HPLC standard deionized water, a product manufactured by Duksan.

3.3 Equipment

A Ponar bucket (model 3-1728-G40, WILCO, USA) was used to collect sediment samples from the bottom of catfish ponds. The moisture content of the dewatered sludge was measured in the laboratory using an automatic moisture meter MA150-Moisture-Analyzer (Sartorius, Germany). This moisture meter is integrated with an analytical balance and infrared drying with results-readability of 0.01% moisture.

The analytical balance manufactured by Mettler Toledo (MS204S) with readability of 0.1mg was used to weigh samples for laboratory experiments. The waste samples such as dewatered sludges, sediments, or animal manures were dried in a forced convection oven (Thermo, USA) and (CE3F-ShelLab, USA) to constant mass at 105^{o}C. To crush the sample for the specific experiment, a crusher machine (PEF100, Jiangxi, CHINA) was used.

To mix the samples, the stirrer (OVAN-JT40E, Spain) at a speed range of 20 to 250 min^{-1} was used during the large-volume leaching experiment. The pH of the liquids was measured using a pH meter HI-8314 manufactured by Hanna, Italy. Hanna provided the 2-point calibration buffer solutions HI70004 pH 4.01 and HI70007 pH 7.01. Additionally, a pH probe storage solution was applied.

A DM0636 centrifuge (DLAB Scientific, China) with a speed range from 300 to 6000 min^{-1} was used to support the liquid-solid separation during the laboratory experiment. The maximum capacity of the DM0636 centrifuge is 100 mL × 4. Additionally, 0.45 to

1 µm pore size polytetrafluoroethylene syringe filters, (Finetech, Taiwan) were used to filter the solids from the liquid solution. In case a large volume of leach liquid was required for precipitation studies, the liquid-solid phase separation was performed using a N035.3AN.18 diaphragm vacuum pump (KNF, Germany) with maximum flow rate of 30 L min^{-1}, combined with polypropylene filter fibers.

Concentration of total phosphorus and metals, such as Al, Ca, Fe, Mg, as well as heavy metals, were analyzed using an inductively coupled plasma optical emission spectrometer (ICP-OES, SPECTROBLUE, Spectro, Germany). Liquid samples for analysis by ICP-OES were prepared according to the manufacturer's recommendations. The HNO_3 5% was used for dilution and preparation of the analytical sample. The liquid was thoroughly filtered to remove as many fine particles as possible before ICP-OES analysis. The detection limit for P and metals was set at 1 mg L^{-1}. The concentration of Pb was also analyzed by energy dispersive X-ray fluorescence spectrometer (EDX- 7000, SHIMADZU, Japan).

An external laboratory (Nano Technology Laboratory, Sai Gon Hi-Tech Park) conducted morphological analysis of input dried sludge and remaining solid after leaching utilizing a scanning electron microscope (SEM) S4800 FE-SEM (Hitachi, Japan). The SEM's rapid voltage varies in the range from 0.5 to 30 kV, with voltage steps of 0.1 kV. The elemental composition of the recovered product samples was analyzed using X-ray fluorescence - S2 PUMA equipment (Bruker, Germany) at the German-Vietnamese Technology Academy, Ho Chi Minh City University of Industry and Trade.

3.4 Sample Treatment

Waste samples

The moisture content of the samples was determined using an automatic moisture meter by drying approximately 50 g of studied samples such as dewatered sludges from wastewater-treatment plants.

The prepared dried waste samples were digested for multielement analysis such as total phosphorus, metals, and heavy metals using the digestion method developed by the European "Horizontal" project (Horizontal, 2006), specifically BS EN 16174:2012– Sludge, treated biowaste and soil. An aqua regia mixture was formed by adding 21 mL of 37% HCl, 7 mL of 65% HNO_3, and 1 mL of distilled water to a 250 mL reaction flask. Following that, 3 g pulverized dry sample sieved with less than 500 µm particle size was added. The mixture was left open at room temperature to release any gas generated from the reaction between the acids and the metals in the sludge before being covered and heated at 100°C for 2 hours. The digestion solution was transferred to a 100 mL flask and diluted with 5% HNO_3 solution. Before analysis, the diluted digestion solution was phase-separated using a 0.45 µm pore size 25 mm syringe filter.

For analyzing the concentration of the organic phosphorus (OP) and inorganic phosphorus (IP), the input sludge samples were pre-treatment following the Standards, Measurements, and Testing (SMT) procedure developed and revised by Ruban et al. and García-Albacete et al. as part of the European Commission's SMT project (García-Albacete et al., 2012; González Medeiros et al., 2005; Ruban et al., 1999).

Leach liquid

Before analyzing the concentration of elements by ICP-OES, all liquids obtained from the experiments were filtered to remove fine particles and prevent precipitation in the solution. To determine the content of P and metals in the leach solutions, the mixture obtained after leaching, including the remaining insoluble solids, was transferred to 50 mL polypropylene centrifuge tubes and centrifuged at 5000 min^{-1} for 6 min. The supernatant was then immediately filtered using a 60 mL syringe combined with a 0.45 µm pore size polytetrafluoroethylene syringe filter to remove any remaining suspended

solids. The leach solution was diluted using HNO_3 5% to minimize the formation of a precipitate, ensuring suitable conditions for analysis by ICP-OES.

3.5 Cascaded Option-Tree Method

The Cascaded Option-Trees (COT) method, as introduced by Bednarz et al., was employed to facilitate a concise and systematic evaluation of process alternatives (Bednarz et al., 2014). This COT method serves to assess diverse process options through establishing relevant criteria. Fig. 3-1 shows an example of a COT applied to evaluate various options. The result of the assessment of each criterion for each option is depicted in the table through distinct symbols and colors. The color green accompanied by the symbol "+" signifies favorable performance of the option relative to the considered criteria; yellow and the symbol "0" denotes acceptable performance, while red and "-" indicate unacceptable performance. If a particular criterion is assessed as unsuitable, it implies that the associated option will not undergo further consideration.

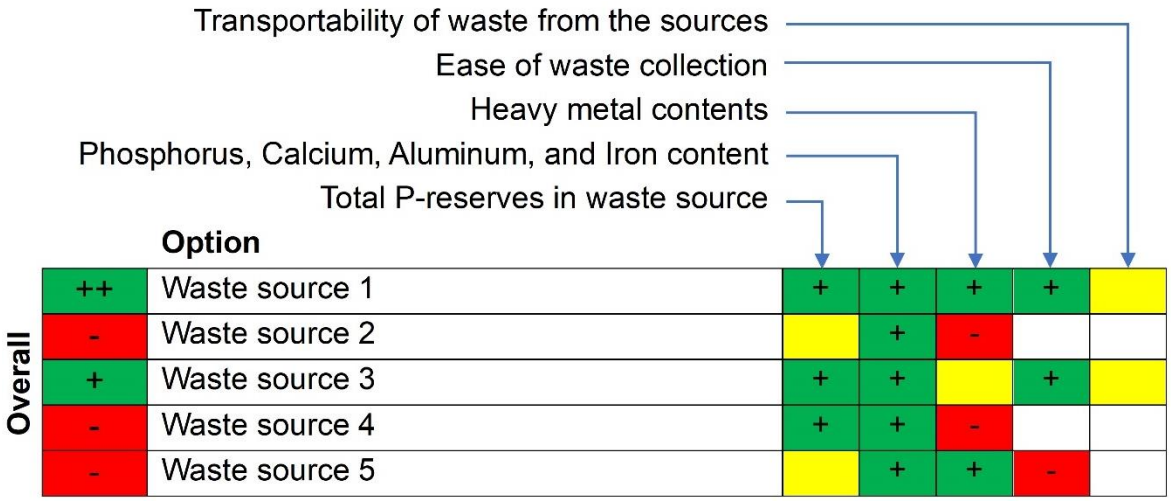

Fig. 3-1: A COT example

The evaluation of the performance of an option is based on the outcomes of a given criterion or sub-criterion. Results from surveys, experiments, literature reviews, simulations, lab or pilot experiments can be used to evaluate each specific criterion. The COT method was used here first to evaluate potential waste sources. Then, the COT method was applied for the overall evaluation of the process and for each step of P the recovery process development. This means the COT tool can be applied at various research levels in the development of the P-recovery process.

3.6 Equilibrium Simulation Tool

A solid-liquid-liquid thermodynamic equilibrium (SLLE) simulation tool adapted from Shariff et al. was applied to develop the P-recovery process (Shariff et al., 2023). In the SLLE simulation, the computation of the equilibrium composition in a chemical system is obtained by solving a system of non-linear equations using the Newton-Raphson (NR) method (Morin, 1985) which was realized in MATLAB. This system consists of the mass balance (MB), the law of mass action (LMA) applied to speciation, precipitation, and liquid-liquid phase equilibrium, and the charge balance (CB). The NR method converges faster than other methods, such as the simplex method. However, the NR method has a smaller convergence radius, i.e., it requires a better initial guess. The procedure of solving a system of non-linear equations using the NR method takes place in three steps, namely

1. obtaining an initial guess,

2. calculating and updating improved values through an iterative procedure, and

3. checking the convergence.

The Newton-Raphson method may not converge if the initial guess value is poorly chosen or if the function exhibits unfavorable characteristics such as a discontinuity or multiple solutions. Therefore, it is necessary to obtain a suitable initial guess. In the SLLE tool developed by Shariff et al. the zero-order positive continuous fraction method (PCF) is used to generate an initial guess value that falls within the convergence region (Carrayrou et al., 2002). This, then is used for "fsolve" function from MATLAB as a starting point to solve the NLEs by first-order derivative of the NR method (Shariff et al., 2023).

In this study, the SLLE simulation tool was adapted and applied to evaluate experimental data and to optimize the P-recovery process. Results from the simulation support the optimization of parameters during the development of the P-recovery process, including specific steps such as leaching, dissolution, and precipitation. Based on the equilibrium simulations with the SLLE tool, the chemical reactions, the concentrations of species of various components, and mineral precipitates are evaluated in the following chapters.

The SLLE simulation tool ensures equilibrium across solid, aqueous, and organic phases by balancing the chemical potentials (μ) and fulfilling the LMA. Activity coefficients (γ) are calculated using Debye-Hückel or Davies models to account for non-ideal behavior in aqueous solutions. To facilitate the simulation, master species are defined, which are the key chemical components that govern the equilibrium conditions of a system involving solid, an aqueous phase, and organic phases (see Shariff et al. for details). These species act as reference points or primary variables to describe the system's state and composition. Morel and Hering noted the criteria for selecting master species to build the appropriate input data set (Morel & Hering, 1993). The main criteria used for selecting master species are:

- Master species are common or dominant in concentration in the relevant mixture at the specific environment.
- Master species should be thermodynamically stable: master species exist for a long time and have little tendency to convert to other forms at equilibrium.
- Master species should be simple, easy to analyze, and calculate.
- Master species should be capable of representing the chemical behavior of that element in the environment.
- Master species should be able to remain in a free ionic state or be less complex.

Based on these criteria, the master species PO_4^{3-}, SO_4^{2-}, Al^{3+}, Fe^{2+}, Fe^{3+}, and Ca^{2+} are selected in this study. Also, H_2O and H^+ should always be chosen as master species.

To describe precipitation, the pure precipitate has an activity normalized to 1. Therefore, in the case of precipitation, the equilibrium chemical reaction constant is expressed as

$$K_p = \frac{1}{\prod_{i=1}^{N_m} a_i^{v_{i,p}}}, \tag{3-1}$$

where, $v_{i,p}$ is the stoichiometric coefficient of the master species relative to the precipitated species p, N_m is a set of chosen master species from the existing species, a_i is the activity of the master species i or the product species p. The solubility or precipitation of a species is expressed through two main indices, the equilibrium

constant K_p or solubility product constant and the ion activity product *IAP*. *IAP* is used to determine a slightly soluble electrolyte's equilibrium state and predict whether precipitation will occur in the solution. The decadic logarithm of the ratio of *IAP* to K_p is so-called the saturation index I_s. Three cases can then result:

- If I_s < 0 or *IAP* < K_p: the solution is in an unsaturated state, which means there is no precipitation.
- If I_s = 0 or *IAP* = K_p: the solution reaches a saturated or equilibrium state.
- If I_s > 0 or *IAP* > K_p: the solution is in a supersaturated state. Under this condition, precipitates of species appear. If I_s for one or more solid species is positive, the PCF algorithm is used to generate updated initial guess values. This iterative process continues until the precipitation state of the species approaches equilibrium (I_s = 0) (Carrayrou et al., 2002; Shariff et al., 2023). The refined initial guess, accounting for aqueous, organic, and solid species, is subsequently utilized as input for the NLE solver to compute the final solution.

4 Potential for P-Recovery of Waste Sources in Southern Vietnam

In this study, waste sources were evaluated to find the most potential and suitable waste source for P recovery in Southern Vietnam. The waste sources selected for evaluation are typical in different sectors in Southern Vietnam, as mentioned in the materials section. The survey, data collection and processing, and sample analysis methods were used to evaluate the potential for P recovery from waste sources by establishing a relationship matrix between waste sources and criteria using the cascaded option-tree method (Bednarz et al., 2014). The most suitable wastes will be used as input material for developing the P-recovery process for application in Southern Vietnam.

4.1 Criteria used to identify the potential waste source

Each waste source is regarded as a prospective option and will undergo evaluation based on relevant and important criteria using the COT method. The criteria selected for evaluation must clarify the potential and suitability of waste sources for P recovery through developing a recovery process suitable to current conditions in Southern Vietnam. Five criteria were used to assess the suitability of waste sources for phosphorus recovery objectives in Southern Vietnam:

- Total P-reserves from potential sources in Southern Vietnam;
- Phosphorus, Calcium (Ca), Aluminum (Al), and Iron (Fe) content in the wastes;
- Heavy Metal contents in the wastes;
- Ability to collect wastes;
- Ability to transport wastes from the sources.

P-reserves in the waste source is a critical criterion for P recovery because P is the main object for developing recovery solutions. This criterion is a necessary condition and, therefore, should be evaluated first. The greater the P-reserve in the waste stream, the greater the attractively for recovery. Removing impurities such as metals in waste is essential to recovering sufficiently pure P-rich products. The lower the level of impurity contamination, the more attractive are waste sources containing P.

Conversely, the higher the P content in the waste, the more suitable it is for recovery. Therefore, the content of P and metals such as Fe, Al, Ca in waste is a criterion to be evaluated. In addition, heavy metal content in waste is a specific criterion that needs to be evaluated. The presence of heavy metals in wastes will reduce their P recovery potential, especially for wastes with high heavy metal content and a high mass ratio of heavy metal to P. A P-recovery process that can run safely, reliably, and practically in any environment in Vietnam does not allow for the complex removal of heavy metals. The ability to collect waste from waste sources for P recovery can be limited by various reasons, including limited access due to livestock diseases or the fragmented distribution of P-reserves. Therefore, the ability to collect waste from waste sources is the next criterion that needs to be evaluated. The potential for P recovery from waste sources is directly affected by the ability to transport waste to a centralized P-recovery unit, especially for waste sources with non-central P distribution. In addition, the state of the waste directly affects how it can be stored and transported to ensure it does not pollute the environment and disperse pathogens. According to Vietnamese government regulations on waste and scrap management, the waste transportation process must ensure that wastewater, dust, odors, and waste are not released into the environment (Vietnam Government, 2015). Therefore, the ability to transport waste is also a criterion that needs to be evaluated.

4.2 Survey and Data Collection

Surveys and statistical-data collection on typical waste sources were conducted to provide a basis for calculating and evaluating criteria for P recovery potential in Southern Vietnam. Statistical data from the General Statistics Office of Vietnam (GSO) was used to identify prominent provinces in each sector with relevant waste sources. These prominent provinces were selected for field surveys and sampling. The provinces selected for survey and sampling corresponding to each type of waste source are shown in Tab. 4-1. Catfish farming is concentrated in the MRD region. Therefore, survey and sample collection activities were conducted in three typical provinces in this area. Pig and cattle farming are widespread sectors in many provinces in Southern Vietnam. Four typical provinces with large output production from each sector were selected for survey and sampling. Survey and sample collection activities from rubber-latex processing wastewater treatment plants were only conducted in the SE region due to the

characteristics of rubber trees and the rubber-latex processing industry that only develops here. Ho Chi Minh City and Binh Duong were selected for survey and sludge sampling of domestic WWTP because they have many operational large-scale WWTPs in Southern Vietnam.

Tab. 4-1: Localities selected for field survey and sampling

Province/City	Sample				
	Pig farming	Cattle farming	Catfish farming	RWWTPs	DWWTPs
An Giang			x		
Dong Thap			x		
Ben Tre (BT)	x	x	x		
Dong Nai (DN)	x			x	
Ho Chi Minh (HCMC)	x	x			x
Tien Giang (TG)	x	x			
Tra Vinh (TV)		x			
Binh Duong (BD)				x	x
Binh Phuoc (BP)				x	
Ba Ria- Vung Tau (BRVT)				x	

The principal information for the survey and data collection are summarized and presented in Tab. 4-2. Based on the GSO (General Statistic, 2018, 2019), the Ministry of Natural Resources and Environment (MONRE), the Ministry of Agriculture and Rural Development (MARD) of Vietnam (MARD, 2019c), the Food and Agriculture Organization (FAO) (FAO, 2023), statistical data such as the head of pigs, cattle, catfish farming area, catfish age, rubber plantation area, and population were collected and used to calculate the P-reserves in waste sources. Waste cleaning and collection methods, waste storage methods, and waste volume reduction methods were used to evaluate the current status of waste management and treatment from the waste sources. The current waste management and treatment situation is a basis for assessing the ability to collect and transport waste to recover P in Southern Vietnam.

Waste samples from waste sources in selected representative provinces were obtained and evaluated. The waste samples were stored in 20-liter plastic containers with lids and then analyzed to determine the P content and impurities such as metals and heavy metals. The P content of each waste was also used to calculate the P-reserves in the waste sources.

Tab. 4-2: The principal information that needs to be obtained from the survey

Heading	Waste source			
	Pig, cattle farming	Catfish farming	RWWTPs	DWWTPs
Head of pig/cattle/person	x			x
Cleaning method and frequency	x			
Catfish age		x		
Type of feeds/wastewater	x	x	x	x
Waste collecting method and frequency	x	x	x	x
Area/yield/capacity	x	x	x	x
Storage method	x	x	x	x
Reducing waste volume method	x	x	x	x
Flow of waste (manure/sediment/sludge)	x	x	x	x

Specialized equipment, specifically the Ponar bucket (model 3-1728-G40, WILCO, USA) was used to collect sediment samples from the bottom of catfish ponds. At each pond, sediment retrieval was performed at five distinct locations, encompassing the central point and four positions at the pond's corners. These individual samples were combined and homogenized to generate an aggregate representation of the sediment profile.

Sludge from RWWTPs can include two types, which are produced from different wastewater treatment methods, namely chemical sludge (CHES) and biological sludge (BIOS). Fig. 4-1 shows an overview of P in the RWWTPs and sludge collection yard at the plant. These sludges originate from chemical and biological treatment stages. Both

types of sludge from RWWTPs were evaluated. Sludges from domestic wastewater treatment plants with capacity above 10,000 m^3day^{-1} were also evaluated.

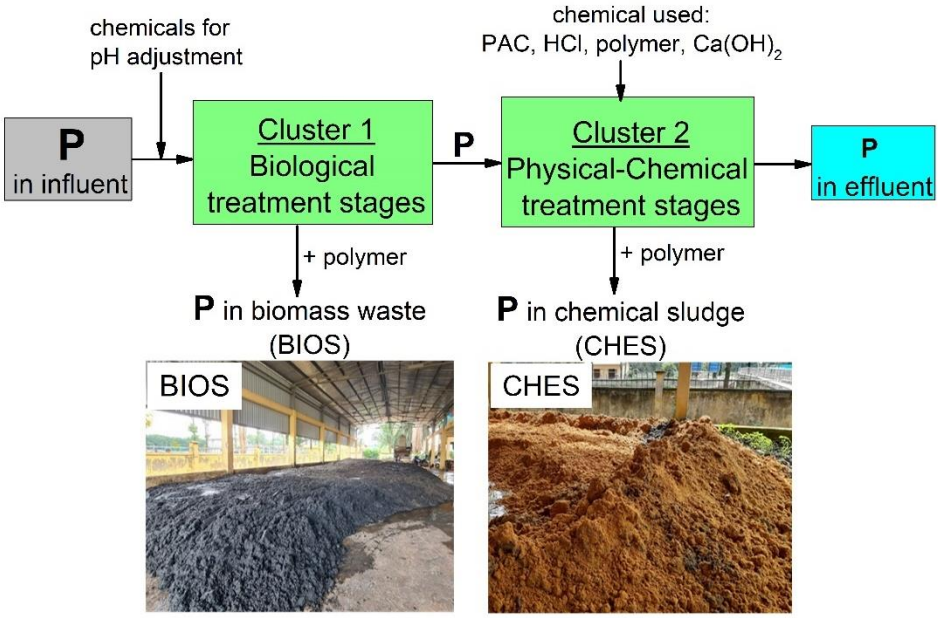

Fig. 4-1: Phosphorus resources at different stages in rubber-latex processing wastewater treatment plant

4.3 Phosphorus-Reserve Calculation

The methods for calculating P-reserves in waste sources are shown in detail in the following sections.

Calculation of P-reserve in sludge from domestic wastewater-treatment plants

Organic matter, N, and P are typical pollutant components in domestic wastewater. P and N in wastewater are used and converted to biomass, known as biological sludge, by microorganisms in biological tanks. Biological treatment is a popular and efficient method for removing P at DWWTPs in Southern Vietnam. The P-reserve from DWWTPs is estimated based on the biological sludge volume generated from the biological treatment stages.

The annual P-reserve in sludge from domestic wastewater treatment plant $\dot{m}_{\mathrm{P,D}}$ is calculated as

$$\dot{m}_{\mathrm{P,D}} = W_{\mathrm{P,sludge}}\, \dot{m}_{\mathrm{S}}\ , \qquad (4\text{-}1)$$

where $W_{\mathrm{P,sludge}}$ is P mass fraction in sludge, and $\dot{m}_{\mathrm{S}}$ is the daily biological sludge produced. $\dot{m}_{\mathrm{S}}$ is calculated based on Lam et al., (2015):

$$\dot{m}_{\mathrm{S}} = \frac{Q\left(C_{\mathrm{BOD,in}} - C_{\mathrm{BOD,out}}\right)Y}{1 + T_{\mathrm{R,S}}\, k_{\mathrm{d}}}\ \frac{1}{0.85} + Q(SS_{\mathrm{in}} - SS_{\mathrm{out}}), \qquad (4\text{-}2)$$

where, $C_{\mathrm{BOD,in}}$ and $C_{\mathrm{BOD,out}}$ are influent and effluent biological oxygen demand (BOD) concentration in wastewater, SS_{in} and SS_{out} are influent and effluent suspended solids, respectively, in which SS_{out} is the biological sludge. The endogenous decay coefficient k_{d} is the mass of volatile suspended solids per mass of volatile suspended solids per time, which can be understood as the loss in cell mass because of the oxidation of internal storage products for energy and for maintenance and cell death in the biological reaction tank. Biomass yield *Y* is the ratio of the amount of biomass produced to BOD consumed. The average time of activated-sludge in the system is called solids retention time $T_{\mathrm{R,S}}$. The typical biomass fraction is the ratio of biomass volatile suspended solids to total suspended solids. A typical biomass fraction usually slightly varies in the range of 0.8 to 0.9. Here, a typical biomass fraction is chosen as 0.85. Q is the total domestic wastewater flow rate. The domestic wastewater flow rate generated according to the population size in the provinces and cities is calculated as

$$Q = \frac{(P_r\, S_r\ + P_u\, S_u\ )}{R}, \qquad (4\text{-}3)$$

where, P_{r}, P_{u}, and S_{r}, S_{u} are the population in rural and urban regions as well as the water supply in both regions, respectively. Water supply standards for domestic purposes are regulated according to the Water Supply-Distribution System and Facilities Design Standard TCXDVN 33: 2006 issued by the Ministry of Construction of Vietnam (MOC, 2006). The generation coefficient R is the percentage of water supply converted into wastewater after utilization for living activities. R = 0.8 is specified in the Vietnam standard No.7957 issued in 2008 by the Ministry of Science and Technology of Vietnam (MOST, 2008) as a typical value.

Calculation of P-reserves in cattle and pig manure

The excretion from pigs and cattle is collected as wet manure and slurry. Thu et al.'s survey results show that most farms in Vietnam and some other Asian countries do not

use bedding in pigpen (Thu et al., 2012). This makes it difficult to clean pigpen and manage manure.

P-reserves from PF and CTF were calculated as

$$\dot{m}_{\mathrm{P,pig}} = W_{\mathrm{P,pig}}\, \dot{m}_{\mathrm{pig\ manure}} \tag{4-4}$$

and

$$\dot{m}_{\mathrm{P,cattle}} = W_{\mathrm{P,cattle}}\, \dot{m}_{\mathrm{cattle\ manure}}\ , \tag{4-5}$$

where $W_{\mathrm{P,cattle}}$ and $W_{\mathrm{P,pig}}$ are P mass fraction in dry cattle manure and pig manure, respectively, and $\dot{m}_{\mathrm{pig\ manure}}$ and $\dot{m}_{\mathrm{cattle\ manure}}$ are the quantities of dry manure production per time.

Calculation of P-reserve in sediment from catfish pond

P-containing waste from catfish farming activities at MRD mainly comes from sediments deposited at the bottom of the pond. It includes excess feed, fish excreta, and possibly dead fish. Therefore, P-reserves is calculated based on the amount of sediment deposited at the bottom of the catfish pond at each stage of a farming cycle.

The amount of sediment produced varies with the fish's growth time. Towards the end of the farming cycle, the fish's need for feed increases, increasing sediment from excess feed and fish excretion. Nguyen et al. (2014) reported that after three months of catfish culture, sediment volume reached approximately 1,600 $m^3\ ha^{-1}$, increasing by 1,000 $m^3\ ha^{-1}\ month^{-1}$ thereafter. Survey results indicate that each catfish growing cycle lasts 6 to 8 months, with an additional 2 to 3 months for pond cleaning and disinfection before starting a new cycle. The P-reserve from catfish farming $\dot{m}_{\mathrm{P,CF}}$ is calculated as:

$$\dot{m}_{\mathrm{P,CF}} = W_{\mathrm{P,catfish}}\, \mathrm{Q_{se}}\, R_{\mathrm{se}}\, \rho_{\mathrm{se}}\, d_m \tag{4-6}$$

where Q_{se} is the annual volume of sediment at the bottom of a pond, which is pumped directly up and then dewatered through an intermediate gravity settling pond to recover wet sediment, R_{se} is the density of the wet sediment to the directly pumped sediment at the pond's bottom, ρ_{se} is the density of wet sediment, d_{m} is dry matter content, which is the ratio of dried sediment to wet sediment, about 0.25, and $W_{\mathrm{P,catfish}}$ is P mass fraction in dried sediment.

Calculation of P-reserve in sludge from rubber-latex processing wastewater-treatment plant

Wastewater from rubber processing has a high concentration of nutrient components, such as phosphorus and nitrogen. Based on the influent and effluent P concentration, the P-reserve from RWWTP is calculated as

$$\dot{m}_{\mathrm{P,R}} = 0.9\, \dot{m}_{\mathrm{rp}}\, q_{\mathrm{w}}\, (C_0 - C), \tag{4-7}$$

where $\dot{m}_{\mathrm{rp}}$ is annual rubber production. These data are collected from the GSO of Vietnam (General Statistic, 2019) and the Vietnam Rubber Association (Vietnam Rubber Association, 2018). The coefficient q_{w} is the water supply for rubber processing, about 10 $m^3\ t^{-1}$ of rubber production, C_0 and C are influent and effluent P concentration, respectively. Before discharge to the environment, outlet wastewater characteristic has to meet the national technical regulation on waste wastewater, in which the maximum total P concentration in effluent must not exceed 4 mg L^{-1} (MONRE, 2011). In this study, the effluent P concentration used for calculation is thus chosen as 4 mg L^{-1}.

4.4 Total P-reserves

P-reserves from the studied waste sources as obtained with the above equation are shown in Fig. 4-2 for the year 2015 to 2018. From 2019 to 2022, economic and social activities were severely affected by the COVID-19 pandemic in Vietnam, so statistical data were not fully guaranteed and could not be used to calculate P-reserves.

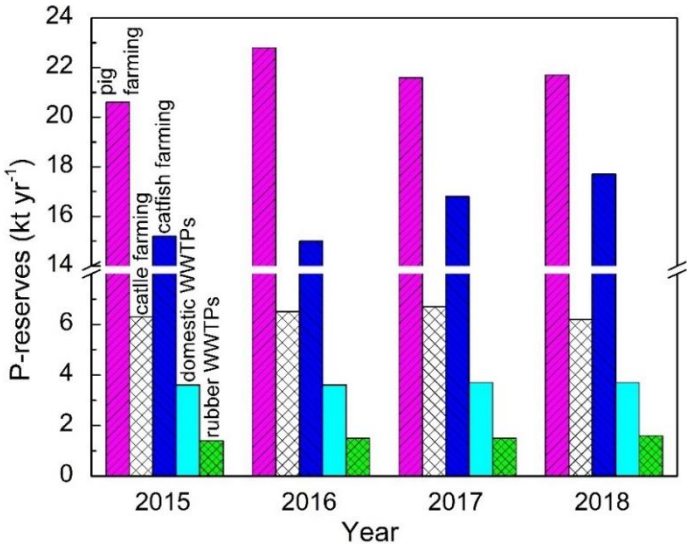

Fig. 4-2: P-reserves from studied waste sources

P-reserves from waste sources mostly increased over the years from 2015 to 2018. P-reserves from pig farming and catfish farming are recorded as the highest group, about 21.7 and 17.7 kt in 2018, respectively. The estimated P-reserves results show that DWWTP and RWWTP are the two waste sources with P-reserves less than 6 kt yr^{-1}, lower than reserves from other studied waste sources.

To evaluate the criterion of the total P-reserves for the COT, the waste source, which has above 6 kt yr^{-1}, appears to be particularly attractive for P recovery and is therefore rated as green and "+" in the COT as shown in Fig. 4-3. They include pig, catfish, and cattle farming. Lower values are considered feasible but less attractive and are therefore rated as 0 and yellow. The further criteria in the COT are explained in the following sections.

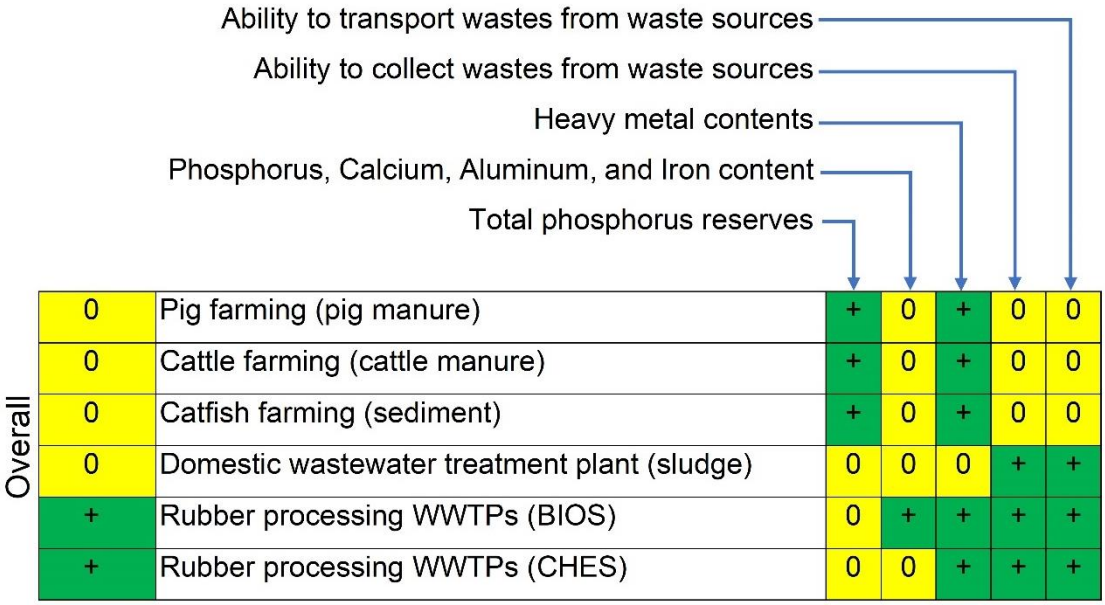

Fig. 4-3: Comprehensive assessment of P recovery potential from waste sources through COT

4.5 Phosphorus and Impurities Content

The composition and level of impurity contamination in studied waste sources depend mainly on the production method, wastewater treatment methods as well as the input materials used in different fields. In particular, most current rubber-latex processing wastewater-treatment plants operate in semi-automatic mode. In addition, the pollutant concentration in feed rubber-latex processing and domestic wastewater are frequently

varied by the seasons of the year. Chemical dosages used in the wastewater-treatment process are mainly prepared according to operating experience and adjusted according to changes in input pollutant concentration. Therefore, the content of substances in sludges is also varied. The content of P and impurities in the dried wastes obtained from the survey, literature are presented in Tab. 4-3.

Phosphorus, Calcium, Aluminum and Iron Content

P contents in wastes from different waste sources show significant differences. The P content in sediment from catfish farming is the lowest. CHES from RWWTPs contains the highest P content among the studied waste sources. Manure from cattle farming and sludge from DWWTPs have quite similar P contents. Comparison with pig manure from Sun et al. (2023) shows that the P content in pig manure collected from South Vietnam is lower. The P content in the sediment from a study by Phu and Tinh (2012) is quite similar to that from sediment in this study. In contrast, the P content in the sediment from Khoi et al.'s study (2012) is much higher than that in the sediment sample collected from the field in this study. The difference in P content in sediments is usually due to the sediment samples being taken at different times during the catfish farming cycle. The closer to the time of fish harvest, the greater the amount of feed used and excreta of the fish. This may lead to higher P content in sediment. The sludge from DWWTP obtained in Southern Vietnam has P content quite similar to that in the study of Alam et al. (2003).

The highest Fe content was recorded in catfish sediment, followed by CHES from RWWTPs. During the raising of catfish, refreshing the water in ponds is a mandatory condition to ensure a living environment for the catfish. Water exchange in the catfish pond occurs once or twice per day, each replacing 30 to 100% of the pond water (Phan et al., 2009). In MRD, most of the freshwater used for daily exchange is taken directly from rivers or canals, which usually pass through the high Fe-content acid-sulfate soils area (Guong & Hoa, 2012). Moreover, the habit of using hydrated lime to disinfect and stabilize pH during fish farming can also cause high Fe content in sediment due to the formation of Fe precipitate. Manure from cattle farming and BIOS from RWWTP were the two wastes with the lowest Fe content. The highest Ca content was recorded in sludges from RWWTP, followed by pig manure, cattle manure, sludge from DWWTP, and sediment from catfish farming.

Tab. 4-3: P, metals and heavy metals in dried waste samples compared to other literature

Sample	Content							
	P	Fe	Ca	Al	Cd	Pb	Cr	Cu
	wt-%	wt-%	wt-%	wt-%	mg kg^{-1}	mg kg^{-1}	mg kg^{-1}	mg kg^{-1}
Pig manure	1.71	1.73	8.50	BDL	BDL	74 ± 2	84 ± 5	400 ± 50
Pig manure (Sun et al., 2023)	3.47	NA	NA	NA	0.3 ± 0.04	12.96 ± 1.92	31 ± 0.50	216.96 ± 11
Cattle manure	0.68	0.16	3	BDL	BDL	BDL	BDL	100 ±10
Cattle manure (Nicholson et al., 1999)					0.1	2	1.4	16.4
Catfish sediment	0.54	4.77	0.80	0.10	BDL	41	89 ± 6	120 ± 10
Catfish sediment (Khoi et al., 2012)	3.89	NA	NA	NA				
Catfish sediment (Phu & Tinh, 2012)	0.62	0.9	0.11	NA	0.02 ± 0.003	0.03 ± 0.01	59 ± 18	2.54 ± 1
CHES from RWWTP	7.01	3.90	11.21	6.23	1	34	167 ± 15	143 ± 10
BIOS from RWWTP	3.94	0.68	4.57	1.16	BDL	BDL	14 ± 5	130 ± 60
Sludge of DWWTP	1.54	1.39	2.29	0.88	BDL	119 ± 14	582 ± 265	440 ± 30
Sludge of DWWTP (Alam et al., 2003)	1.40	NA	0.13	NA	5 ± 1	133 ± 14		121 ± 16

NA: not analyzed; BDL: below the detection limit

In wastewater treatment plants, chemical methods are used to remove suspended impurities as well as P from wastewater. The commonly used chemicals are hydrated lime, polyaluminum chloride (PAlC), ferrous sulfate heptahydrate, and also polymers or ferric alum. The use of these chemicals leads to high metal content such as Al, Ca, or Fe in the sludges from wastewater-treatment plants, especially CHES and BIOS from RWWTPs. Feeds for livestock such as cattle and pigs are mostly industrial feed, in which Ca is supplemented from fish bones and animal bones. Pig and cattle manure, therefore, contain a high Ca content. In catfish farming, lime used in pond renovation and in rising catfish is the cause of increased Ca content in sediment (Phu & Tinh, 2012), but this is not too high. Al was present in all types of sludge from wastewater treatment systems. The Al content was recorded highest in CHES, followed by BIOS and sludge from DWWTPs. Al was not detected in pig and cattle manure. Sediment from catfish farming has an Al content 60 times lower than that in CHES.

The higher the P content in the waste, the greater the potential for P recovery. Conversely, the higher the impurity content in the waste, the higher the cost of removing the impurity. The mass ratio of metal to P in the wastes, as shown in Tab. 4-4, gives a general overview of the two opposite aspects of P and impurities in waste sources. The mass ratio of Fe to P in sediment was recorded at the highest level, about 8.3. Although the Fe content in CHES is high, just lower than that in catfish sediment, the mass ratio of Fe to P in CHES is much lower than that in sludge of DWWTPs and pig manure. BIOS had the lowest mass ratio of Fe to P. The Al to P mass ratio is recorded at the highest in CHES from RWWTPs. However, this ratio is lower than 1, which indicates that the P content is high enough to increase the attractiveness of this waste source. Manure from pig and cattle had the highest mass ratio of Ca to P.

Tab. 4-4: Metal to P ratio by mass from studied materials

Mass ratio (mg mg^{-1})	Studied waste					
	Pig manure	Cattle manure	Catfish sediment	Sludge of DWWTP	BIOS of RWWTP	CHES of RWWTP
Fe to P	1.01	0.24	**8.27**	0.9	0.17	0.55
Al to P	-	-	0.18	0.57	0.29	0.88
Ca to P	**4.97**	**4.41**	1.48	1.48	1.16	1.6

In the COT in Fig. 4-3, only RWWTP (BIOS) is evaluated positively because of the high P content and comparably low impurities content. All other sources were evaluated as 0, because they have either lower P content or higher content of Al, Fe, or Ca. It should be noted that RWWTP (CHES) has somewhat higher metal content but, at the same time, the highest P content, which renders this option slightly better than the other option, rated 0.

Heavy Metal Contents

The heavy metal (HM) contents in the studied samples and literature are shown in Tab. 4-3. The HM content varied significantly among the wastes. Cd was not detected in most of the waste samples, except for RWWTP-CHES. Pb was detected in most of the samples, except for manure from cattle farming and BIOS of RWWTPs. The sludge of DWWTPs contained the highest Pb content and is quite similar to the results of Ahadi's study. In addition, the Cr and Cu contents in the sludge of DWWTPs are also recorded as the highest among the studied waste sources.

The standards for the limit of heavy metal contents in fertilizers and the mass ratios of heavy metal to phosphorus in the studied wastes are shown in Tab. 4-5. The Cu content in cattle manure, catfish sediment, and sludges of RWWTPs are all lower than the limits in fertilizer standards, as shown in Tabs. 4-3 and 4-5. A comparison with the standards for the limit of HMs in fertilizers in Vietnam, Europe, or Canada shows that most of the wastes in this study have lower Cd and Pb contents.

The mass ratio of heavy metal and P in the waste plays a decisive role in the attractiveness of waste sources for direct use as fertilizers or P recovery. The composition analysis results show that cattle manure is the purest waste in all waste sources. Next, BIOS is the second purest waste with very low mass ratios of Cr, Cu to P. Cd and Pb were not detected in BIOS. CHES of RWWPT has high P content, and most of the HMs are low. Thus, the mass ratio of HMs to P is very low, lower than many other wastes, such as sediment, pig manure, and sludge of DWWTP. The mass ratios of heavy metals to P in the sludge of DWWTP are recorded as the highest. In Vietnam, in general, and in the South of Vietnam in particular, most domestic wastewater is collected by the sewer system, which can increase the content of heavy metals due to surface pollutants being washed into the wastewater treatment plant, especially when raining. In addition, wastewater from small industrial and commercial producers not located in

industrial zones can still carry heavy metals to centralized domestic wastewater treatment plants.

Tab. 4-5: Mass ratios of heavy metal to P in studied wastes and standard for heavy metal con-tent limits in fertilizers

Mass ratio	Studied waste					
	Pig manure	Cattle manure	Catfish sediment	Sludge of DWWTP	BIOS of RWWTP	CHES of RWWTP
Cd to P	BDL	BDL	BDL	BDL	BDL	1.43E-05
Pb to P	4.33E-03	BDL	7.59E-03	**7.73E-03**	BDL	4.85E-04
Cr to P	4.91E-03	BDL	1.65E-02	**3.78E-02**	3.55E-04	2.38E-03
Cu to P	2.34E-02	1.47E-02	2.22E-02	**2.86E-02**	3.30E-03	2.04E-03

Standard	Heavy metal contents				
	Cd	Pb	Cr	Hg	Cu
	mg kg^{-1}	mg kg^{-1}	mg kg^{-1}	mg kg^{-1}	mg kg^{-1}
Vietnam Standard (MARD, 2019a)	< 5	< 200		< 2	
Chinese Standard (MARA, 2021)	3	50	150	2	
British Standard (BSI, 2018)	1.5	200	100	1	200
Canadian Standard - Category A (CCME, 2005)	3	150	210	0.8	400
Canadian Standard - Category B (CCME, 2005)	20	500	1060	5	757
European regulation (EU, 2019)	1.5	120	100		300

BDL: below the detection limit

The presence of heavy metals in waste will reduce its appeal, especially when it has high HM content and a high mass ratio of HMs to P. The removal of HMs from waste requires using complex and expensive techniques in terms of investment and operating costs, as discussed in the overview of Chapter 2. These requirements are not appropriate in most applications in Vietnam due to limited investment and technical application capabilities. P-recovery process that can run simply, safely, and effectively in all conditions in Vietnam only when it is applied to input material from waste sources with no heavy metal problems. The sludge from DWWTPs is only rated at acceptable

performance due to high HM contents and high mass ratios of heavy metal to P. Most of the mass ratio of HM to P and HM contents in wastes of cattle farming, catfish farming, PF, and RWWTPs are very low and below the limits set by most fertilizer standards. Therefore, these wastes are indicated as a favorable potential for P recovery applications, as shown in Fig. 4-3.

4.6 Ability to Collect Waste from Waste Sources

Two sub-criteria that directly affect waste-collection efficiency are the accessibility to waste sources and the distribution of fraction of P-reserves in each waste source by province, which were assessed.

Waste can only be collected when there are no restrictions on access to the waste source. Therefore, the sub-criterion of accessibility to waste sources needs to be carefully considered. Pigs, cattle, and catfish are especially sensitive to animal diseases. Waste collection activities can increase the risk of disease spread in fields between regions. Therefore, most farm owners are very cautious about activities that may pose a risk to the safety of their animals. In catfish farming, hemorrhagic disease is the primary cause of significant losses, mainly caused by *Aeromonas hydrophila* and *Edwardsiella ictalurid* (Ly et al., 2009). These bacteria rapidly spread through water, sediment, or unconsumed food, resulting in mortality rates of up to 80% among infected catfish (Ly et al., 2009, Esteve et al., 1993, Ho et al., 2008). African swine fever (ASF) is a devastating disease of swine and the pig industry (Nga et al., 2020). In February 2019, the ASF appeared first in Hung Yen province and then spread to 62 provinces of Vietnam through July of the same year. There were about 5.7 million pigs infected to be killed during the ASF outbreak in Vietnam in 2019 (MARD, 2019c). ASF is characteristic of a hemorrhagic phenomenon and suppresses the immune system in pigs (Carrasco et al., 1997, Dixon et al., 2019). Highly virulent strains of the virus that cause acute illness can lead to a mortality rate close to 100% within 4 to 15 days of infection (Dixon et al., 2019).

These pathogens from CF, cattle farming, and PF are easily spread through many different infectious pathways. In particular, waste collection is a pathway of a high risk of spreading any of these diseases. The attractiveness of these wastes is therefore very low even if they completely meet the requirements to prevent disease

transmission. Methods of disinfecting pathogens, such as using chemicals or heat, can be applied to limit the spread of disease. However, these methods cause expensive chemical costs and high energy consumption. As a consequence, accessing sludges from RWWTPs or DWWTPs is more convenient, since this avoids these issues.

The second sub-criterion that needs to be assessed is the distribution of the fraction of P-reserves in each waste source by province. This sub-criterion represents the level of distribution of P-reserves. In the case of the fraction of P-reserves being widely distributed in provinces, it may lead to higher costs for transport of the waste to the P-recovery unit, especially for provinces with low P-reserves in waste, such that it would not be for operating units in that province. Fig. 4-4 presents the distribution of the fraction of phosphorus reserves for each waste source by province. Quantitatively, the distribution of the P-reserves is assessed by calculating the coefficient of variation C_v. A lower C_v value indicates a more balanced distribution of P-reserves among provinces.

Pig and cattle farming are on a small scale and spontaneously developed in almost all provinces and cities in Southern Vietnam. Households, especially in rural areas, can raise pigs and cattle on different scales. Therefore, P-reserves from cattle and pig farming are widely and evenly distributed among provinces. Results from the survey and data analysis show that P-reserves from catfish farming are concentrated mainly in some provinces, such as Dong Thap, An Giang, Ben Tre, and Can Tho.

The P-reserves in sludge from DWWTPs in Southern Vietnam show a fairly even distribution. Ho Chi Minh City has the highest P-reserves fraction. P-reserves from the sludge of domestic wastewater treatment plants depend on population, the level of wastewater generation, and the collection rate. The domestic wastewater collection rate in Ho Chi Minh City is the highest in Southern Vietnam but only reaches about 21.2% (MONRE, 2019). By June 2021, there were only five wastewater treatment plants in Ho Chi Minh City, six plants in the Southeast region, and 13 plants in the Mekong Delta with over 10,000 m^3/day capacity. The low wastewater collection rate and few wastewater treatment plants with a high capacity lead to current unattractiveness due to P still being lost through untreated wastewater and small amounts of sludge from small-capacity DWWTPs. One positive point is that wastewater

treatment plants are designed with high capacities so that the volume of sludge is large enough to install their own P-recovery unit at the discharge site.

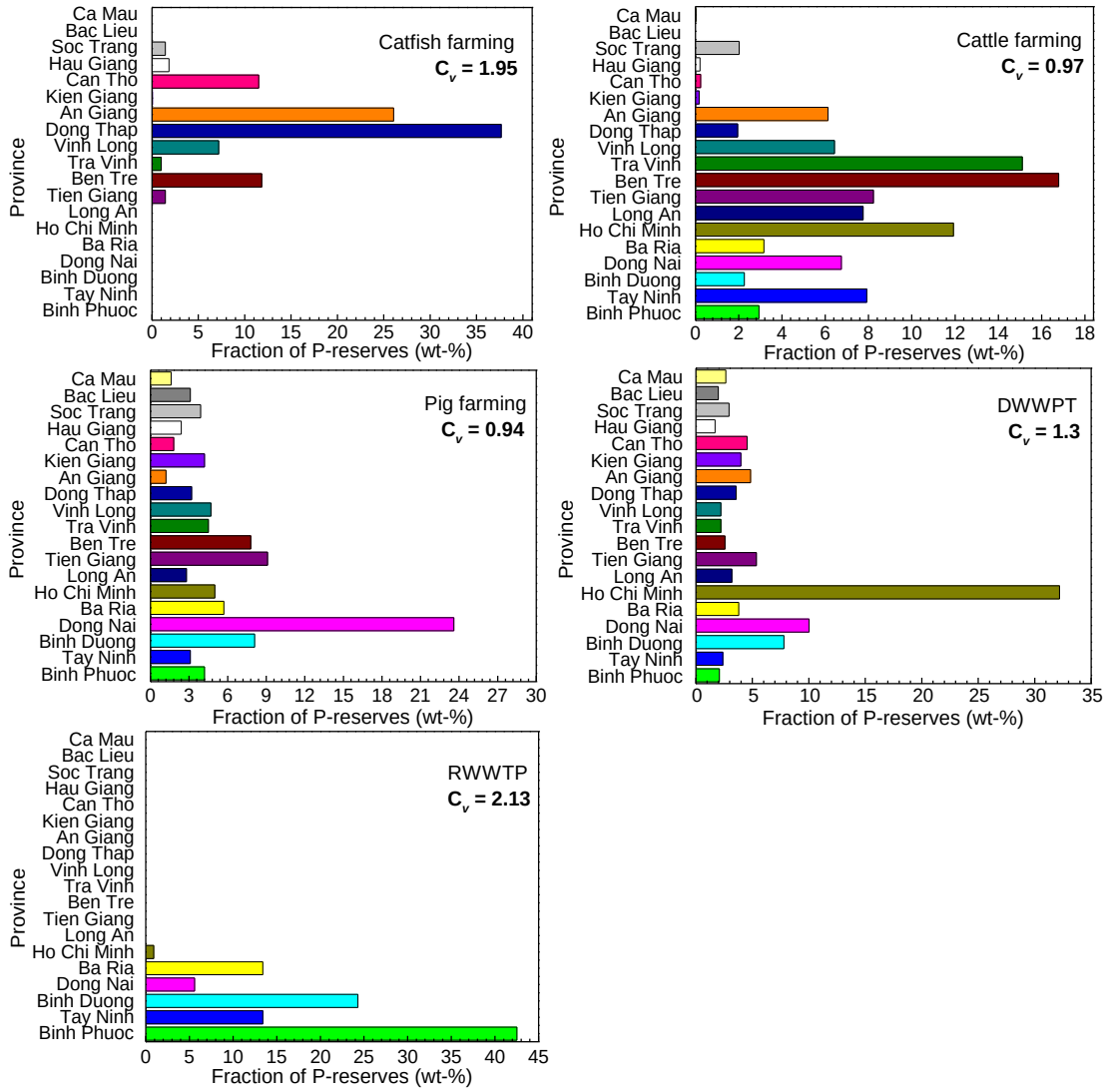

Fig. 4-4: Fraction of P-reserves by province for the different waste sources

The C_v from RWWTPs is recorded as the highest compared to other studied waste sources. Most of the P-reserves from RWWWTPs are concentrated in the southeastern provinces because rubber-processing factories are also concentrated in this area. Similarly to DWWTPs, A large-capacity RWWTPs can install their own P-recovery unit. An additional advantage is that the obtained P-fertilizer can actually be reused directly on the rubber plantation.

In summary, the combined assessment results from the sub-criteria show that it is easy to access and collect sludges from DWWTP and RWWTP for P recovery since both are already using chemical-engineering steps, so some more technical steps for P

recovery are easily possible to operate. Therefore, these two waste sources are assessed as highly suitable and are colored green in Fig. 4-3. Manure from pig and cattle farming cannot satisfy both of the sub-criteria specified. Sediment from catfish farming does not satisfy the sub-criterion on accessibility for collection due to pathogen problems. Therefore, manure from pig, cattle farming, and catfish sediment are rated only at acceptable performance.

4.7 Ability To Transport Waste from Waste Sources

Two sub-criteria that directly impact the ability to transport waste were assessed. The first sub-criterion is the distance of the waste collection route between waste points, and the last one is the characteristics of the collected waste.

Waste is collected between discharge points when the reserve is not enough to set up an individual P-recovery unit at the discharge site. Waste then has to be collected and transported to a centralized P-recovery unit. The length of the waste collection route from each waste source is calculated based on the distance between the four provinces with the largest P-reserves. The P-recovery unit is assumed to be located in the province, which has the largest P-reserves. Then, the transportation effort between the other provinces to the central unit is the smallest. Four provinces with the largest P-reserves in each type of waste source are shown in Tab. 4-6. In all case, the total P-reserve fraction from the four provinces with the highest reserves is greater than or roughly equal to 50% of its reserves from Southern Vietnam.

Tab. 4-6: Four provinces with highest P-reserves by waste source

	Pig farming	Cattle farming	Catfish farming
Province	Dong Nai	Ben Tre	Dong Thap
	Tien Giang	Tra Vinh	An Giang
	Binh Duong	Ho Chi Minh City	Ben Tre
	Ben Tre	Tien Giang	Can Tho
∑P-reserves, %	49	52	87

The waste collection route distance is measured in the field based on the global positioning system device GARMIN GPS MAP 78S. The route and length of the waste transportation route for each waste source are shown in Fig. 4-5. P can be recovered at each RWWTP and DWWTP using its P-recovery unit. Therefore, the transportation distance for sludge collection is not a critical factor in these waste sources. The transport route for manure from pig farming is determined to be the longest, followed by the transport route for sediment from catfish farming. The route to transport cattle manure between provinces with the largest P-reserves to the concentrated place is determined to be the shortest.

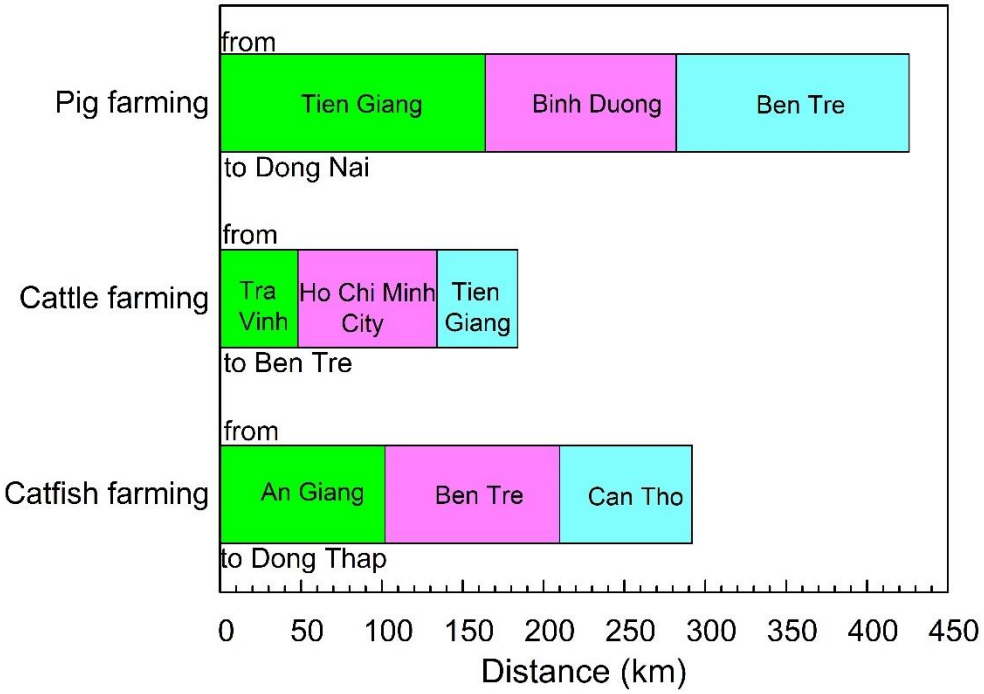

Fig. 4-5: Distance of waste-collection route from the group of provinces with the largest P-reserves according to each waste source

In addition, the means of transporting waste used according to the topographical features are also considered in Southern Vietnam. There are two major means of transportation that can be considered for waste transport, namely land and the inland-waterway transport. Fig. 4-6 shows the dense river and canal network in the Mekong River Delta region. The MRD has a low terrain and a very dense river and canal network. The Mekong River divides into nine branches before flowing into the sea. Therefore, inland-waterway transport is very convenient and well-developed in the provinces of the MRD. The provinces in the southeast region have high terrain and

very few canals and rivers, so land transport is strongly developed. Catfish farming is concentrated in the MRD region, with a dense network of rivers and canals. Moreover, catfish ponds are often located next to rivers or canals, which facilitates the collection and transportation of sediment by inland-waterways. Transportation by the inland-waterways often leads to longer routes and requires more time than by land transport. However, each ship can transport a larger quantity of waste than by road transport such as trucks. Other types of waste are most conveniently transported by land transport.

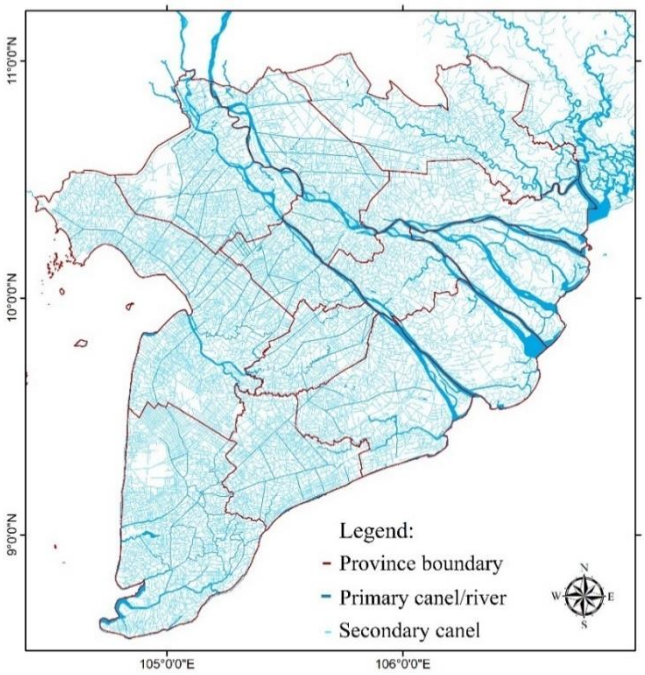

Fig. 4-6: River and canal networks in the lower Mekong River basin

The character of the waste, e.g., if it is obtained as liquid, slurry, or solid, affects the mode of transportation and storage. The current waste character, management, and treatment from waste sources in this study are shown specifically in Fig. 4-7. The diagram illustrates the waste management and treatment levels for each waste source. The red dashed line divides the graphic into two parts. The left side shows the current status of waste generated and treated at the waste sources. The right side indicates pre-collection and transportation requirements. Slurry from cattle and pig farming requires additional dewatering before it can be transported. Slurry, after dewatering, reduces its volume significantly, making it easier to transport and less expensive. Most livestock households and farms have biogas systems as a alternative way of utilization and for treating the wastewater after dewatering. Liquid after biogas can be used for

irrigation purposes. Sediment which pumped from catfish pond, primarily composed of surplus food and fish excretion (Bosma et al., 2011), also requires dewatering due to its high water content. Most sludges from DWWTPs and RWWTPs are dewatered on-site using dewatering equipment. Dewatered sludge significantly reduces its volume and is very convenient for storage and transportation. The lower the water content of dewatered sludge, the lower the pre-treatment costs such as drying for P recovery. Tab. 4-7 summarizes and presents the current status of sludge treatment from some typical RWWPs and DWWTPs in the Southern Vietnam.

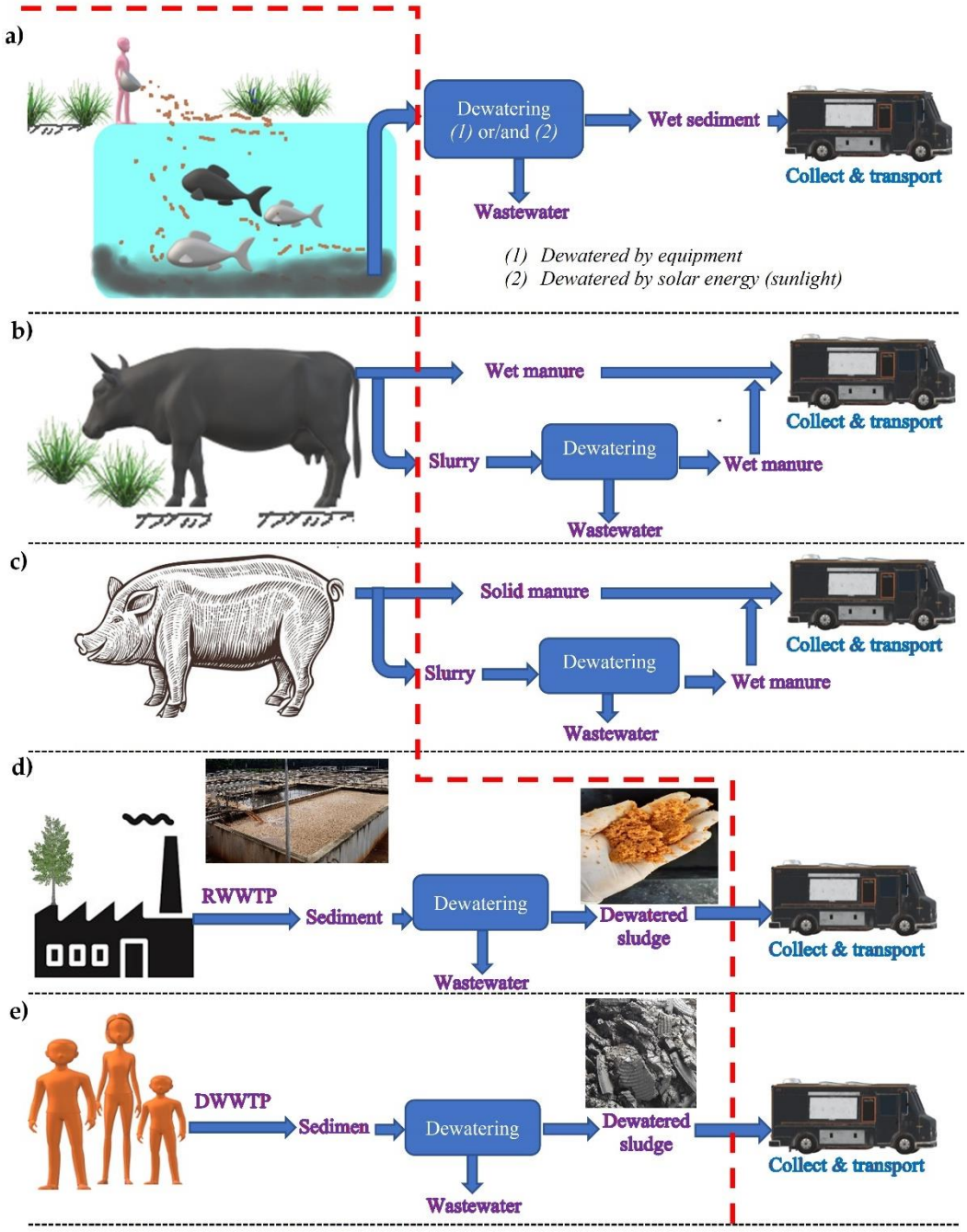

Fig. 4-7: The current situation of waste physical forms, management and treatment

Many of the wastewater treatment plants show a trend of using specialized dewatering equipment such as multi-disk screw press and belt press to reduce sludge volume, except for Binh Hung Hoa DWWTP, where the sludge is not dewatered by machine but stored in a settling pond and then pumped for treatment once a year. Binh Hung Hoa DWWTP has been operating since 2006 under the cooperation of the Belgian and Vietnamese governments. The aeration and stabilization pond technology are used for treating wastewater in Binh Hung Hoa DWWTP. Dewatering by natural drying such as drying by solar energy has not been used in any wastewater treatment plant.

Tab. 4-7: Sludge treatment method at RWWTP and DWWTP via survey data

Enterprise	Wastewater type	Sludge	Dewatered by	
			Dewater-ingequip-ment	Natural drying
Ben Suc Rubber Corporation	Rubber	Both(*)	Yes	No
An Lap Rubber Corporation	Rubber	Both(*)	Yes	No
Xuan Lap Rubber Corporation	Rubber	Both(*)	Yes	No
Cam My Rubber Corporation	Rubber	Both(*)	Yes	No
Hang Gon Rubber Corporation	Rubber	Both(*)	Yes	No
Ba Ria Rubber Corporation	Rubber	Both(*)	Yes	No
Loc Ninh Rubber Corporation	Rubber	MixS(*)	Yes	No
Binh Phuoc Rubber Corporation	Rubber	MixS(*)	Yes	No
Binh Hung plant	Domestic	BIOS	Yes	No
Tham Luong plant	Domestic	BIOS	Yes	No
Binh Hung Hoa plant	Domestic	BIOS	No	No
Di An plant	Domestic	BIOS	Yes	No

MixS(*): CHES and BIOS are mixed before dewatering
Both(*): CHES and BIOS are separately obtained

The general assessment of the criteria for the ability to transport waste from discharge sources for P recovery showed that sludge from wastewater treatment plants is very convenient for transporting. In addition, for large-scale wastewater treatment plants, P

recovery units can be established at their plants. Thus, RWWTP and DWWTP are positively evaluated with respect to criterion in Fig. 4-3. Transporting waste from catfish, cattle, and pig farming is more complicated, so that are evaluated only as acceptable.

4.8 Discussion of Results

Pig, cattle, and catfish farming require large investments in infrastructure for possible dewatering, for transport and collection networks, including intermediate storage. Thus, while they have large potential for the future, they are less attractive in the short term. Heavy metal appears in the sludge of DWWTP, and variations of their concentration are expected between the dry and rainy seasons. Therefore, DWWTP requires a complex process. Also, a wide variety of process options are readily available for them (see literature chapter). Thus, here RWWTP with CHES and BIOS shall be the focused as the most suitable waste source because that allows for some local technology, which should nevertheless not be significantly more complex as compared to the process operated at RWWTP already today. In prospective scenarios, the comprehensive recovery of P-reserves from studied waste sources holds the potential to resolve approximately 16% of the aggregate nutrient phosphorus (P) volume utilized as fertilizers in Vietnamese agriculture during 2019. Also, once established for RWWTPs, these may be used as demonstrators for medium-sized P-recovery plants for regional P-recycling from pig farming, catfish farming, and cattle farming.

5 Phosphorus Recovery Process Concept and as Basis for Developing a Corresponding Process

The current status of P-recovery processes from different waste sources was summarized in the literature review section. BIOS and CHES from RWWTP were assessed as one of the most suitable waste for recovering P in Southern Vietnam. Sludges from RWWTP are a rich source of P but also contain Al, Fe and Ca. In addition, the heavy metal contents in CHES and BIOS are low, so complex solutions to remove heavy metals in leach liquid are not necessary. The development of the P-recovery process at the same time has to meet a number of criteria such as:

- high P recovery efficiency,
- simple technical methods to remove impurities such as the mentioned metals,
- ability to reuse chemicals, and low negative impact on the environment,
- respect current economic and technical conditions in Vietnam.

The comprehensive literature review in chapter 2 shows that no single technology is optimal for all input materials. Therefore, developing an appropriate P-recovery process depends on the input material composition.

Pre-treatment methods such as drying or incineration are applied in most P-recovery processes to reduce sludge volume and enrich P significantly. However, the incineration of sewage sludge at high temperatures to produce sewage sludge ash may consume more energy than just drying sewage sludge. In addition, the pre-treatment method of P-rich waste at high temperatures as an incineration method requires an additional exhaust gas treatment system due to the possibility of containing toxic organic vapors.

Wet chemical leaching is then the major step suitable for leaching P in input solid materials such as sewage sludge. Available P-recovery processes, which included the wet chemical leaching step, show high leaching efficiency, reaching more than 90%. In addition, the techniques and equipment used for wet chemical leaching are simpler than thermal P-recovery methods.

Impurity removal is the next major step in the P-recovery process to recover pure P-product. The composition and level of contamination in the input material influence the

choice of purification technique. Since the sludges from RWWTPs contain heavy metals only at very low concentration, a simple-impurity removal technique is fully sufficient. Ion exchange and solvent extraction have been shown to achieve very high metals and heavy metals removal efficiency. Thus, the selective precipitation and dissolution as simple and effective methods to remove unwanted impurities, can be applied for RWWTP sludges, since they allow dealing with the high content of Al, Ca, and Fe. The difference in solubility of metal-precipitates of Al and Fe at different pHs is thus the basis for removing impurities through liquid-solid phase separation. Selective precipitation and dissolution do not require the use of specialized chemicals or materials such as extractants, ion exchange material, or high temperatures.

The resulting P-recovery process proposed here is shown in Fig. 5-1. First, dewatered sludges from RWWTP are dried to stabilize the input material and to reduce chemical consumption in successive steps. Phosphorus is then leached from this feed by using a strong acid. Metals Ca, Al, and Fe from sludge dissolve into the leached liquid. After filtration for recovering the pregnant leach solution, the remaining insoluble solids are washed with water to recover the maximum amount of dissolved P and remaining acid. This washing solution is reused to prepare the acid medium for the next leaching batch. In addition, washing with water also significantly reduces the acidity of this insoluble secondary waste. In the next step, the leached liquid undergoes the first selective precipitation by increasing the pH adding NaOH to precipitate Al-P salt and to remove other impurities such as metals remaining in the liquid. The precipitated products consist mainly of Al-P salts and Fe-precipitates. They are recovered again through filtration. Subsequently, the Al-P salt is dissolved by again shifting the pH by adding NaOH, which selectively dissolves Al-P salt, while Fe-precipitates remain in the solid phase. The liquid obtained after filtration contains mainly dissolved Al and P.

Finally, $Ca(OH)_2$ solution is used for the final selective precipitation of the Ca-P precipitate. After filtration, the Ca-P precipitate is washed and collected as final product. The Al dissolved as Al^{3+} can be recovered and reused in the wastewater of the RWWTP.

The proposed P-recovery process shows advantages for P recovery from RWWTP sludges. It achieves the criteria set for the process to be applied in the current economic and technical conditions of Vietnam. The techniques used in the P-recovery

process are simple but highly effective in both leaching and removing unwanted impurities. The by-products created in the P-recovery process, such as the remaining solids after leaching, are washed with water, significantly to reduce environmental impacts.

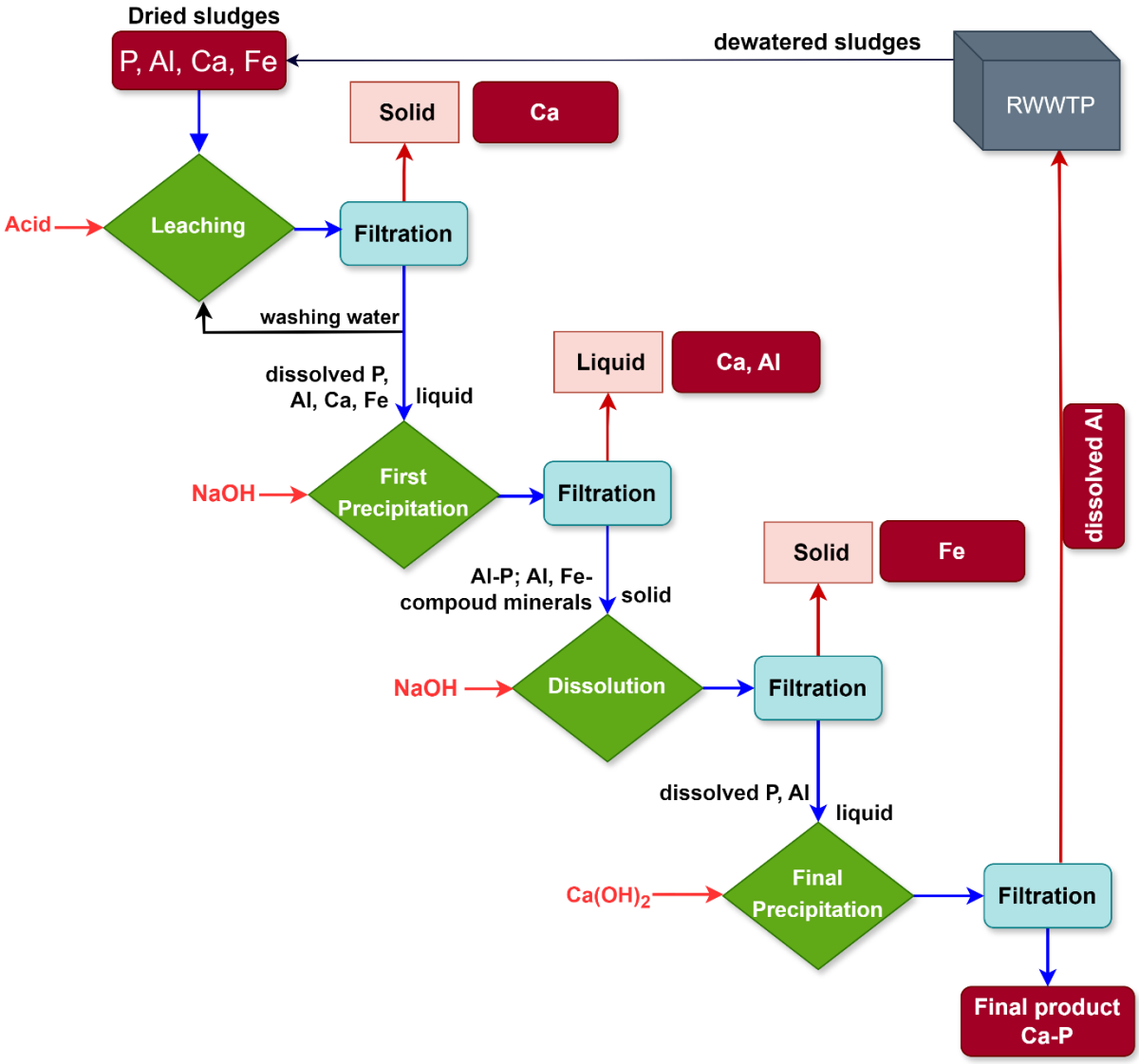

Fig. 5-1: Schematic diagram of P-recovery process concept

To fully design the process for real RWWTP sludges, the parameters of the proposed P-recovery process are first to be investigated in laboratory experiments. Then, simulations with the SLLE tool are used to optimize the process parameters. Finally, the P-recovery process with the optimized parameters is then validated in a small-scale pilot plant.

6 Lab experiments

Laboratory experiments were performed simultaneously for both types of sludge generated from RWWTP, namely CHES and BIOS. These sludges were taken from the wastewater treatment plant of Dong Nai Rubber Corporation (DONARUCO) in Dong Nai province. The experiments were performed following the sequence of steps of the conceptualized P-recovery process. Results from the experiments were used to evaluate, develop, and optimize the parameters of each stage as well as the entire P-recovery process step by step. The leaching agents were tested to evaluate their ability to solubilize P in the input material by using the COT method. The most suitable leaching agent was then used for subsequent experiments. Variables affecting P leaching efficiency, such as sludge drying method, sludge particle size, leaching time, phase ratio, equilibrium pH, and leaching agent concentration, were investigated. Along with the results from the simulation tool, lab experiments on the step of precipitation, dissolution of P-precipitates, such as Al-P salt, and final precipitation to create the final product of P were performed to determine the optimal parameters, which are then to be validated through the pilot plant in the following chapter.

6.1 Sludge Preparation

The dewatered BIOS and CHES from RWWTP were prepared in different ways depending on the intended uses. These included sludge preparations to determine sludge composition and elements' content or to optimize P leaching. Immediately after collection from the RWWTP, the dewatered sludge was dried in a forced-convection oven (CE3F-ShelLab, USA) and (Thermo, USA) at 105^{o}C to a constant mass. Depending on the moisture content, the mass of dewatered sludge, the time required to reach a constant mass of the sludge was between 8 and 10 hours.

The dewatered sludge was shaped into "spaghetti sludge" before drying. According to the study published by Fraikin et al. (2015), shaping sludge into spaghetti sludge improves drying efficiency. For sludge digestion, the dewatered sludge after drying to constant mass was ground into a powder with a particle size of about 500 µm using a grinder (H2.HHM800, Hanil, South Korea). Then, dried sludge power was digested for analysis of composition and content of elements. The dried CHES and BIOS prepared for digestion are shown in Fig. 6-1.

Fig. 6-1: Sludge preparation for digestion

For the leaching study, the particle size of the dried sludge was chosen to study its effect on the leaching efficiency of P. Therefore, dried sludge particles of different sizes were prepared. The extrusion equipment for creating spaghetti sludge of various sizes is shown in Fig. 6-2. A hand-operated extruder was used to form sludge samples of different sizes by using extrusion plates with 1.5 mm to 8 mm extrusion holes.

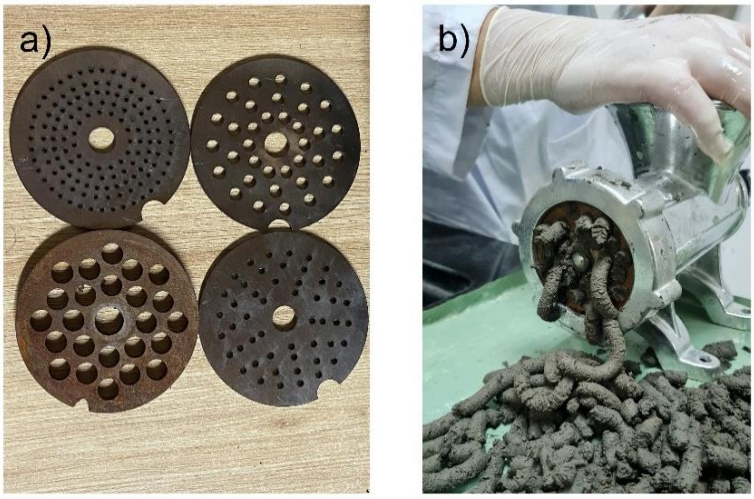

Fig. 6-2: Different pore sizes of extrusion plates (a) and extruder (b)

The spaghetti sludge was evenly distributed on a metal tray before being placed in the drying oven. The dried sludge was stored in 2 L polypropylene plastic containers with lids before further use. For the experiment to determine the effect of dried sludge particle size on P leaching, the dried sludge was cut into pieces manually with sizes smaller than 1 mm, 1 to 2.5 mm, 2.5 to 5 mm, and above 5 mm. These dried sludge

pieces were then separated to uniform size using a sieve before being used for the leaching experiments.

6.2 Experimental Procedures

Based on the conception for P-recovery process developed in section 5, the optimization study of each step of the P-recovery process was carried out step by step through laboratory experiments. The experimental procedures for each step of the P-recovery process are detailed in the subsections below.

6.2.1 Leaching

The leaching was investigated at different conditions, varying the type of leaching agent, particle sizes, contact time, liquid-solid phase ratio, and leaching-agent concentration. The liquid-solid phase ratio was defined as the volume of leaching solution to the mass of dry sludge, expressed as L:S. HCl, HNO_3, and H_2SO_4 were use for leaching. For each leaching experiment, 2 g of dry sludge sorted according to particle size was placed in a 20 mL to 100 mL glass flask or test tube with a lid, then acid was added. The mixture was then mixed using a rotary shaker at 30 min^{-1} at room temperature. The leaching time was varied from 30 to 270 min, incrementally varying by 30 min. The phase ratio is adjusted to vary from 5 to 30 mL g^{-1}. The acid concentration for leaching was varied from 0.1 to 3 $molL^{-1}$. Immediately after leaching, the leach mixture was transferred to 50 mL polypropylene centrifuge tubes and centrifuged at 5000 min^{-1} for 6 min using a DM0636 centrifuge (DLAB Scientific, China). The centrifuged supernatant was then filtered through a 1 µm polytetrafluoroethylene syringe filter (FINETECH, Taiwan) to obtain the leaching liquid, which was then analyzed for its composition and element contents.

In order to study the subsequent steps of the P recovery process, such as precipitation, the leaching was as shown in Fig. 6-3. In this case, P leaching was carried out in a 1L glass beaker. The sample mixture was mixed using a Jartest stirrer (OVAN-JT40E, Spain) at 100 min^{-1} under laboratory room temperature. After 60 min of leaching, the liquid-solid mixture was transferred to 50 mL polypropylene centrifuge tubes for centrifugation at 5000 min^{-1} for 6 min. Immediately after that, a vacuum filtration device

was used to separate the leach solution and the residue solid through a 100 µm polypropylene filter fabric.

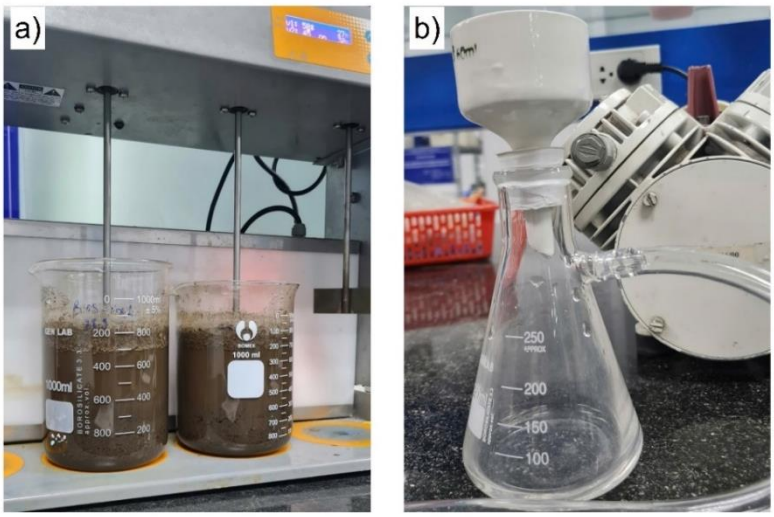

Fig. 6-3: Large-volume leaching in 1 L beaker (a) and vacuum filter equipment (b)

The degree of P leaching or metals leaching η_L was calculated by the formula

$$\eta_L = \frac{C_e L}{C_{e,0}} \quad (6\text{–}1)$$

where, C_e is the dissolved element concentration in leach liquid, L is the leach liquid volume and $C_{e,0}$ is the element concentration in the dried sludge.

6.2.2 First Precipitation

The leached liquid from BIOS and CHES was subjected to precipitation to gradually remove the unwanted Ca and Fe, which stayed in the solution while the Al-P precipitate is the expected primary product in the P-recovery process. The selective precipitation was performed by using NaOH solution to adjust the equilibrium pH of the leached liquid. The precipitation experiment was performed in a 200 mL glass beaker at room temperature in the laboratory. The room temperature varied from 29°C to 34°C. The leached liquid was filled into the glass beaker and then NaOH solution was slowly added to reach the desired equilibrium pH. During the pH adjustment process, the mixture was stirred with a stirrer (OVAN-JT40E, Spain) at a speed of 100 min^{-1}. The precipitation was assumed to be completed 60 min after reaching the equilibrium pH. Then, the liquid-precipitate mixture was transferred to 50 mL polypropylene centrifuge

tubes for centrifugation at 4000 min^{-1} for 10 min. A typical liquid-solid mixture before and after centrifugation is shown in Fig. 6-4.

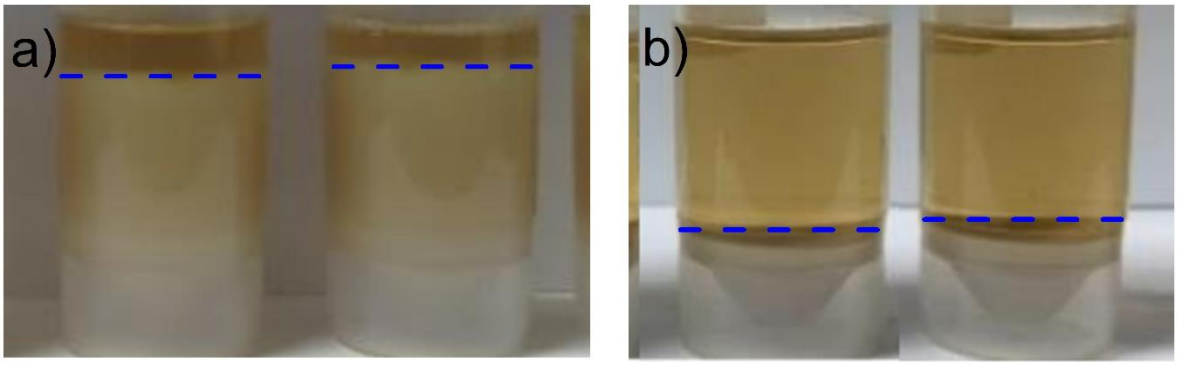

Fig. 6-4: Liquid-solid mixture before centrifugation (a) and after centrifugation (b)

Immediately after centrifugation, the liquid in the centrifuge tube was collected using a 1 µm polytetrafluoroethylene syringe filter (FINETECH, Taiwan). The liquid was separated from fine solids and then acidified with 30% HNO_3 solution with the equivalent volume to prevent any further precipitation. The P and remaining dissolved metals concentrations in the filtered liquid were analyzed by using ICP-OES to determine the degree of precipitation. The degree of precipitation η_P is calculated by

$$\eta_P = 1 - \frac{C_{e,\mathrm{a}} V_\mathrm{a}}{C_e V_\mathrm{b}}, \qquad (6\text{–}2)$$

where, $C_{e,\mathrm{a}}$ is the element concentration in liquid after precipitation, V_a is the liquid volume after precipitation. V_a is the total volume of liquid obtained after the liquid-solid phase separation and the volume in wet precipitates, which is quantified after drying the precipitate. The volume of leach liquid used for precipitation is V_b.

6.2.3 Dissolution

The precipitate obtained from the precipitation stage is mainly Al-P compounds as well as other compounds of metals such as $Fe(OH)_3$, $Al(OH)_3$. To recover dissolved P and remove metal impurities, the precipitate was dissolved again at a selected equilibrium pH using NaOH solution. The efficiency of P dissolution was studied at equilibrium pHs varying from 7 to 14. 1 g of dried precipitate was placed into a 200 mL glass beaker. 100 mL of NaOH solution were then added with the corresponding initial pH. Then, 0.5M NaOH solution was added to adjust the mixture to the desired equilibrium pH. A MaXtir-TM MS500 magnetic stirrer (Daihan Science, Korea) was used to stir the

mixture at 150 min^{-1} for 30 min at room temperature. The solid-liquid mixture was centrifuged using a DM0636 centrifuge (DLAB Scientific, China) before being phase-separated by vacuum filtration using 100 µm polypropylene (PP) filter fabric. The P dissolution degree η_d was calculated according to the formula

$$\eta_d = \frac{C_{e,\mathrm{d}} V_\mathrm{d}}{C_{p,e}}, \qquad (6\text{–}3)$$

where, $C_{e,\mathrm{d}}$ is dissolved element concentration in liquid after dissolution, V_d is the liquid volume obtained after dissolution, the element content in the dried precipitate is $C_{p,\mathrm{e}}$. $C_{p,\mathrm{e}}$ is calculated after the digestion of the dried precipitate after washing by aqua regia and measurement concentration of the element by ICP-OES.

6.2.4 Final Product Precipitation

The experimental setup for precipitation at varied equilibrium pH is shown in detail in Fig. 6-5. The dissolved P in the liquid obtained from the previous dissolution step was recovered as a salt precipitate with Ca^{2+} ions at equilibrium pH to form the final Ca-P product. Ca^{2+} ions were added using $Ca(OH)_2$ or $CaCl_2$ solution. For the precipitation at a selected equilibrium pH lower than the pH of the dissolution liquid (pH_e X), 1N HCl and $CaCl_2$ were used to adjust the pH. In the opposite case, $Ca(OH)_2$ or $CaCl_2$ and 1N NaOH were added. The equilibrium pH for final precipitation was varied from 6 to 14.

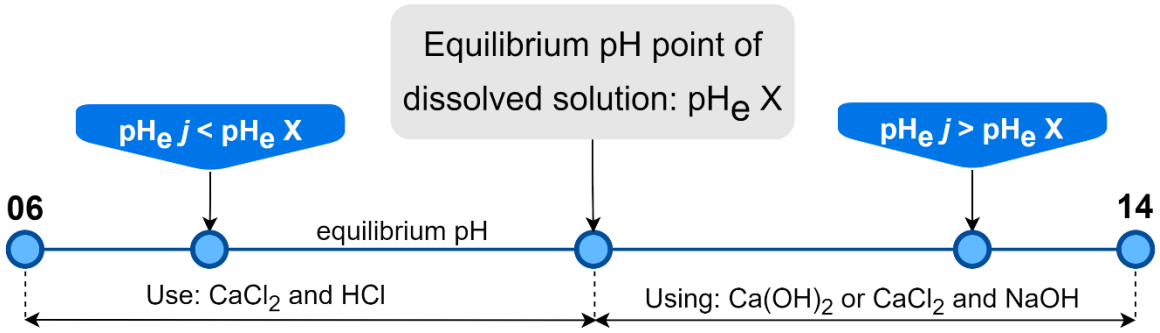

Fig. 6-5: Experimental procedure to reach the desired pH for the final precipitation step

The precipitation experiment was carried out in a 100 mL glass beaker, the reaction mixture was stirred with a stirrer (OVAN-JT40E, Spain) at 100 min^{-1} and room temperature. After 60 min of reaction at equilibrium pH, the liquid-precipitate mixture was transferred to a 50 mL PP centrifuge tube for centrifugation at 5000 min^{-1} for 10 min

using a DM0636 centrifuge (DLAB Scientific, China). Next, liquid-solid separation was performed using a 1 µm polytetrafluoroethylene syringe filter (FINETECH, Taiwan). The resulting solid precipitate was dried after washing for composition analysis, and the separated liquid and fine solid were used for analysis of the remaining dissolved element concentration.

6.3 Validation of Simulation Tool

The SLLE simulation tool used was developed in Matlab by Shariff (Shariff et al., 2023). The simulation results from the developed SLLE tool have been validated and experimentally studied for application in the development of the P-recovery process from dried sewage sludge (Shariff et al., 2023). In this study, the simulation tool has been updated to add SO_4^{-2} species to suit the leaching simulation using H_2SO_4 solution. The SLLE simulation results were compared with the Aqion tool, which is a currently commercialized hydrochemistry software tool (Aqion, 2024). The reference Aqion tool is a developed product for application in chemical equilibrium simulation. It is especially suitable for the simulation of inorganic reactions.

To validate the developed SLLE tool, its simulation results were compared with those obtained from the Aqion tool under the same input conditions. The input species concentrations used for simulation were C_{Na^+} = $C_{Ca^{2+}}$ = 0.1 molL^{-1}, $C_{PO_4^{3-}}$ = 0.3 molL^{-1} while $C_{SO_4^{2-}}$ was varied from 0.1 to 1.5 molL^{-1}. The results of the chemical equilibrium simulations from two simulation tools are compared in Fig. 6-6. The results of both simulation tools showed a high degree of similarity, especially for the formation of soluble P compounds such as $H_2PO_4^-$ and H_3PO_4. There is nevertheless a slight difference in the simulation results between the two tools. Part of the reason for this discrepancy are differences in the thermodynamic reaction constants introduced into each simulation tool. In addition, the Aqion tool still has certain limitations, such as an incomplete mineral database, which may cause certain limitations for simulation in more complex studies. For example, the Aqion tool did not show the NaH_2PO_4 precipitate, while the developed SLLE simulation tool indicated it very clearly. A comparison of the simulation results of the two tools shows that the developed SLLE simulation tool has at least the same accuracy as the Aqion tool. In addition, the limitations of the Aqion tool on the mineral database are advoided in the developed SLLE simulation tool to handle more complex reactions

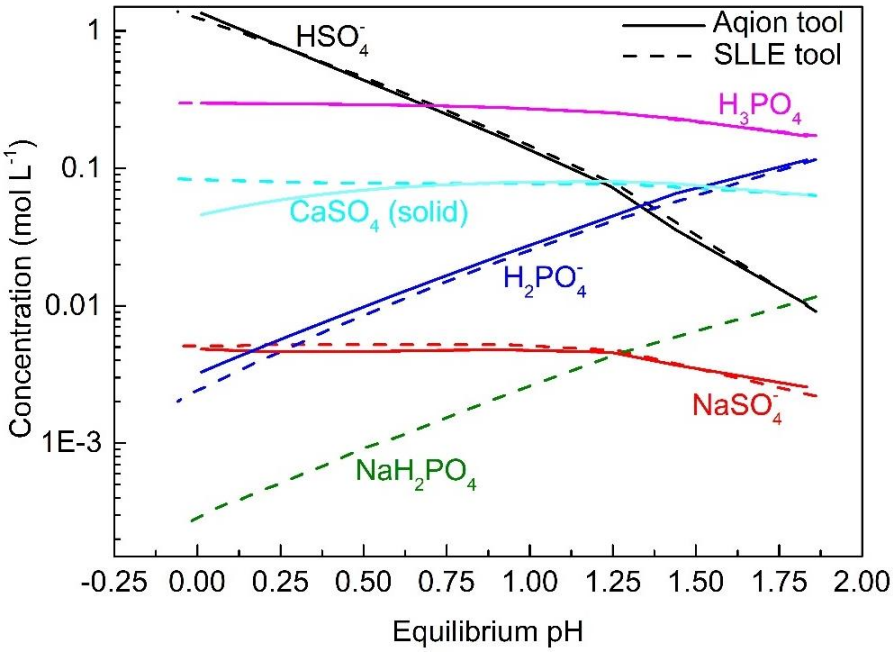

Fig. 6-6: Comparison of primary chemical equilibrium simulation results

6.4 Results and Discussion

The experimental results for the development of the P-recovery process from RWWTP sludge are presented in the order corresponding to each stage of the P-recovery process. In addition, the simulation results from the developed SLLE tool were used to optimize the conditions and operating parameters of the P-recovery process.

6.4.1 Input Dried Sludge Compositions

The chemical fractions of phosphorus from CHES and BIOS, such as inorganic phosphorus, and organic phosphorus, were determined, where total phosphorus (TP) is the sum of IP and OP (García-Albacete et al., 2012; González Medeiros et al., 2005; Ruban et al., 1999). The concentrations of these and other components are presented in Tab. 6-1. CHES and BIOS contained approximately 93% and 76% IP, respectively. The observed difference in P fractions between the two sludge types primarily results from the phosphorus removal methods employed during wastewater treatment. Tab. 6-1 shows that phosphorus, calcium, aluminum were the elements with the highest mass fractions in both sludge types. The high aluminum content in CHES can be attributed to the use of poly-aluminum chloride for phosphorus precipitation and adsorption during the chemical treatment stage at the wastewater-treatment plant, leading to the formation of Al–P salts (Hwang & Cheon, 2009; Toor et al., 2019), as well as

$Al(OH)_3$ formed during adsorption (Gon Kim et al., 2002; Hwang & Cheon, 2009; Toor et al., 2019). Hydrated lime, $Ca(OH)_2$, was used to adjust the pH and remove phosphorus by forming Ca–P salts during the wastewater treatment process (Pengthamkeerati et al., 2008; Rietra et al., 2001; Yan et al., 2007), contributing to the high concentrations of both Ca and P in CHES as well as BIOS.

Tab. 6-1: Input dried sludge composition

Element		Concentration, $C_{e,0}$	
		mg g^{-1} dried sludge	
		CHES	BIOS
P		54.60 to 63.00	42.70 to 48.23
of which	OP	3.82 to 4.41	10.25 to 11.58
	IP	50.78 to 58.59	32.45 to 36.65
Al		100.40 to 129.30	16.53 to 20.97
Ca		28.80 to 36.80	26.43 to 30.57
Fe		4.60 to 19.50	8.44 to 12.92
Mn		0.30 to 0.50	0.57 to 0.63
Zn		1.30 to 1.60	1.17 to 1.73
K		5.80 to 11.30	7.40 to 9.35
Cu		0.125 to 0.164	0.083 to 0.196
Cr		0.155 to 0.189	0.010 to 0.019
Cd		7×10^{-4} to 10^{-3}	BDL
Pb		0.030 to 0.040	BDL

BDL: below detection level

The concentrations of heavy metals, such as copper, chromium, cadmium, and lead, were generally higher in CHES compared to BIOS. In particular, the Cr content in CHES was nearly 12 times higher than in BIOS. However, the concentrations of Cu, Cd, and Pb relative to phosphorus content in both CHES and BIOS were lower than the maximum allowable limits for fertilizers as specified by quality standards in Vietnam and Europe (EU, 2019; MARD, 2019b) as shown in Chapter 4.

6.4.2 Leaching

For the recovery of P from CHES and BIOS, P is first dissolved. The efficiency of P leaching affects the overall P recovery efficiency as well as the cost of energy, water, and chemicals used for successive steps. The COT has been utilized to evaluate HNO_3, HCl, and H_2SO_4 to determine the most suitable leaching agent, as shown in Fig. 6-7. The criteria evaluated for selecting the leaching agent are leaching efficiency, impurity co-solubility, and market price. Leaching efficiency and impurity co-solubility in the leach liquid affect the efficiency and complexity of the entire P-recovery process. The market price of the leaching agents directly affects the operating cost of the technical process. Developing a P-recovery process that meets the goals of simplicity, efficiency, and lowest operating costs will be suitable for the application conditions in Vietnam.

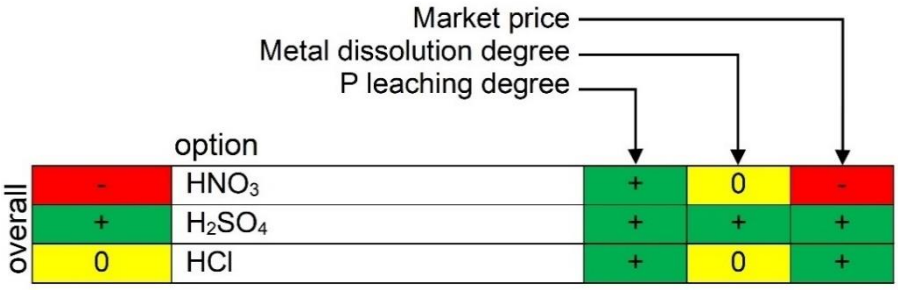

Fig. 6-7: The cascaded option-tree for leaching agent

The leaching efficiencies for P, Al, Fe, and Ca in CHES and BIOS for the three acids investigated are shown in Fig. 6-8. At identical conditions, the P leaching efficiency in BIOS is higher at 89% compared to 77% in CHES but is essentially independent of the acid used in both cases. All three leaching agents have shown high P leaching degree. Therefore, all three are considered to be suitable for the criterion of P leaching degree and then positively evaluated in the COT.

The efficiency of Ca leaching using H_2SO_4 is much lower than that by using HCl and HNO_3 for CHES as well as BIOS. This is induced by gypsum ($CaSO_4$) formation with H_2SO_4 (Donatello, Freeman-Pask, et al., 2010; Ottosen et al., 2013). The higher dissolved Ca content in the leached liquid obtained with HCl and HNO_3 limits the ability to separate impurities in the subsequent selective precipitation step. Therefore, it is advantageous to minimize dissolved Ca leading to a positive evaluation in the COT of

only H_2SO_4. In addition, the price of H_2SO_4 and HCl is lower compared to that of HNO_3 (Houssaine Moutiy et al., 2020; Levlin & Hultman, 2004; VINACHEM, 2024), as shown in Appendix Tab. A 9-1. The price of HNO_3 is especially high, leading to a negative evaluation in the COT.

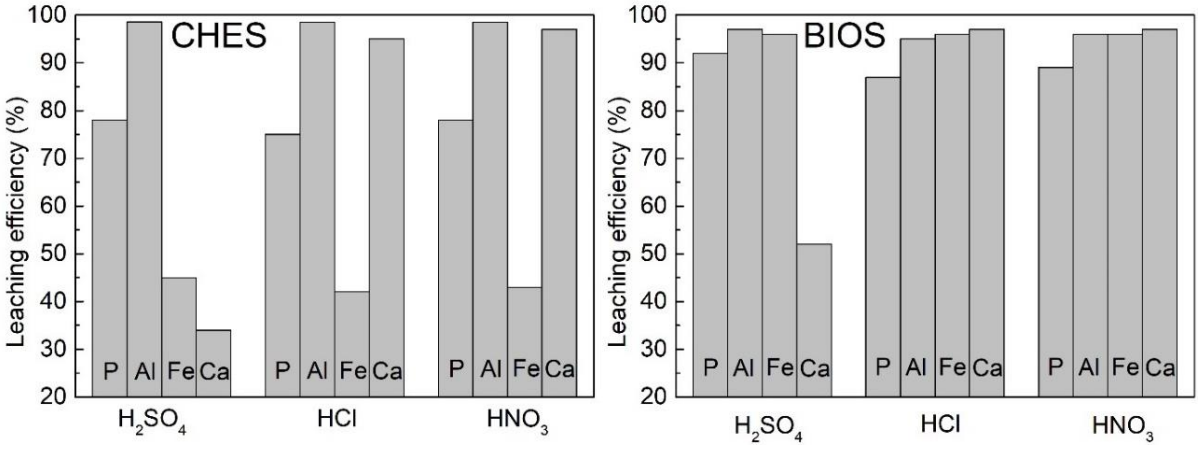

Fig. 6-8: Leaching efficiency of P, Al, Ca and Fe with different 1M acids at phase ratio 20 mL g^{-1} for CHES and BIOS

Overall, the completed COT shows that H_2SO_4 is the most suitable acid for the leaching of P in CHES and BIOS.

Leaching time and particle size

In a next step, the optimization of the leaching with H_2SO_4 was carried out through the variation of leaching conditions such as sludge particle size, leaching time and acid concentration, the liquid-solid phase ratio, both of which affect equilibrium pH. Since phase ratio and acid concentration both affect pH, which is the relevant leaching parameter, both parameters are first individually varied in the experiment. The optimum is then chosen based on the simulations. Leaching time and particle size have been varied using 1M H_2SO_4 and a phase ratio of 20 mL g^{-1}. The P, Al, Ca, and Fe leaching efficiencies were analyzed and shown in Fig. 6-9 and Fig. **6-10**. Maximum P leaching efficiency can be reached for CHES and BIOS already after 60 to 90 min, especially for smaller particle sizes. Leaching times exceeding 180 min show that the P leaching efficiency tends to decrease slightly, possibly due to the onset of chemical reactions that re-precipitate to create P mineral compounds (Stark et al., 2006).

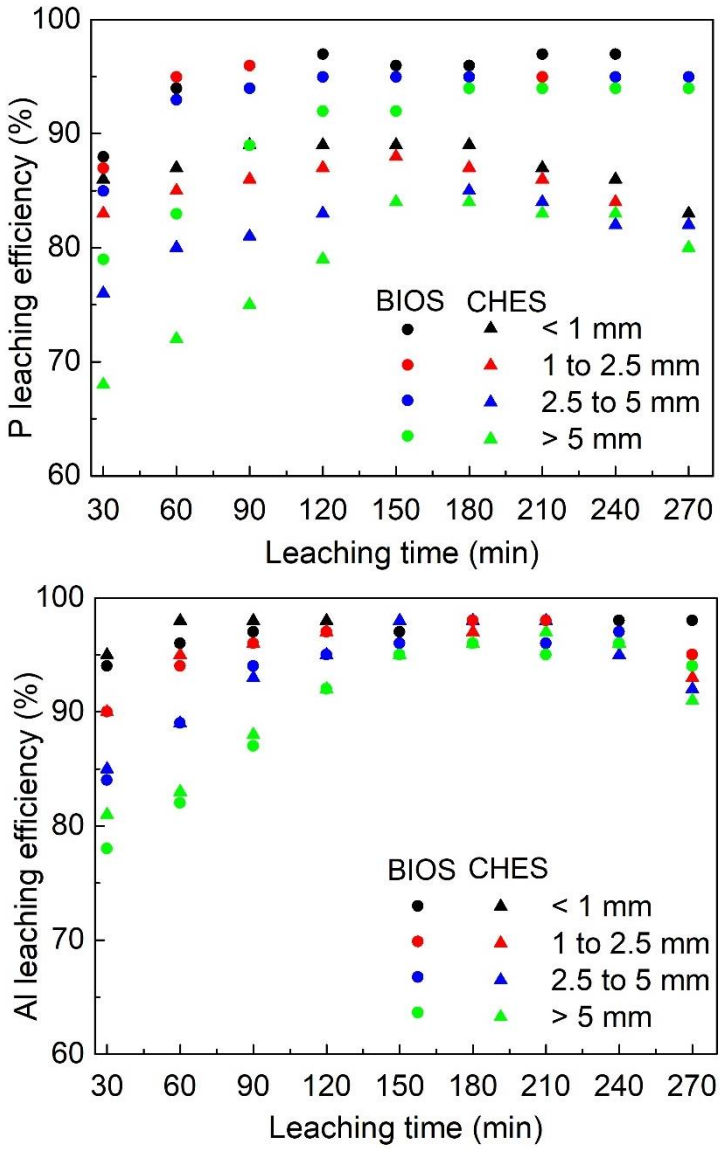

Fig. 6-9: The leaching efficiency at varying leaching times and input dried particle sizes of P and Al.

P leaching efficiency decreases as sludge particle size increases, especially at short leaching times from 30 to 60 min, but the difference between particles < 1 mm and 1 to 2.5 mm is significantly less than compared to larger particles. At a leaching time of 60 and 90 min, P leaching efficiency for particles below 2.5 mm reached a maximum of over 92% for BIOS and 85% for CHES, respectively. Thus, in the proposed process, leaching time can remain below 90 min and particle size should be below 2.5 mm. This result is consistent with previous studies by Ali & Kim (2016).

Already, after 30 min, more than 90% of the Al is leached in both types of sludge with a particle size of less than 2.5 mm. There is no significant difference in Al leaching

efficiency in CHES and BIOS under the same leaching conditions. Thus, Al will always be co-leached to a large fraction under conditions where P is efficiently leached.

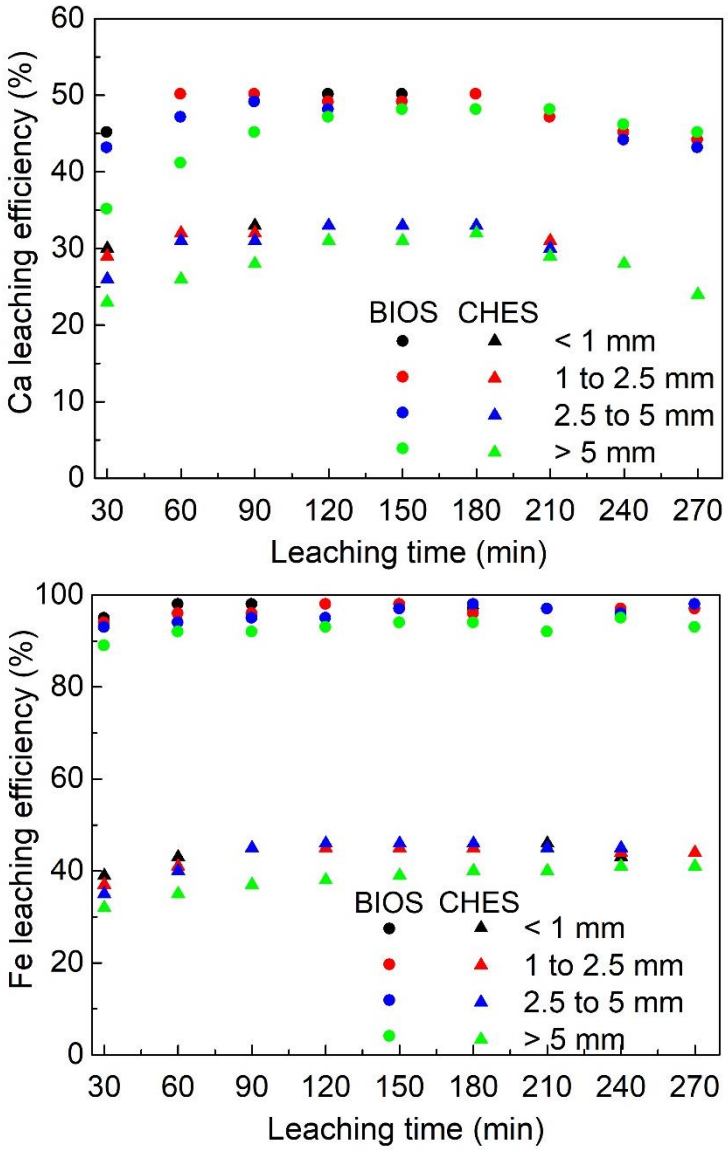

Fig. 6-10: The leaching efficiency at varying leaching times and input dried particle sizes of Ca and Fe.

As already shown in Figs. 8-6 and 6-10, there is a significant difference in the Ca and Fe leaching efficiency between CHES and BIOS. Beyond 60 min of leaching time, the leaching efficiency of Ca and Fe varies only a little, almost independent of particle size. Thus, also the fraction of Ca and Fe leached cannot be avoided at conditions suitable for P leaching. Thus, a sludge particle size between 1 and 2.5 mm and leaching times between 60 and 90 min are the optimal P leaching conditions for both, BIOS and

CHES. At these conditions, co-leaching of metals such as Al, Fe, and Ca cannot be avoided, which makes further separation steps necessary.

Phase ratio and leaching time

The phase ratio in leaching defines the water and acid consumption and thus needs to be optimized as well. The water consumed increases as the phase ratio increases, which reduces the attractiveness of the P-recovery process by increasing recovery costs (Semerci et al., 2021). Using 1M H_2SO_4 for leaching, the phase ratio was varied between 5 mL g^{-1} and 30 mL g^{-1}, and the leaching time between 60 and 180 min. CHES and BIOS particles between 1 mm and 2.5 mm were used. The experimental results on P leaching efficiency for CHES and BIOS are shown in Fig. 6-11. The dependence of Al, Ca, and Fe leaching efficiency on leaching time and phase ratio are also shown in Figs. 6-12 and 6-13, respectively. One major result shown in Fig. 6-11 is that the P leaching efficiency is not significantly influenced by leaching times. This applies to the leaching of Al, Ca, and Fe as well. Therefore, 60 min is the most suitable leaching time.

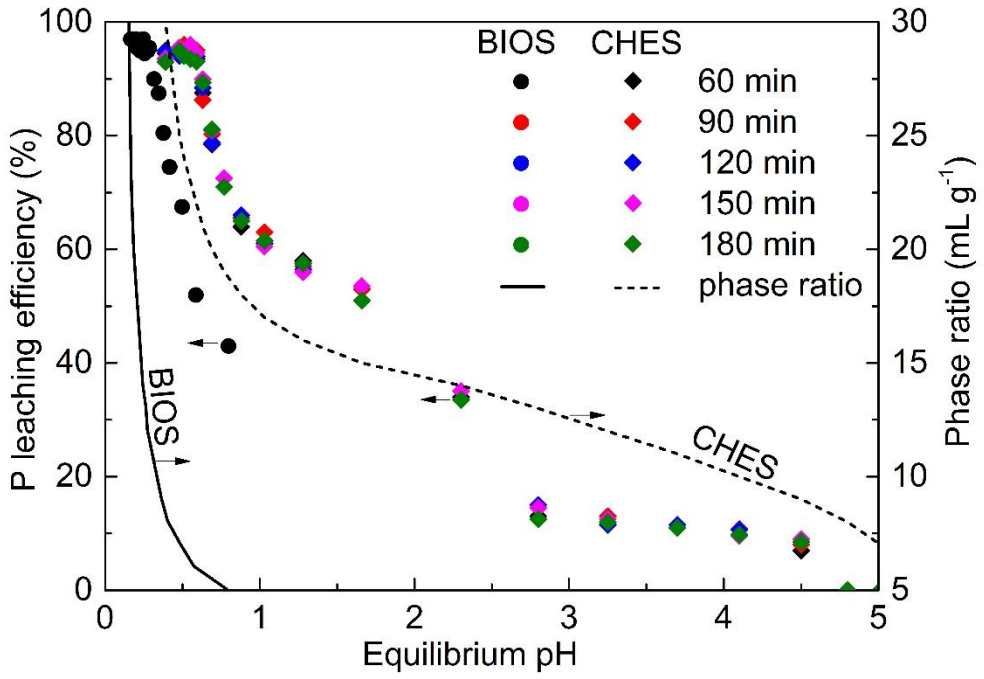

Fig. 6-11: Dependence of P leaching efficiency on leaching time and phase ratio

P leaching efficiency shows a very clear difference between the leaching of CHES and BIOS. The lowest P leaching efficiency for BIOS is about 43% at phase ratio 5. At the same phase ratio, the P leaching efficiency is less than 10% at the same phase ratio for CHES. An increase in phase ratio leads to a decrease in equilibrium pH and

correspondingly to an increase in P leaching efficiency. For CHES, P leaching efficiencies of over 95% were reached at phase ratios greater than 23, at equilibrium pH below 0.55, and for BIOS, a phase ratio above 12 with an equilibrium pH below 0.28.

As mentioned above, under conditions of high P-leaching efficiencies, Al is leached at least with 95% efficiency for both CHES and BIOS. Especially for BIOS, at all phase ratios and leaching times, most of the equilibrium pH was recorded to be below 1, and the Al leaching efficiency above 95%. For CHES, above a pH of 3, a very different behavior is observed for Al, which is much less efficiently leached, and its leaching efficiency decreases rapidly further as pH increases.

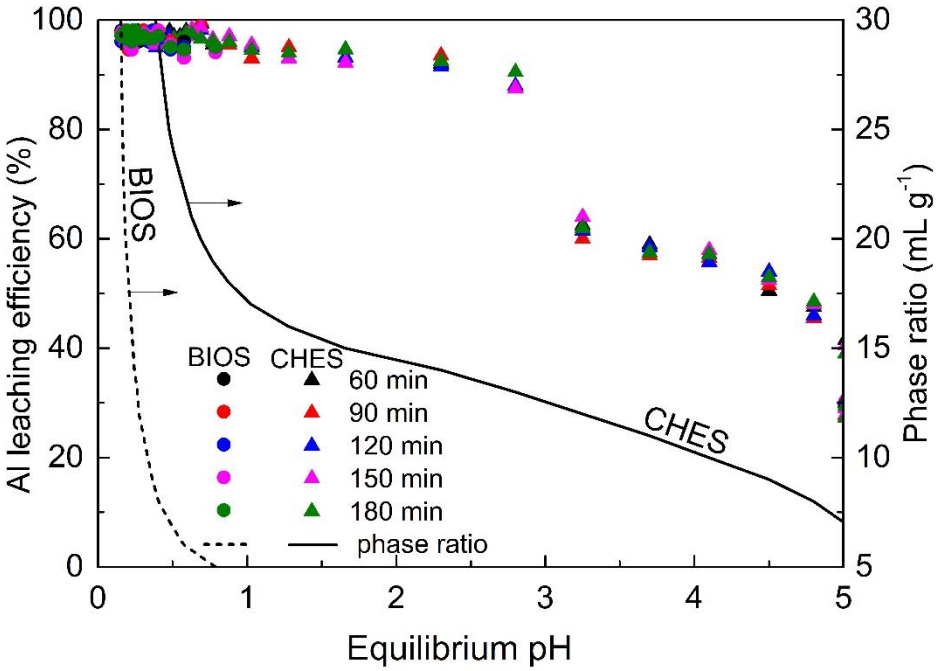

Fig. 6-12: Dependence of Al leaching efficiency on leaching time and phase ratio

Since, performing leaching at such high pH shows a significant decrease in P leaching efficiency, an equilibrium pH > 3 is not a suitable parameter for P leaching even though the co-Al leaching would be reduced.

The Ca and Fe leaching efficiencies in BIOS and CHES tend to increase as the phase ratio is increased and equilibrium pH is decreased. Again, Ca and Fe leaching develop similar to P-leaching, so that their co-leaching cannot be avoided in an efficient P-recovery process.

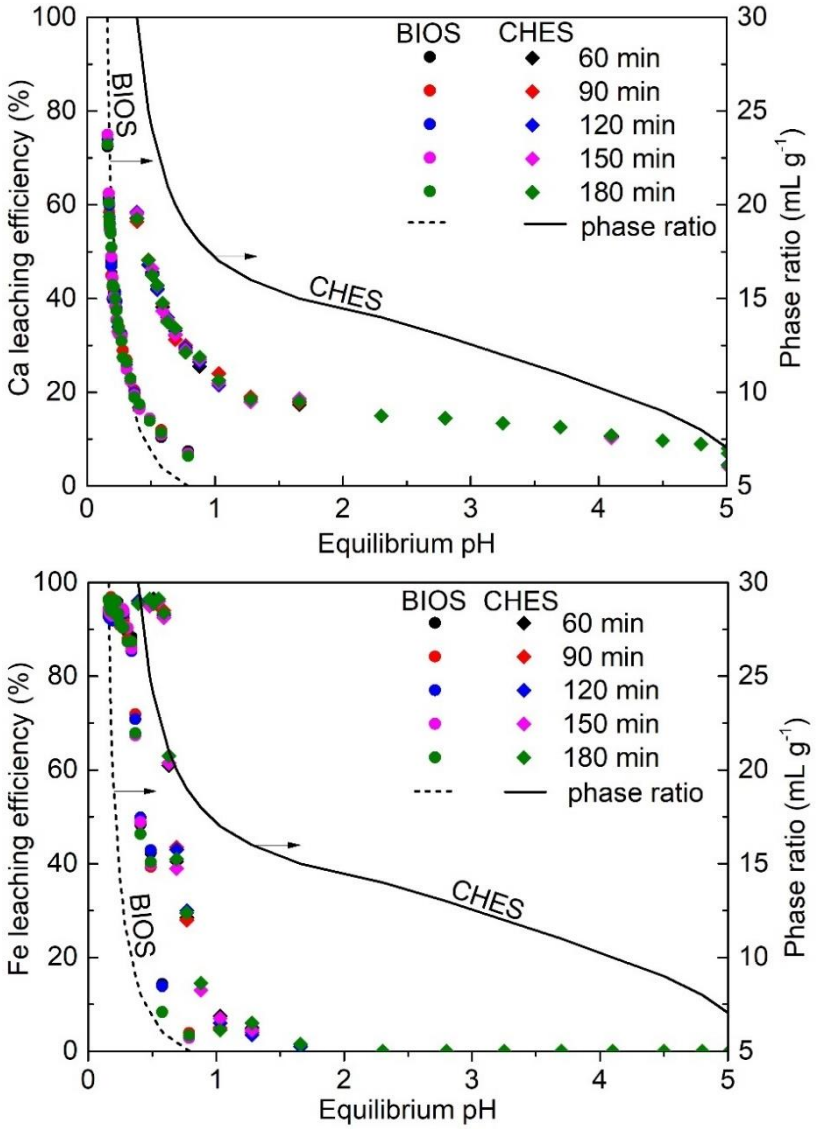

Fig. 6-13: Dependence of Ca, Fe leaching efficiency on leaching time and phase ratio

Simulation with the SLLE tool based on input conditions at different phase ratios is performed for both CHES and BIOS to understand the trends of P and metals when leached with H_2SO_4. Fig. 6-14 shows precipitation results for CHES and BIOS, which indicate the possibility of precipitates formed during the leaching process. Simulation results show that not only Al compounds such as $Al(OH)_3$ and $AlPO_4$ are formed but also Fe compounds and Ca compounds. Similar results on Al-P precipitation, especially for pH ≥ 4 were reported by Truong et al. (2021). The $AlPO_4$ precipitate starts to be formed above equilibrium pH of 2.7 for CHES, which reduces the Al as well as the soluble P content in the leaching solution (Gon Kim et al., 2002; Hwang & Cheon, 2009; Toor et al., 2019).

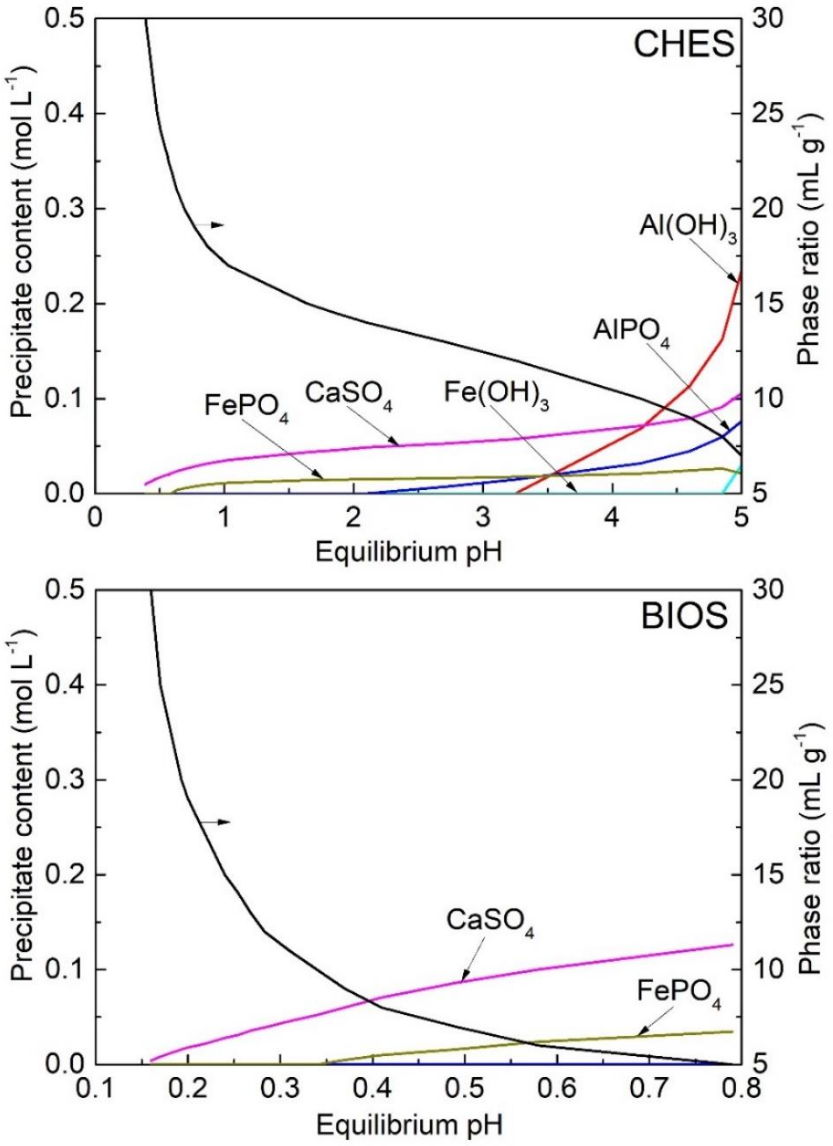

Fig. 6-14: Simulation of precipitated with 1M H_2SO_4 at varying phase ratios

The results from SLLE simulations show that the gypsum precipitation gradually increases as equilibrium pH increases, leading to a decrease in dissolved Ca. The lower the phase ratio, the higher the fraction of gypsum precipitate. The formation of $FePO_4$ precipitate, as shown in Fig. 6-14, reduces the dissolved Fe content in the leach liquor, but $FePO_4$ precipitate formed at high pH also reduces the P leaching efficiency.

The strong influence of phase ratio on P leaching efficiency shown here has also been noted by some published studies (Donatello et al., 2010; Semerci et al., 2021; Shiba & Ntuli, 2017). The higher the phase ratio, the better the P leaching achieved. However, increasing the phase ratio also leads to an increase in amount of chemicals and water consumed as well as equipment size. Thus, a small phase ratio is actually desired.

Acid concentration

From the above leaching study results, it has been realized that equilibrium pH is a major influencing parameter for the leaching, as expected. There, equilibrium pH was varied by varying phase ratios for a given molarity of acid. Alternatively, equilibrium pH can be varied by changing acid concentration for a given phase ratio. Additionally, increasing the H_2SO_4 concentration can favorably influence the P-leaching efficiency (Biswas et al., 2009; Liu & Qu, 2016; Naoum et al., 2001). Fig. 6-15 shows the leaching efficiency of P, Ca, Al, and Fe at different H_2SO_4 concentrations at phase ratio of 20. The dissolved P content in leach liquid increases with increasing H_2SO_4 concentration and decreasing pH.

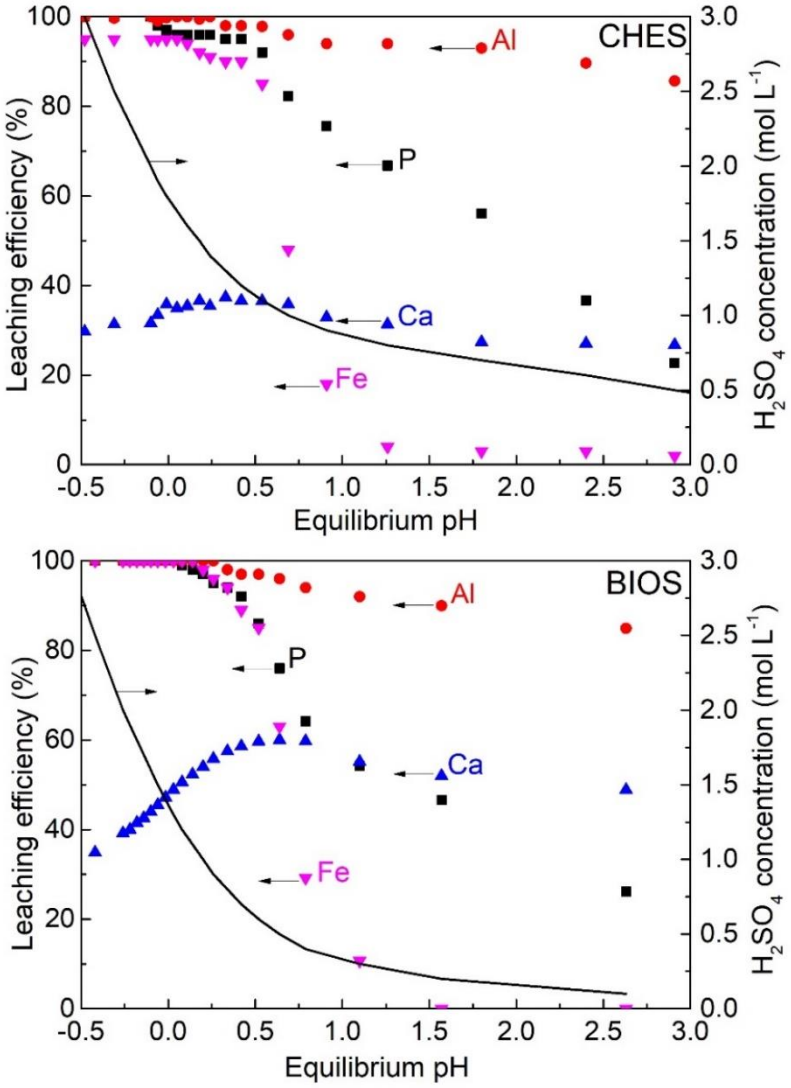

Fig. 6-15: Leaching efficiency of P, Al, Ca, and Fe at different H_2SO_4 concentrations, a phase ratio of 20 mL g^{-1}

In the pH range of 0.5 to 2.5, P leaching is slightly worse for BIOS than for CHES. At lower pH, i.e. for H_2SO_4 concentrations above 1 mol L^{-1}, the difference in P leaching efficiency from CHES and BIOS is negligible. Both are greater than 90%. Liang et al. (2019) reported similar trends in P leaching efficiency from sewage sludge under different H_2SO_4 concentrations. The trends for Al and Fe leaching efficiencies depend essentially identically on pH for both types of sludge as well. A significant difference between CHES and BIOS can only be observed for Ca leaching. Around a pH of 0.5, a maximum in Ca leaching is observed, which is around 60% for BIOS and 35% for CHES. For lower pH, especially for BIOS, the Ca-leaching efficiency decreases significantly.

In general, the leaching results showed that varying phase ratios and H_2SO_4 concentrations affected the value of equilibrium pH, the leaching efficiency of P, and the metals dissolved in the leaching liquid. The general trend was that increasing the phase ratio and the H_2SO_4 concentration increases the leaching efficiency of P.

SLLE simulation and experiment validation of optimal leaching parameters

It is obvious that equilibrium pH is a decisive parameter, which can be varied by phase ratio as well as initial acid concentration. Both parameters need to be varied simultaneously for process optimization. This variation has been realized by simulation with the SLLE tool.

Fig. 6-16 shows how P leaching efficiency and the amount of H_2SO_4, which are decisive parameters for judging the economic feasibility of the leaching, depend on the phase ratio and H_2SO_4 concentration for CHES and BIOS. It is obvious that lines of constant P leaching efficiency and the amount of H_2SO_4 used show a rather similar behavior. Nevertheless, from a given P leaching efficiency decreasing the phase ratio but increasing H_2SO_4 concentration leads to a certain reduction in the amount of H_2SO_4 required due to the slightly different slope of the iso-lines of P leaching efficiency and amount of H_2SO_4 used. It is thus beneficial to reduce the phase ratio. At the same time, this reduces the amount of water required and equipment size. The amount of H_2SO_4 used to leach more than 95% P in 1 kg of dry CHES is about 20 mol and 8.5 mol for BIOS.

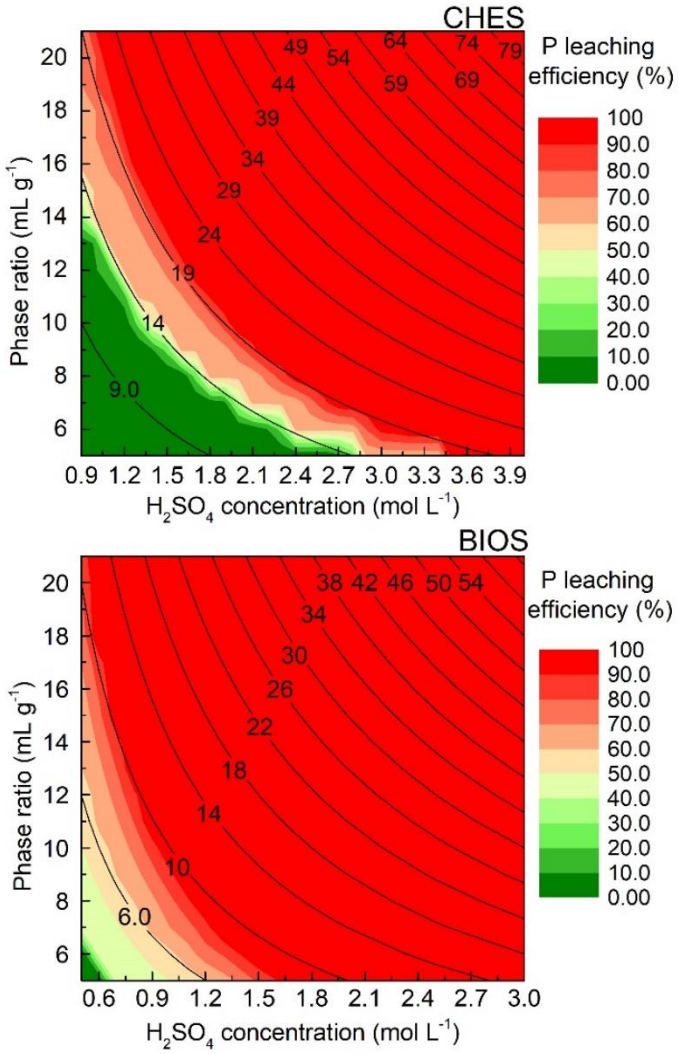

Fig. 6-16: Simulation results on the dependence of P leaching efficiency and the amount of H_2SO_4 on phase ratio and H_2SO_4 concentration used. The labeled iso-lines show the amount of H_2SO_4 required for leaching per kg dry sludge in mol kg^{-1}

On the other hand, performing leaching at too low a phase ratio limits the ability to filter and separate the leached liquor from the solid phase after leaching. The molar ratio of gypsum precipitate produced to input P from the SLLE simulation at different phase ratios and H_2SO_4 concentrations for CHES are shown in Fig. 6-17. This is especially critical due to the formation of gypsum precipitate, especially for sludges with high Ca content, i.e. for both BIOS, and especially for CHES. At lower phase ratios, the molar ratio of gypsum precipitate to input P is larger. This is a limitation when comparing the amount of P that can be recovered and the problems of phase separation filtration and by-product treatment caused by gypsum after leaching.

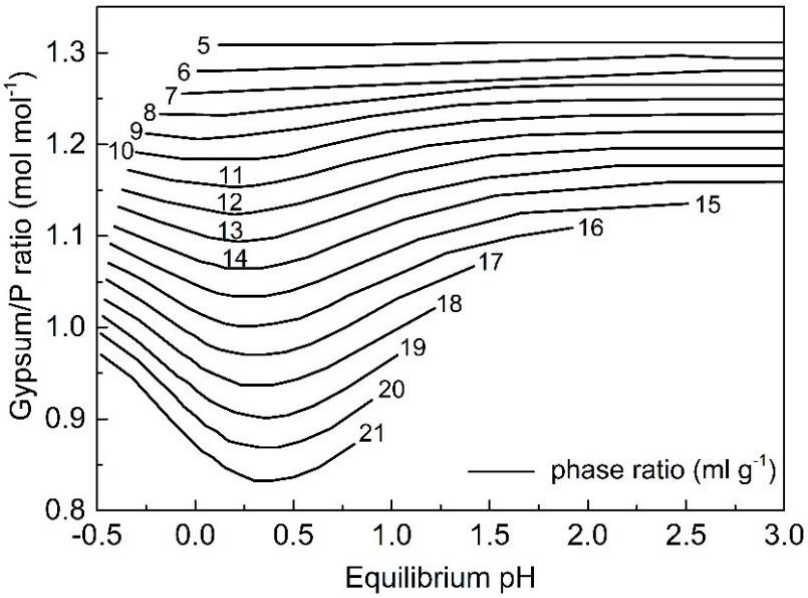

Fig. 6-17: The mol ratio of gypsum produced for CHES to input P according to simulation results at different phase ratios, and H_2SO_4 concentration from 0.9 to 3M

In addition, Fig. 6-18 shows the liquid-solid mixture after the experiment of P leaching from CHES at phase ratio 5 using 2M H_2SO_4. The mixture is like a slurry, including the remaining undissolved solids, gypsum precipitate, and leached liquid. This mixture is almost impossible to filter by gravity filtration. Therefore, applying P leaching at the lowest phase ratios investigated in the simulation is not feasible in practice

Fig. 6-18: The liquid-solid mixture as thick slurry after leaching at phase ratio 5 mL g^{-1}, 2M H_2SO_4 for CHES

To eliminate disadvantages such as difficulty in phase separation when leaching at a low phase ratio or excessive water use for leaching at a high phase ratio, the optimal choices for leaching P from CHES are a 2M H_2SO_4 and a phase ratio of 10 mL g^{-1}, and for BIOS are 1.7M H_2SO_4 and a phase ratio of 5 mL g^{-1}, leading to a P leaching efficiency of at least 90%. Validation experiments have been performed for these cases, as shown in Fig. 6-19, where the experimental data are compared to the simulations. Leaching experiments at the optimal conditions for BIOS and CHES show that Ca-leaching efficiency is very low, with only about 10% for BIOS and 15% for CHES. Most dissolved Ca reacts with SO_4^{2-} in the H_2SO_4 solution to form a gypsum precipitate. The data also show that the experiments match the values expected from the simulation. Also, this good agreement justifies using the simulation for optimization.

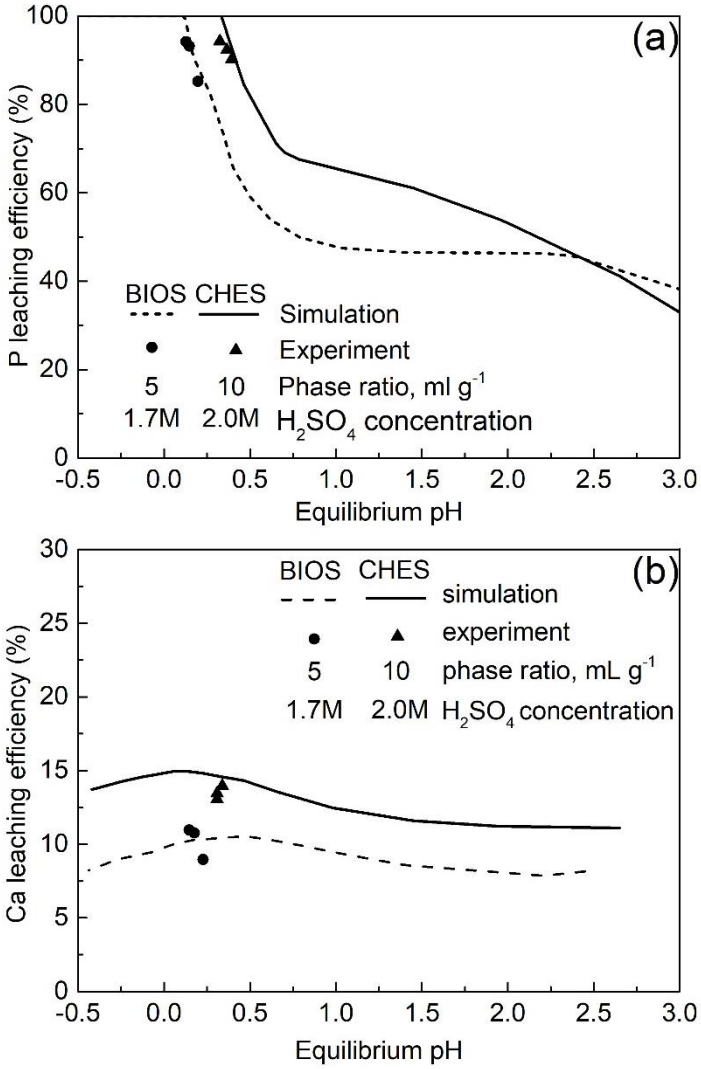

Fig. 6-19: Leaching efficiency of P (a) and Ca (b) from simulation and experiment at optimal parameters

Fig. 6-20 finally shows SEM images before and after P leaching in CHES and BIOS at optimum parameters. These images clearly show the increase of gypsum precipitate in the solid residue after leaching. The amount of gypsum precipitate formed increases the volume of solids that needs to be processed after the leaching. However, this also indicates that by using H_2SO_4 for leaching, the content of the unwanted Ca dissolved can be significantly reduced in leach liquid.

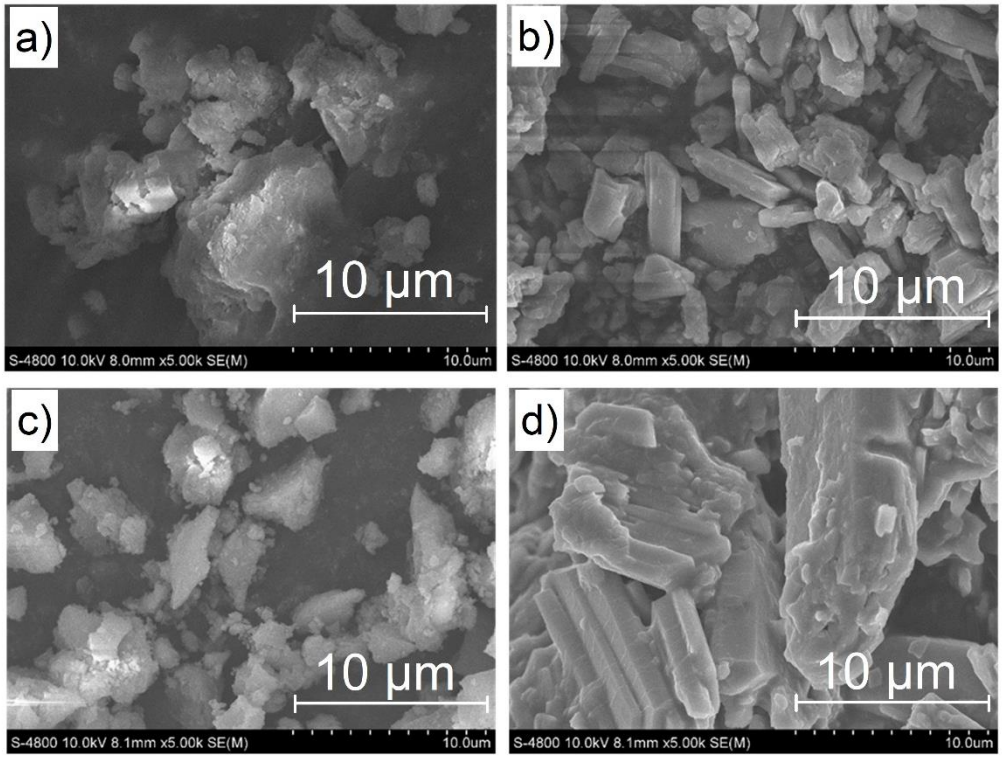

Fig. 6-20: SEM images of input dried sludge for (a) CHES and (c) BIOS as well as residue dried solid after leaching at optimal leaching parameters for (b) CHES and (d) BIOS

Conclusions

Summarizing the results of the experiment and simulation results for sludge leaching shows that the equilibrium simulations with the SLLE tool allow P leaching optimization with H_2SO_4 consistent with experimental lab results. Under optimal conditions, P leaching efficiency can reach above 95%. Al and Fe in both, CHES and BIOS, will always be co-leached. The equilibrium pH is the determining parameter as expected for the leaching of P, Al, Fe, and Ca. It also determines the precipitation of minerals. Ca precipitation is unavoidable if H_2SO_4 is applied to Ca-containing sludge. Gypsum

precipitation significantly reduces the dissolved Ca content in the leached liquid, which is the expected result. Therefore, gypsum precipitation formed in the leaching step is favorable for developing the next selective precipitation step. Unfortunately, gypsum precipitation significantly increases the volume of solid waste generated, which needs to be treated.

6.4.3 First Precipitation

The leached liquid obtained from CHES and BIOS contains dissolved P and other dissolved metals such as Al, Fe, and Ca. In the proposed process, selective precipitation method was chosen using a highly alkaline solution such as NaOH as a function of equilibrium pH, precipitation of impurities such as metals will differ due to the difference in saturation index and solubility product. Thus, impurities can be selectively removed after liquid-solid phase separation.

Experimental results

NaOH solution was used to react with leached liquids from the leaching step for BIOS and CHES until the desired equilibrium pH was reached. The stirring was continued for 60 min. The results presented in Fig. 6-21 for CHES and BIOS shows a very clear trend. At an equilibrium pH of less than 2, the degree of P precipitation is very low. In the pH range from 2 to 3.5, the degree of P precipitation increases strongly for both CHES and BIOS. The highest degree of P precipitations at equilibrium pH 5.5 are about 0.99 for CHES and about 0.92 for BIOS. The high degree of P precipitation is maintained up to about equilibrium pH 9. The degree of P precipitation tends to decrease sharply above a pH of 9. A comparison between CHES and BIOS shows that P in CHES has a slightly higher degree of precipitation than in BIOS. The decrease in the degree of P precipitation of CHES at equilibrium pH > 9 is also more substantial than that of BIOS. P in leached liquid can react with other metals such as Al, Fe, or Ca to form Metal-P precipitates. The decreasing trend of P and Al precipitation at equilibrium pH > 9 shows that Al-P precipitates do not form at high pH. Al is an amphoteric element. Therefore, Al^{3+} will precipitate to form $Al(OH)_3$, in principle, but at highly alkaline environments such as the equilibrium pH range of 11 to 13, $Al(OH)_3$ will not precipitate and will be re-dissolved.

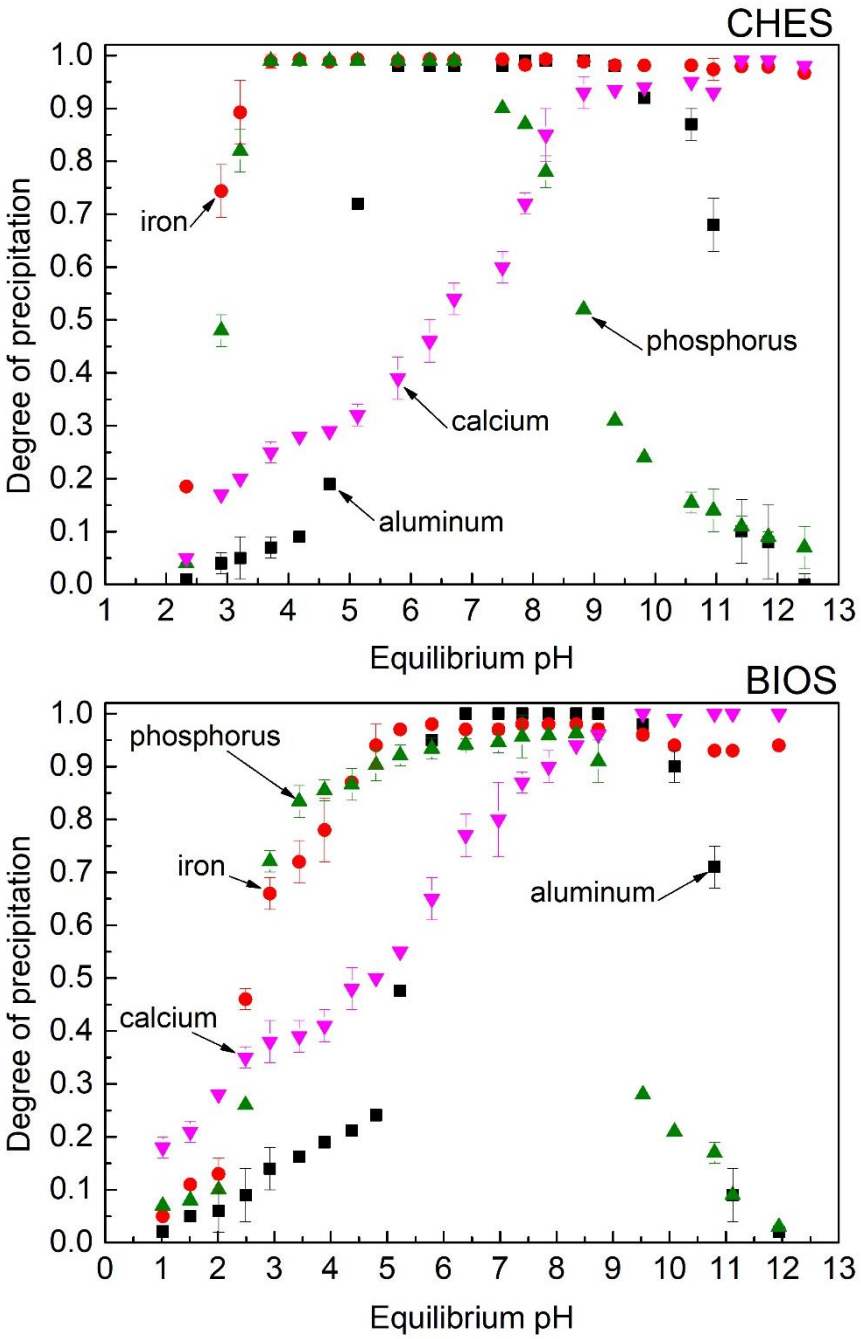

Fig. 6-21: Degree of precipitation of P and metals by using NaOH solution

The precipitation trends of Fe in CHES and BIOS are very similar. The highest degree of Fe precipitation can reach over 0.95 for both CHES and BIOS. Increasing the equilibrium pH > 10 does not show a decrease in the degree of Fe precipitation. Similar results are also recorded for Ca in both CHES and BIOS. But the degree of Ca precipitation increases less with increasing pH than that of P, Al and Fe. The removal efficiency of Ca is therefore higher than that of Al and Fe impurities after filter, especially at pH below 8.5.

SLLE simulation for precipitation

The results from the experiments clearly show the precipitation trends of P as well as metals at different pHs. To determine the trends of not only specific precipitates such as Al-P salts, Fe-P salts, $Al(OH)_3$ and $Fe(OH)_3$ but also for the total elemental content at each pH, the SLLE tool is applied to simulate the precipitation. In particular precipitated Al-P salts, are the desired products in the precipitation step. Simulation results of precipitates formed at different pH for P and primary metals are shown in Fig. 6-22. For CHES, at an equilibrium pH of less than 4.5, the simulations show that P precipitates with both Fe and Al to form Al-P and Fe-P salts. The precipitation at the range of equilibrium pH 4 to 5 shows an increase in Al-P salts and a decrease in Fe-P salts. At the same time, in that pH range, the dissolved Fe reacts with OH^- to form $Fe(OH)_3$. At pH above 5, the precipitates mainly $Al(OH)_3$, Al-P salts, and $Fe(OH)_3$. Similar trends are observed for BIOS.

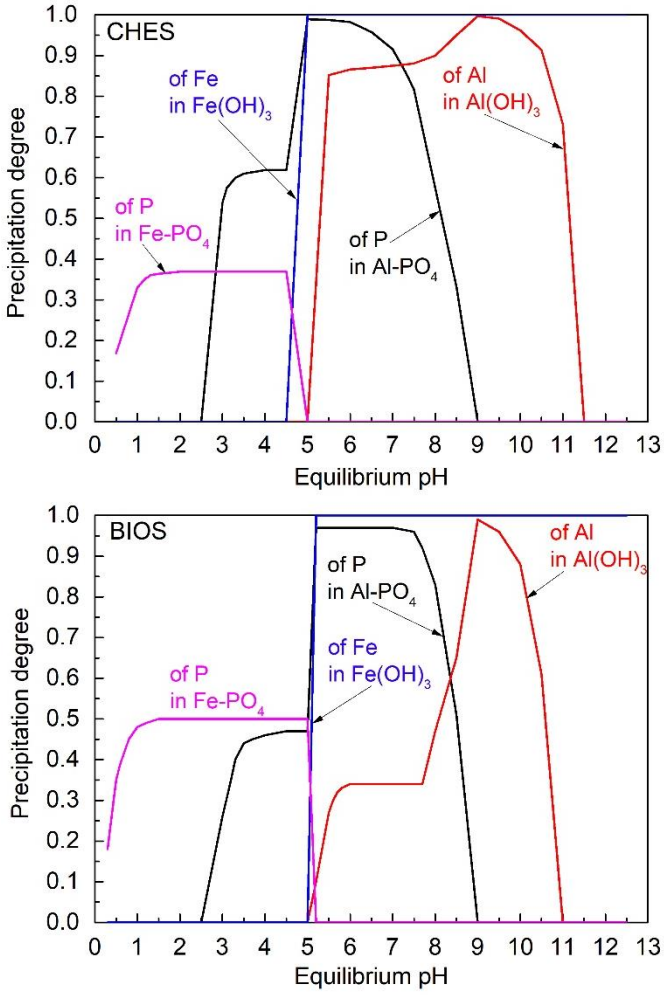

Fig. 6-22: Simulation on precipitation of P and metals at different equilibrium pH

The simulation results show that more than 90% of the P precipitates as Al-P salts at pH ≥ 5 and ≥ 5.2 for both CHES and BIOS, respectively. These degrees of precipitation meet the goal of maximizing P recovery as Al-P in the first precipitation step. If precipitation is performed at a higher pH, more NaOH will be consumed. The COT method is used to determine the optimal pH for the precipitation process. Figs. 6-23 and 6-24 show the COT evaluation results for the most suitable pH for precipitation. The first criterion for evaluation is the degree of P precipitation as Al-P salts. Al-P salts are the desired products in the first precipitation step, so the higher the degree of P-precipitates as Al-P salts, the better. $Fe(OH)_3$ precipitate is expected due to it can then be removed in the next dissolution step. Therefore, a high degree of Fe precipitation as $Fe(OH)_3$ is desired. Al in Al-precipitates from the first precipitation step will be recovered in the following steps of the P-recovery process for reuse at RWWTPs. So, a high degree of Al precipitation as $Al(OH)_3$ and a high amount of Al that can be recovered are expected. The final criterion is the benefit-cost ratio for performing precipitation at different pHs. This criterion was considered to obtain a first impression of the economy for this first precipitation step. The benefit-cost ratio was evaluated based on all chemicals used and the potential products. The cost was calculated based on the amount of chemicals used, mainly NaOH. The benefit was calculated based on the potential amount of Al that can be recovered. The amount of recovered Al was converted to equivalent poly aluminum chloride using the price in the Vietnamese chemical market (HANTECO VIETNAM, 2014; HPDON, 2024; VINACHEM, 2024). The evaluation of the individual criteria and their consequences will be explained in the following.

In the case of CHES, the equilibrium pH for precipitation is evaluated in the range of 5.0 to 5.8 with a variation of 0.1. From the simulation results, over 90% P is precipitated as desired Al-P salt at the equilibrium pH ≥ 5. However, at pH 5, the precipitated Al content is very low, which results in a low value of the benefit-cost ratio. At equilibrium pH 5.1, a positive economic result is obtained for P precipitation – mainly as Al-P precipitate and $Al(OH)_3$ precipitate. The benefit-cost ratio exceeds even the break-even point at pH 5.1. The simulation results show that P precipitation at equilibrium pHs above 5.1 does not reduce the degree of P precipitation, but increases NaOH consumption, which means an increase in precipitation cost. The simulation results also show that most of the Fe reacts with OH^- to precipitate $Fe(OH)_3$ at pH ≥ 5, which is

evaluated as a good feature because this result minimizes P loss due to the absence of Fe-P precipitates. Fe-precipitates will be removed in the next step.

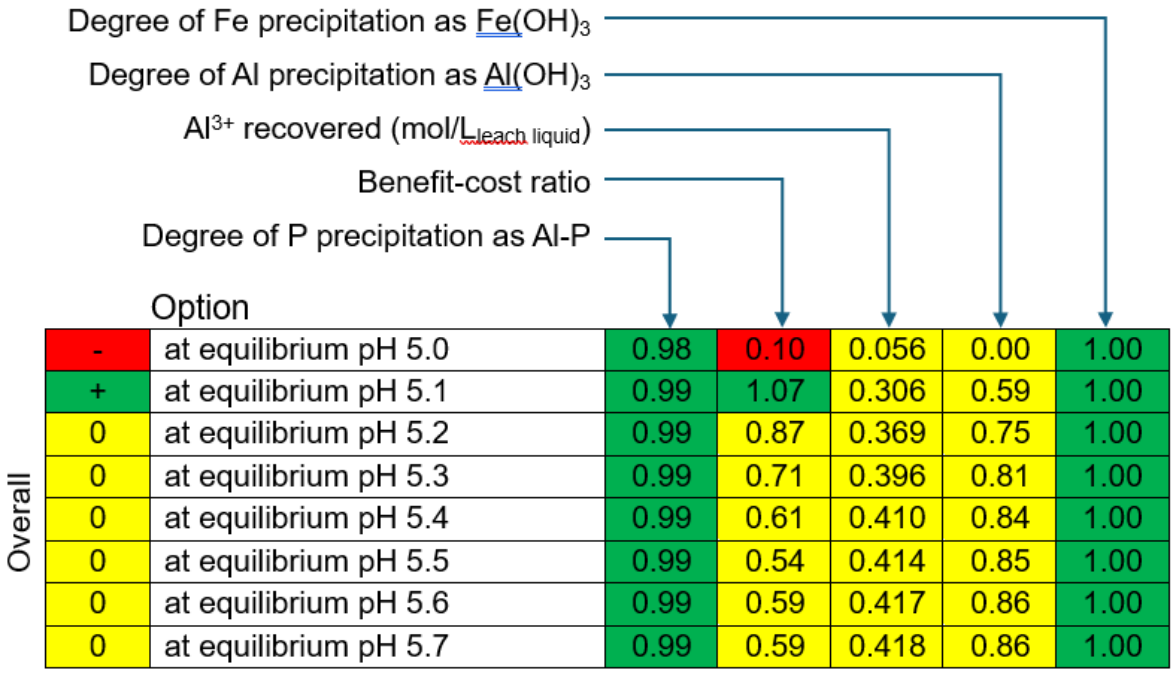

Overall	Option					
-	at equilibrium pH 5.0	0.98	0.10	0.056	0.00	1.00
+	at equilibrium pH 5.1	0.99	1.07	0.306	0.59	1.00
0	at equilibrium pH 5.2	0.99	0.87	0.369	0.75	1.00
0	at equilibrium pH 5.3	0.99	0.71	0.396	0.81	1.00
0	at equilibrium pH 5.4	0.99	0.61	0.410	0.84	1.00
0	at equilibrium pH 5.5	0.99	0.54	0.414	0.85	1.00
0	at equilibrium pH 5.6	0.99	0.59	0.417	0.86	1.00
0	at equilibrium pH 5.7	0.99	0.59	0.418	0.86	1.00

Fig. 6-23: COT evaluation for optimal precipitation parameter, for CHES

The precipitation at a pH of 5.1 meets all criteria. Therefore, it is the optimal parameter for the first precipitation step for CHES.

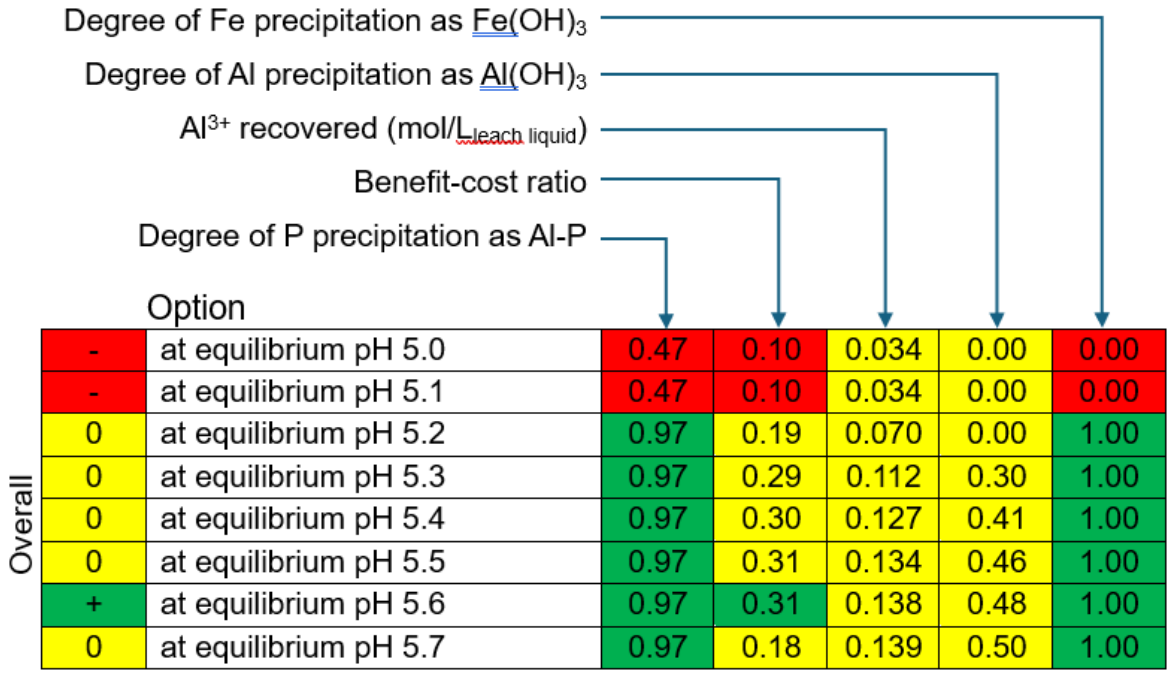

Overall	Option					
-	at equilibrium pH 5.0	0.47	0.10	0.034	0.00	0.00
-	at equilibrium pH 5.1	0.47	0.10	0.034	0.00	0.00
0	at equilibrium pH 5.2	0.97	0.19	0.070	0.00	1.00
0	at equilibrium pH 5.3	0.97	0.29	0.112	0.30	1.00
0	at equilibrium pH 5.4	0.97	0.30	0.127	0.41	1.00
0	at equilibrium pH 5.5	0.97	0.31	0.134	0.46	1.00
+	at equilibrium pH 5.6	0.97	0.31	0.138	0.48	1.00
0	at equilibrium pH 5.7	0.97	0.18	0.139	0.50	1.00

Fig. 6-24: COT evaluation for optimal precipitation parameter, for BIOS

In the case of precipitation simulation for BIOS, in the range pH below 5.1, about 47% of total P precipitations are as Fe-P salt. Thus, P precipitation at pH below 5.1 is not feasible. At pH ≥ 5.2, over 90% of P precipitates as Al-P salt, and most of the Fe precipitates as $Fe(OH)_3$. Thus, pH ≥ 5.2 is considered suitable for P recovery as Al-P salt and $Fe(OH)_3$ precipitation. In contrast, Al precipitation as $Al(OH)_3$ has not appeared at pH 5.2 and only increased slightly above pH > 5.2. At pH 5.6, the benefit-cost ratio and potential amount of Al recovered are the highest. Even so, the benefit-cost ratio shows a huge imbalance at pH 5.6. If Al is also desired as a product, it can be precipitated at pH 5.6.

Precipitation procedure options

The pH in the leached liquid obtained from the leaching step is less than 1 for both CHES and BIOS. There are two precipitation procedure options to reach the desired optimal pH for the first precipitation. In the first option, NaOH solution is gradually added to the leached liquid. The pH of the mixture will gradually increase to reach the desired equilibrium value. In the second option, the leached liquid is slowly added to the NaOH solution so that the pH of the mixture gradually decreases and finally reaches the desired pH. These two precipitation procedures have in common the desired optimum pH for precipitation, but the precipitate products may differ. For the first option, the simulation results shown in Fig. 6-22 indicate that the Fe-P and Al-P salts can be simultaneously formed in the range pH of 2.5 to 5. Fe-P salt is an undesirable product in the first precipitation step. There is a potential kinetic limitation due to the conversion of Fe-P to $Fe(OH)_3$. Meanwhile, for the second option, directly desired Al-P salts, $Fe(OH)_3$ products are formed first. Thus, there is no conversion required. The second procedure is therefore selected for precipitation implementation.

Conclusions

Summarizing the findings shows that a high amount of desired Al-P precipitates can be formed by adjusting the pH of the leached liquid with NaOH solution to equilibrium values of about 5.1 for CHES and ≥ 5.2 for BIOS. In addition, for CHES, performing P-precipitate at equilibrium pH 5.1 also provides a good opportunity to recover Al from the Al precipitates. For BIOS, the benefit-cost ratio is much lower than the balance level, so Al recovery may or may not be considered. If Al-P salts and $Fe(OH)_3$ and Al

are the desired products, pH 5.6 is the optimum precipitation parameter for BIOS. If not Al recycling, about pH of 5.2 is the most suitable.
The wet precipitate obtained from the experiments is then used for the next dissolution step.

6.4.4 Dissolution

In the next step, the P-containing precipitates recovered from the previous precipitation step are dissolved in the equilibrium pH range from 8 to 14 by adding NaOH. Al-P salts are dissolved while Fe and Ca components remain in the solid.

The experimental and simulation results obtained for the degree of dissolution of P, Al, Fe, and Ca for CHES and BIOS, are shown in Figs. 6-25 and 6-26. First of all, the diagrams show that the SLLE tool also allows to predict the equilibrium behavior in good agreement with lab experiments.

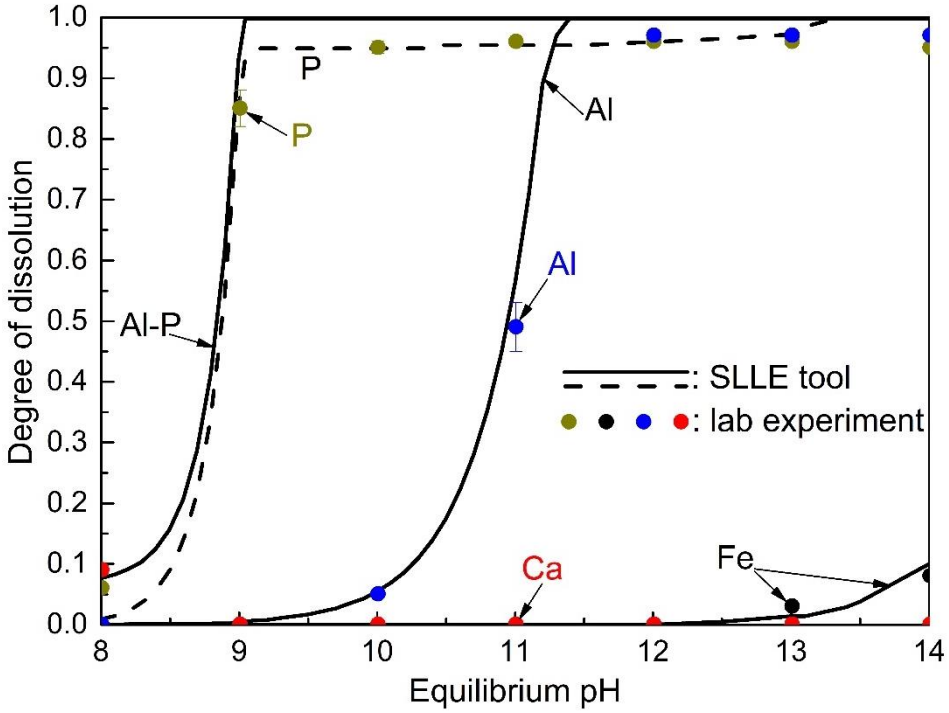

Fig. 6-25: Experimental and simulation results on dissolution at different pHs, for CHES

For both CHES and BIOS, one of the desired products, Al-P, dissolved essentially completely above pH 9.2. Since other metals, which are presented in the sludges (ref. Tab. 6-1), can also form P-precipitates, the degree of P dissolution reaches only about 95% for CHES and 92% for BIOS in the relevant pH range.

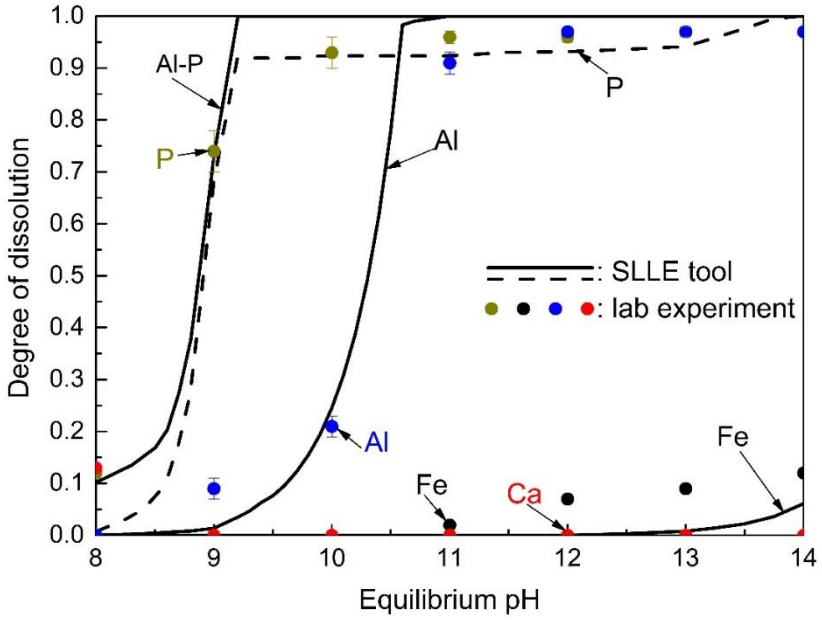

Fig. 6-26: Experimental and simulation results on dissolution at different pH, for BIOS

If also Al^{3+} is desired as a product, that can be dissolved essentially completely above 11.4 for CHES and above 10.6 for BIOS. Between pH of 9 and these pHs, $Al(OH)_3$ precipitate will still be presented. Fig. 6-27 shows the $Al(OH)_3$ precipitate formation trend at different pH. At equilibrium pHs above 9.1, $Al(OH)_3$ is re-dissolved, leading to a rapid increase in total Al solubility. The dissolution trend of $Al(OH)_3$ for BIOS begins to occur from an equilibrium pH of 9.2 for BIOS and pH of 9 for CHES.

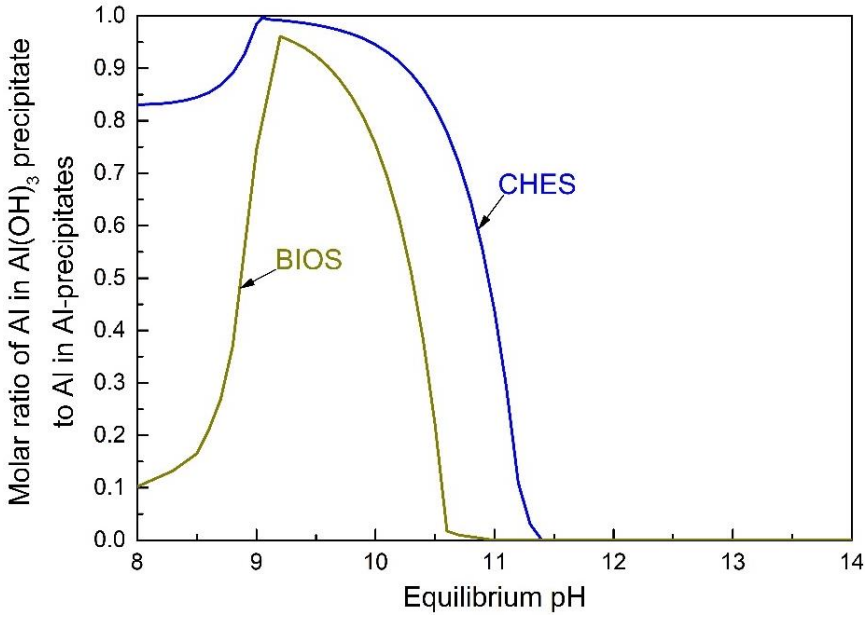

Fig. 6-27: Simulation results on molar ratio of Al in $Al(OH)_3$ precipitates and Al in Al-precipitates at different pH

In all these relevant pH ranges, Fe-precipitates, which mainly is $Fe(OH)_3$ as seen in the simulation results in the previous section (section 6.4.3) and Ca components almost remain essentially undissolved. Thus, at the dissolution step, most of the Fe and Ca are removed after liquid-solid filtration.

In the specific case of CHES, P as well as Al^{3+} are desired products. Therefore, it is necessary to choose the most suitable pH for dissolution to simultaneously obtain maximum dissolved P and Al content. The simulated molar ratio of dissolved Al obtained to NaOH used as a function of equilibrium pH, is shown in Fig. 6-28. The optimal pH for the dissolution step, minimizing the NaOH amount required, is about 11.4. For BIOS, the corresponding range is between pH 10.5 to 10.6. As mentioned in Chapter 6.4.3, if the small benefit of recovering Al^{3+} is not aimed at, the optimal pH range would thus be from 9.2 to 9.5 for BIOS.

The dissolved P is recovered in the next precipitation step, while the dissolved Al can be recovered for reuse in wastewater treatment plants.

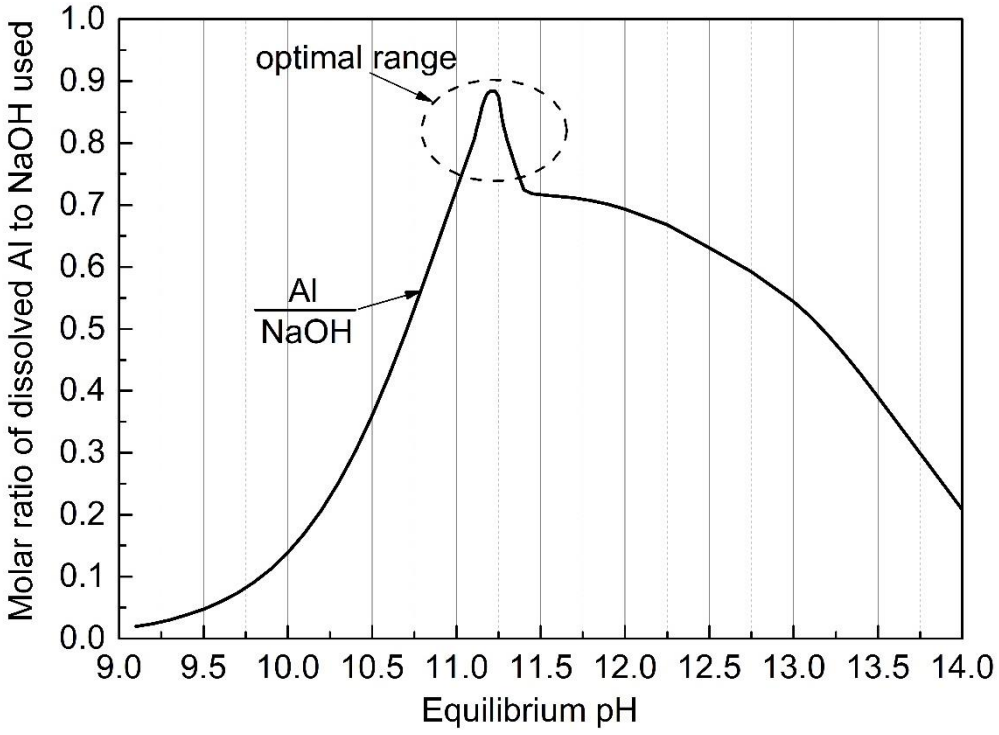

Fig. 6-28: Simulation of the molar ratio of dissolved Al to NaOH used at equilibrium pHs, for CHES

6.4.5 Final Product Precipitation

Ca-P salts precipitation is the final step of the conceptualized P-recovery process. The liquid solution obtained from the dissolution step mainly consists of dissolved P and Al in a highly alkaline environment. A $Ca(OH)_2$ solution is then used to perform the final precipitation by further increasing the pH. The $Ca(OH)_2$ solution also provides Ca^{2+} ions such that Ca-P salts are precipitated. Alternatively, NaOH can be combined to precipitate Ca-P salts, where $CaCl_2$ needs to be added to simultaneously provide Ca^{2+}. This alternative unfortunately can lead to unwanted impurities in the final recovered product due to the Cl^- ion added.

Starting out from the solution obtained in the previous step at equilibrium 11.4 for CHES and 10 for BIOS containing dissolved Al and P, the precipitation experiments were focused at high equilibrium pHs from 11 to 13. The upper limit is chosen to limit the formation of $Al(OH)_3$ precipitate and thus to lose the desired Al^{3+} from the supernatant as shown in Fig. 6-22.

Fig. 6-29 and 6-30 show the results from the experiment and simulation for the Ca-P salt precipitation for CHES and BIOS, respectively. Results from simulation with the SLLE tool show a remarkable agreement in P precipitation with experimental results. In the experiments, the $Ca(OH)_2$ slurry was used to conduct the Ca-P salt precipitation experiments. Since amount of $Ca(OH)_2$ affects the benefit-cost ratio, the molar ratio of $Ca(OH)_2$ used to P in the dissolved liquid was used to evaluate a quantitative impression of cost-benefit of this process step. The precipitation can form different compounds, such as calcium hydrogen phosphate dihydrate ($CaHPO_4 \cdot 2H_2O$), calcium phosphate ($Ca_3(PO_4)_2$), or stable compounds, such as hydroxyapatite ($Ca_5(PO4)_3OH$) (HAP). At a pH of about 13, the degree of P precipitation reaches over 95%, for both BIOS and CHES. In addition, the molar ratio of Ca to P in HAP of 5:3 is quite similar to the molar ratio of Ca^{2+} required to essentially completely precipitation dissolved P. Thus, Ca-P salts, including HAP, reach the maximum degree of P precipitation at the pH of about 13, for both CHES and BIOS.

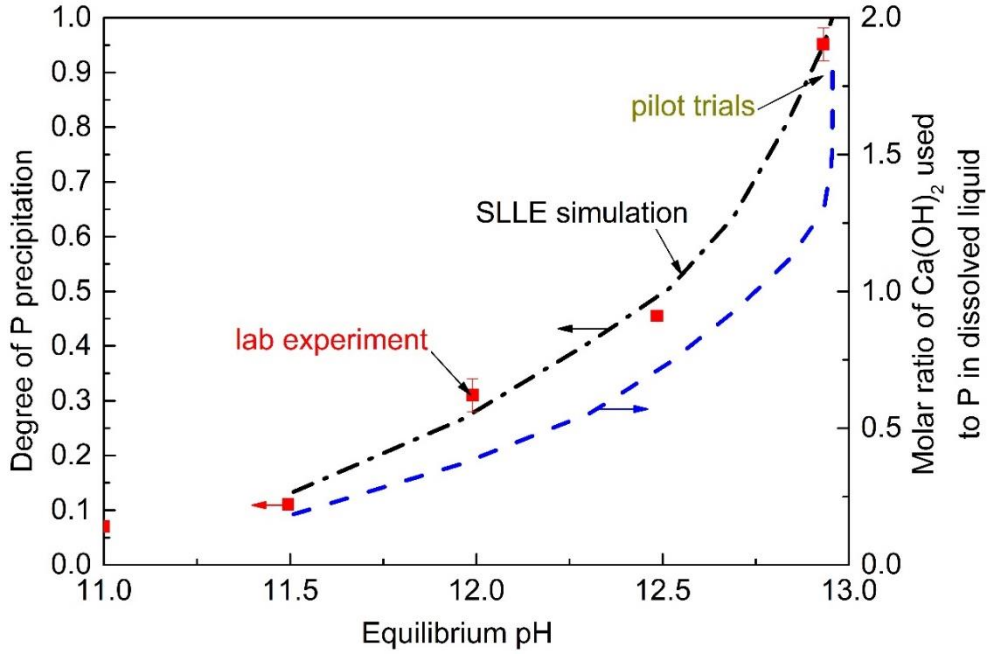

Fig. 6-29: Degree of P precipitation from lab experiments and simulations, for CHES

As can be seen in Fig. 6-27, dissolved Al is almost not precipitated at pH of 13. The dissolved Al can thus be recovered for reuse in RWWTP after filtration. The effect of Fe on the quality of recovered products and the efficiency of Ca-P precipitation was insignificant because the Fe content in precipitates was removed by more than 90% in the previous dissolution step. In addition, Fe did not precipitate with P at pH of 13, as shown in Fig. 6-22.

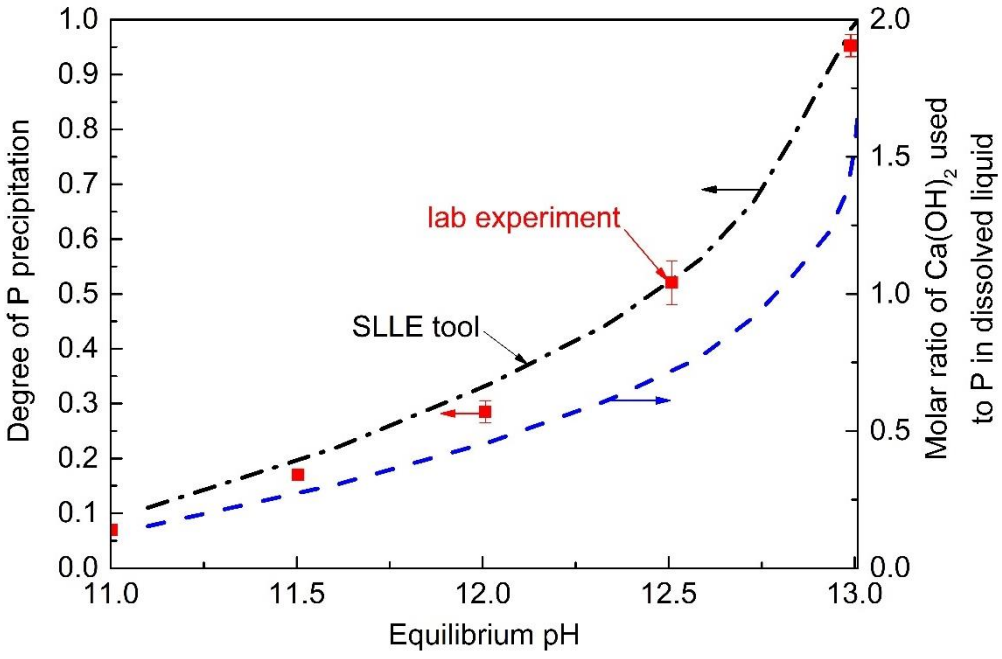

Fig. 6-30: Degree of P precipitation from lab experiments and simulations, for BIOS

As a conclusion, the final product precipitation should be carried out at pH of at most 13, by using $Ca(OH)_2$. The final precipitated solid product obtained is than mainly Ca-P salts, which Al remaining in solution. Fig. 6-29 and 6-30 indicate a very steep slope of the $Ca(OH)_2$ compared to the P ratio in the pH range of interest. This indicates that the technical process should possibly not aim at a specific pH but at a specified molar $Ca(OH)_2$ compared to the P ratio, for example of 5:3 corresponding to HAP.

7 Pilot Plant

The optimal parameters have been determined through lab experiments and the SLLE simulations for the proposed P-recovery process. Here, the determined optimal parameters are to be validated on a pilot scale. The pilot is developed to target goals on simple operation, minimizing the use of equipment and energy consumption as well as maximizing the function of each pilot unit. The pilot is designed to operate on a batch basis, where each batch has a capacity of 1 kg of dried sludge. The goal was for each unit tank in the pilot to perform different functions according to the specific steps in the P-recovery process, thus reducing the number of unit tanks in the pilot. The designed pilot is shown in Fig. 7-1. It consists of 4 glass tanks, tank 1 where the main steps of the P-recovery process occur, and tank 2 for filtration to separate the liquid and solid phase by using different pore-size polypropylene filter plates. A 50 L temporary storage tank 3 and tank 4 containing chemicals used in the process steps, are used. Tanks 1 and 2 are conical reactors, with dimensions of D x H = 300mm x 650mm. Each tank is connected to a liquid transmission pipeline system, metering pumps, and valves. Three metering pumps (Bluewhite, C-6250HV, USA) are used for the pilot. An online pH meter (HI-8314, Hanna, Italy) is installed in tank 1 to measure the pH of the mixture at different steps of the process. In tank 1, a motor (4GN15K, Oriental Motor, Japan) is installed with mixer blades for mixing. All electrical equipment is connected and controlled by a central electrical cabinet.

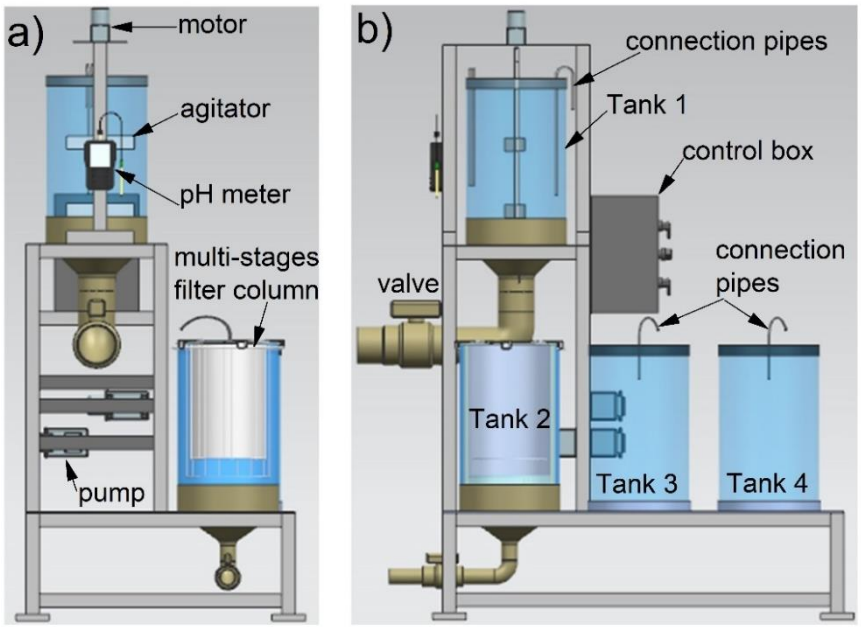

Fig. 7-1: Pilot 3D design drawing, a) left side view, and b) front view

The pilot operating procedure is shown in Fig. 7-2, which allows for the minimization of the tanks while performing process steps. The pilot operation procedure for each batch is divided into eight specific steps. The four main steps of the pilot operation procedure, namely leaching, precipitation, dissolution, and final precipitation, are performed in tank 1 and are colored yellow. The filtration steps are the filtration are performed in tank 2, which is colored green.

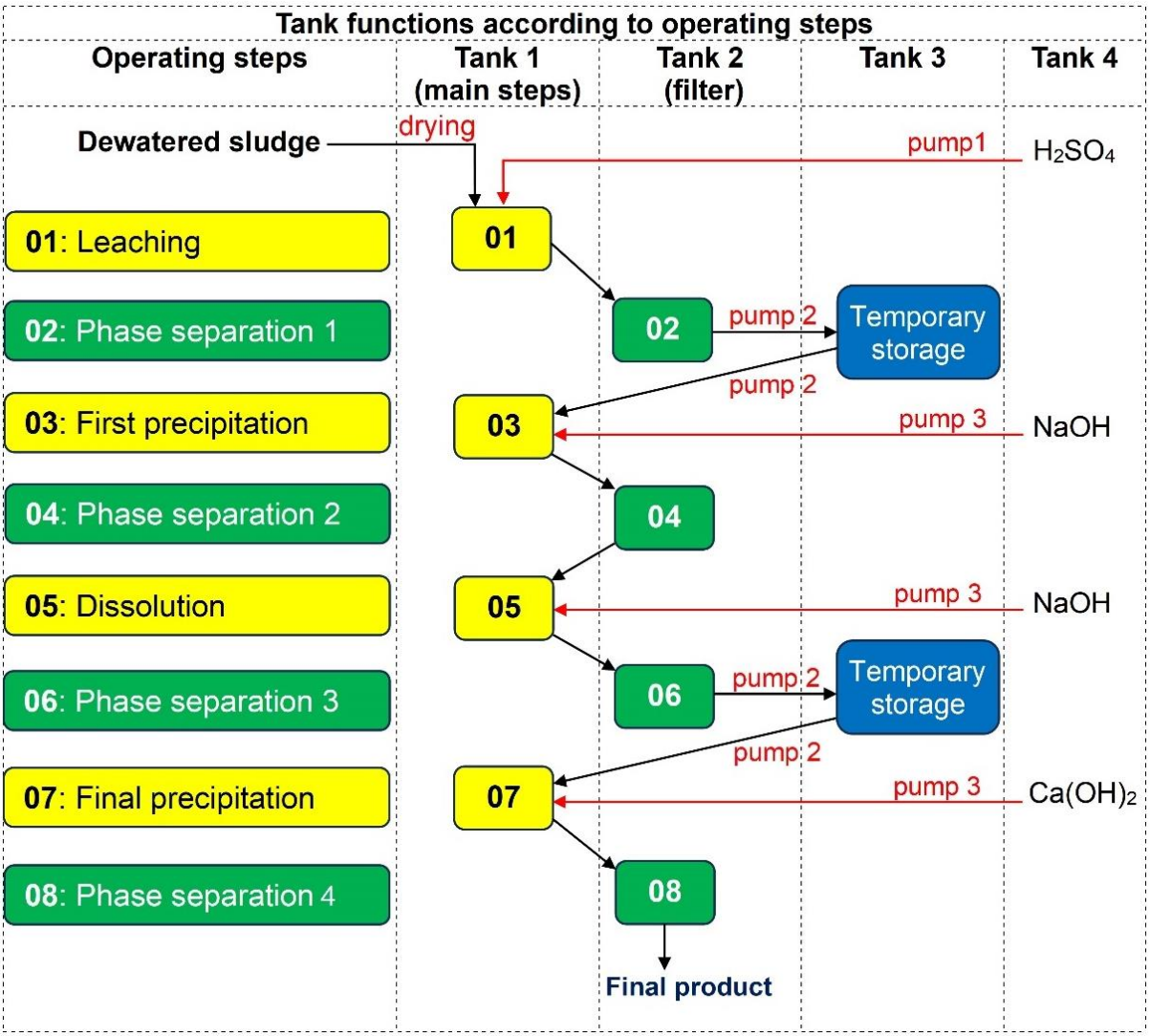

Fig. 7-2: Tanks of pilot and operating procedure

The liquid obtained from the liquid-solid separation process will be transferred to temporary storage in tank 3. The chemical solutions for the leaching, precipitation and dissolution, namely H_2SO_4, NaOH and $Ca(OH)_2$ solutions, are prepared in tank 4 and used for the respective step. The first metering pump is used only to deliver H_2SO_4 solution. The second pump is used to pump leached liquid and the solution from the

dissolution step. The third metering pump delivers the NaOH and $Ca(OH)_2$ solutions for precipitation and dissolution.

Overall, it can be seen that with the pilot operating in batches, this design and the operating procedure minimize the number of units required. More other details of tanks, filter phase separation procedure, and pilot setting up are presented in the appendix Chapter 9. Photos of the installed pilot are shown in Fig. 7-3.

Fig. 7-3: Phosphorus recovery pilot at Industrial University of Ho Chi Minh City

7.1 Results and Discussion

7.1.1 Input Dried Sludges for Pilot Plant

CHES and BIOS for pilot operation were collected from the sludge dewatering area of Xuan Lap-An Loc rubber processing wastewater treatment plant of Dong Nai Rubber Corporation in Dong Nai province, about 65 km from Ho Chi Minh City, immediately after being dewatered. The moisture contents in CHES and BIOS are approximately 80 and 76%, respectively. The dewatered sludges were then shaped into sludge

spaghetti using a hand-cranked extruder before being placed onto inox trays and dried by a forced-convection oven to constant mass at 105°C. Fig. 7-4 shows the sludge spaghetti and the dried sludge prepared for pilot operation. Although a larger mass of dry sludge was required for pilot operation than for the lab experiments, the pilot's capacity of 1 kg of dry sludge per batch did not exceed the capacity of the drying equipment at IUH. Therefore, the forced-convection oven (CE3F-ShelLab, USA) equipment was still used to dry the sludges for the pilot operation. After drying, the sludge was crushed using a crusher machine (PEF100, Jiangxi, CHINA) to a particle size of less than 2.5 mm, which was determined in Chapter 6 to be the most suitable particle size for P leaching.

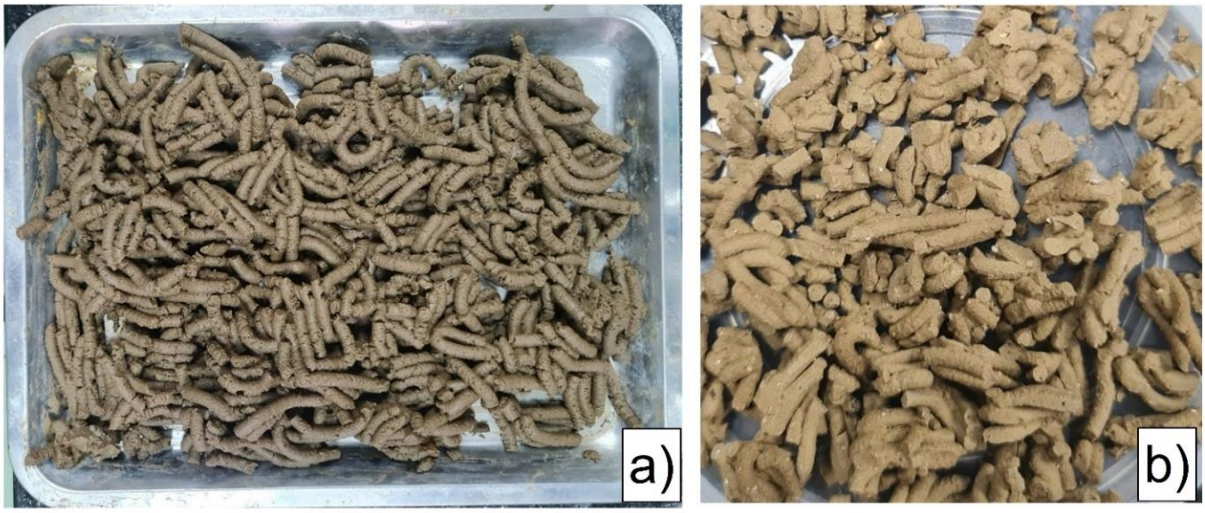

Fig. 7-4: Dewatered sludge "sludge spaghetti" (a) and dried sludge (b)

The dried sludge for pilot trials was then analyzed for the composition of relevant components, presented in Tab. 7-1. The composition sludges for the pilot trial are fully within the range of those in Tab. 6-1.

Tab. 7-1: Input dried sludge composition for pilot trials

Element		Concentration, $C_{e,0}$ g kg^{-1} dried sludge	
		CHES	BIOS
P		59.10	45.10
of which	OP	4.14	11.28
	IP	54.96	33.83
Al		113.10	17.80
Ca		32.30	27.70
Fe		11.50	9.80
Mn		0.41	0.58
Zn		1.40	1.51
K		7.90	8.50
Cu		0.141	0.130
Cr		0.153	0.014
Cd		9×10^{-4}	BDL
Pb		0.034	BDL

BDL: below detection level

7.1.2 Leaching

Optimized leaching parameters from lab experiments and simulations were used for the pilot trials. The dried sludges were leached on a pilot with 1.7M H_2SO_4 at a phase ratio of 5 L kg^{-1} for BIOS and 2M H_2SO_4 at 10 L kg^{-1} for CHES. The dried sludge was transferred to tank 1 which already contained H_2SO_4 solution. Right after transferring the sludge to tank 1, the stirring system was operated continuously to limit the phenomenon of sludge clumping due to the possibility of gypsum formation. The temperature of the reactor, as well as the pH of the mixture, were continuously measured and monitored. After 60 min of leaching and mixing, the solid-liquid mixture was transferred to tank 2 for filtration to remove fine solids and to recover the pregnant leach solution. The leached liquid obtained after the multi-stage filtration is a clear fluid, as shown in Fig. 7-5. The dried mass of residual solid after leaching of BIOS was 1.2 times higher

than that of CHES, although, the amount of gypsum precipitated from CHES leaching is higher than that from BIOS leaching due to the higher Ca content of CHES.

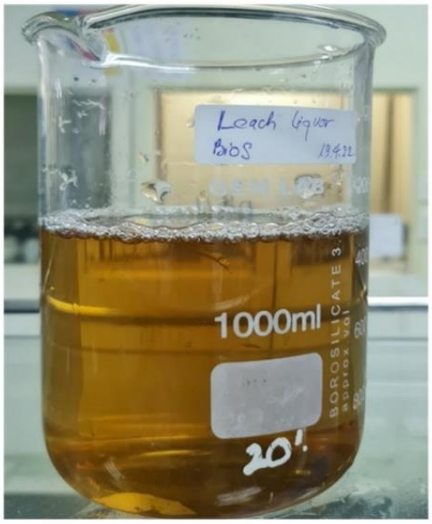

Fig. 7-5: Leached liquid after filtering

A portion of the leached liquid remained in the residue solid after filtration. For every 1 L of H_2SO_4 used to leach P, after the multi-stage filtration process about 0.9 L of leached liquid was obtained for BIOS, and about 0.92 L for CHES. To minimize P loss from the multistage filtration process, the solids after the phase separation were further washed with water to recover the remaining dissolved P, and the washing water was used to prepare the acid solution for the next leaching batch.

The results of P leaching from lab experiments together with simulation with the SLLE tool and pilot trials for BIOS and CHES at the optimal parameters are shown in Fig. 7-6. For pilot trials, P leaching efficiency was calculated considering the amount of dissolved P recovered including the washing step. The P leaching results from the pilot trials for the two sludges showed a good agreement with the results from the lab experiments and simulations. The P leaching efficiencies in the pilot trials were, as expected, about 90% for both CHES and BIOS.

The equilibrium pH of the mixture after pilot leaching was less than 0.5 for both CHES and BIOS. By washing with water, the acidity of the residue solid was significantly reduced reaching a pH of about 5.2, which facilitated the further treatment of this residual waste.

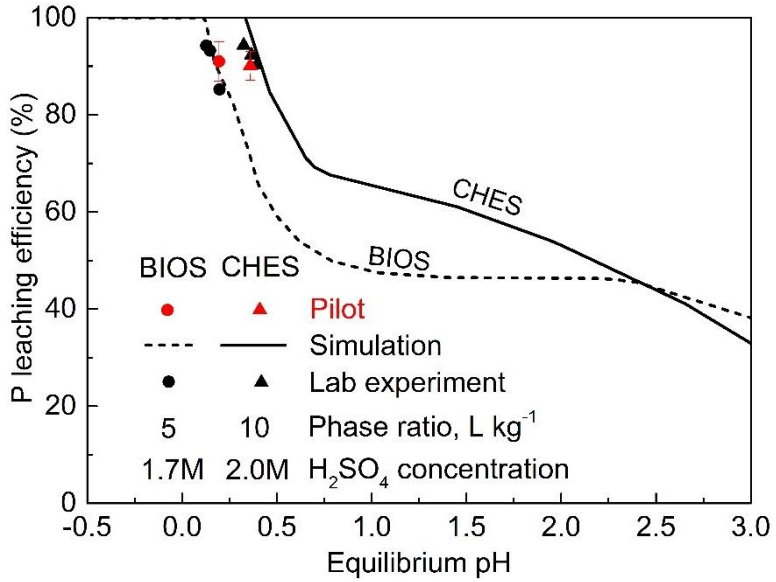

Fig. 7-6: Degree of P leaching from pilot trials, simulation, and lab experiments at optimal parameters

The degree of metals leaching in BIOS and CHES from the pilot trials is shown in Fig. 7-7. Ca had the lowest degree of leaching due to the formation of gypsum precipitate, while Fe and Al in both BIOS and CHES had a high degree of leaching of about 95%. Along with P, Al, and Fe are thus almost completely co-leached, while the Ca concentration has been decreased significantly compared to the original sludge.

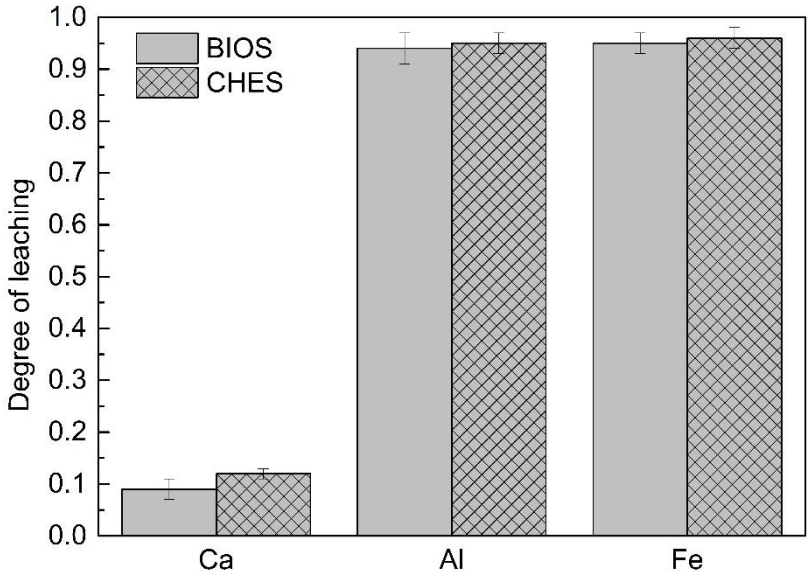

Fig. 7-7: Degree of leaching of metals at optimal parameters, at 1.7M H_2SO_4, phase ratio 5 L kg^{-1} for BIOS and 2M H_2SO_4, phase ratio 10 L kg^{-1} for CHES

7.1.3 First Precipitation

For the first precipitation, the pregnant leach solution was added to the NaOH solution until the desired pH of 5.1 for CHES and 5.2 for BIOS was reached. The result is shown in Fig. 7-8. At the first precipitation, Al-P salt is expected to form and to be recovered as a P-rich product.

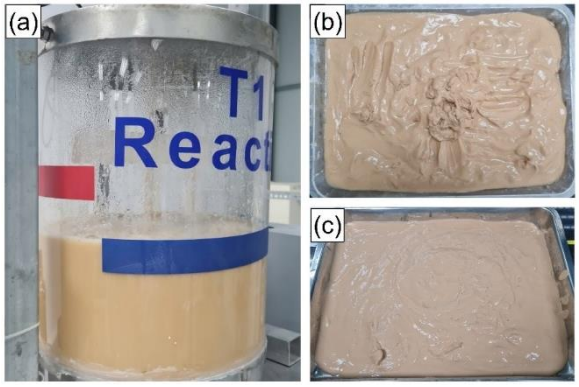

Fig. 7-8: First precipitation on the pilot (a), precipitate for BIOS (b), and for CHES (c)

The precipitation efficiencies of P and metals from lab experiments, simulations, and pilot trials are compared in Fig. 7-9. The results of lab experiments and pilot as well as the simulations agree well. More than 90% of the dissolved P and Fe in the pregnant leach solution of both BIOS and CHES are precipitated. The simulations show that most Fe is precipitated as $Fe(OH)_3$ at pH > 5.1 (see Fig. 6-22). Thus Fe is removed as insoluble $Fe(OH)_3$ precipitate.

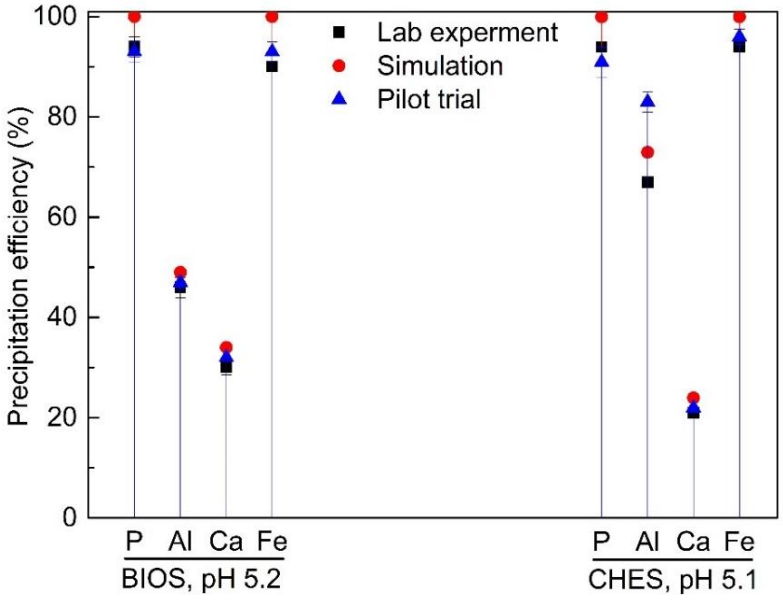

Fig. 7-9: Precipitation efficiency of P and metals at optimal parameters

7.1.4 Dissolution

The precipitate from the previous step was dissolved in tank 1 by adding NaOH solution to reach the optimal dissolution parameters determined above, i.e., pH 9.5 for BIOS and 11.4 for CHES. As discussed in Chapter 6.4.4, here, the pH for CHES has been chosen to allow recovery of Al for use in the WWTP process. For BIOS, the pH has been selected to only 9.5 to minimize NaOH consumption at the price of not being able to recover Al^{3+} for the WWTP process. These choices were made so as to explore the influence of these different options. The degree of dissolution of P and metal compounds for BIOS and CHES is shown in Fig. 7-10. Lab experiments, simulations, and pilot trials on precipitate dissolution show good agreement at the selected pH for both BIOS and CHES. At the selected pHs, only about 6 to 8% of the Fe and about 1% of Ca are dissolved from the precipitate in the pilot trials for CHES and BIOS. Therefore, Fe and Ca-precipitates can be easily removed through filtration, while Al-P is dissolved and recovered as leach liquid. Similar to the filtration from the leaching step, filtration after the dissolution step also results in significant losses of dissolved P remaining in the solid. Therefore, NaOH solution is used for washing the residue solid after the filtration to recover dissolved P, limiting P loss.

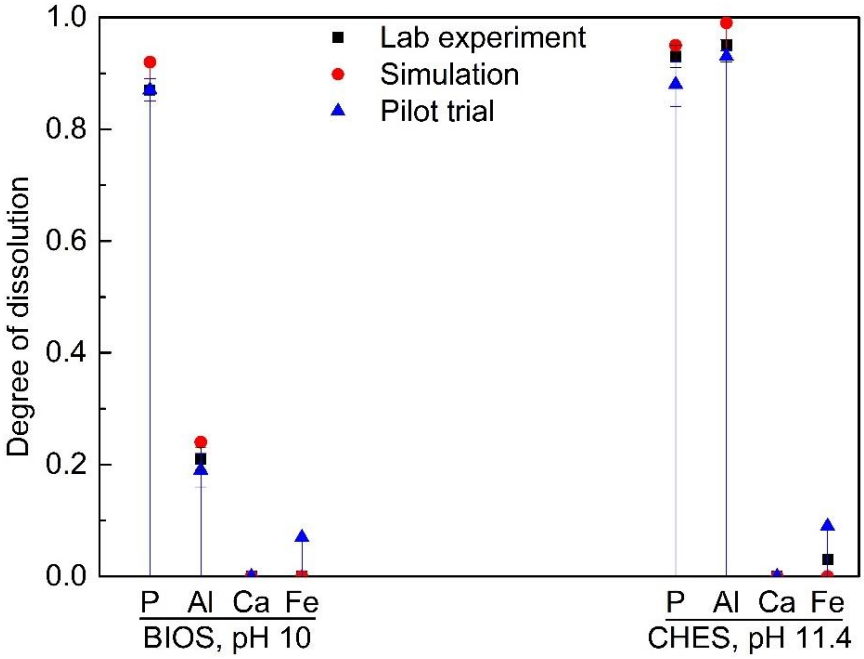

Fig. 7-10: Degree of dissolution during the pilot trials, simulation, and lab experiments at optimal parameters

At the corresponding pH for both sludges, the degrees of P dissolution were greater than 85%. Corresponding to the difference in choice for Al recovery between BIOS and CHES, the degree of dissolution of Al was 4.5 times higher for CHES than for BIOS under the chosen condition, in agreement with the findings in Chapter 6.4.4. The results show that at pH 11.4, Al can be dissolved essentially completely for CHES, as desired.

The desired products recovered after the dissolution step are the leached liquid containing mainly dissolved P for BIOS and both, dissolved P and Al, for CHES.

7.1.5 Final precipitation

The final precipitation is the last step in the P-recovery process. The expected final product is Ca-P salt, especially HAP.

$Ca(OH)_2$ slurry is used to provide Ca^{2+} ions for the Ca-P salt precipitation. Theoretically, the molar ratio of Ca to PO_4^{3-} in the HAP salt formed is 5:3, or the mass ratio of Ca to P in the HAP is 2.15. Based on the concentration of P in the leached liquid from the previous step, the concentration and volume of the $Ca(OH)_2$ slurry were adjusted to match this stoichiometry. More than 90% of the dissolved P precipitated for both BIOS and CHES at the equilibrium pH of around 13 as shown in Fig. 7-11 and 7-12. The agreement between lab experiments, simulations, and pilot trials is excellent.

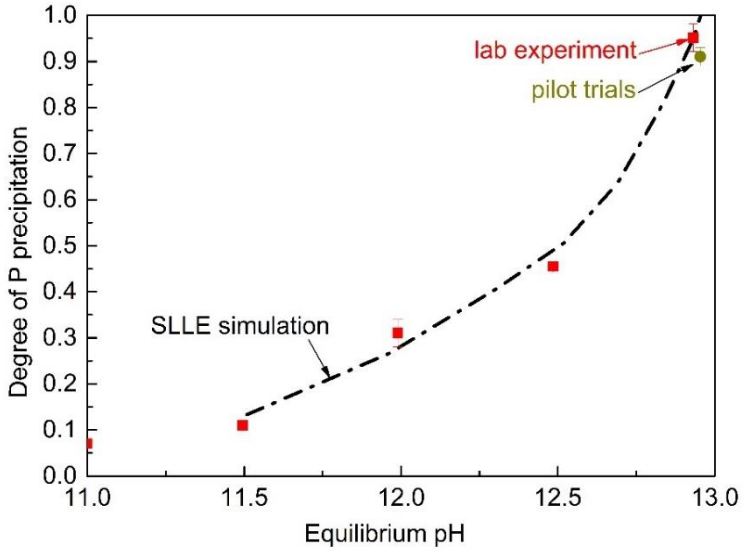

Fig. 7-11: Degree of P precipitation from pilot trials and lab experiments at precipitation optimal parameters, for CHES

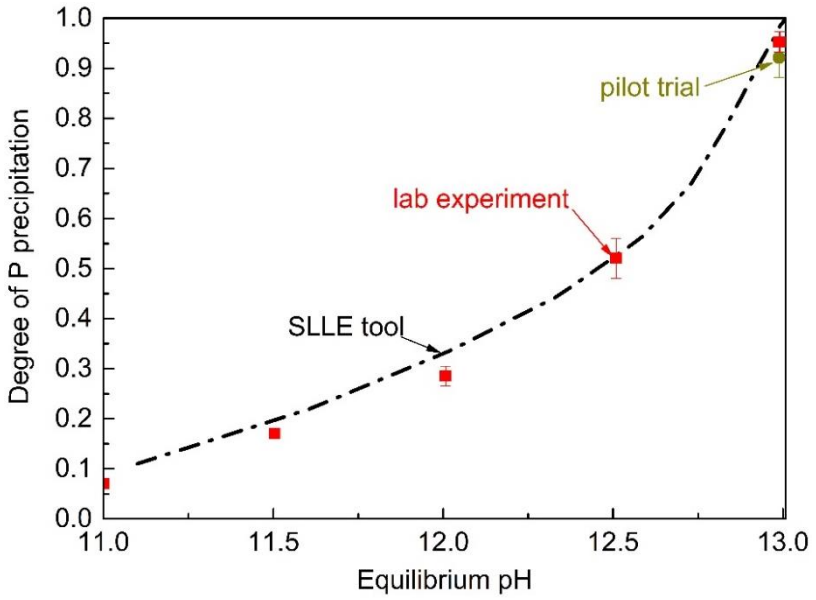

Fig. 7-12: Degree of P precipitation from pilot trials and lab experiments at precipitation optimal parameters, for BIOS

The final precipitates from the pilot trials were recovered after filtration are shown in Fig. 7-13. The recovered final product was washed with water to reduce the Al content significantly.

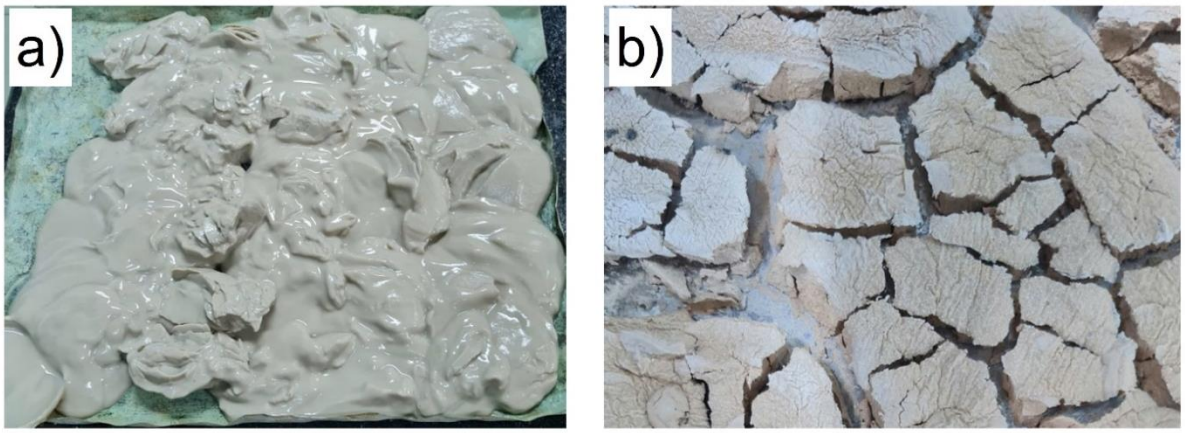

Fig. 7-13: The wet precipitate recovered after multistage filtration (a) and the recovered product after drying (b)

The content of the main elements in the recovered final dried products are shown in Fig. 7-14. The P content is about 15 wt-% for both sludges, corresponding to 32.8% P_2O_5 for BIOS and 35.4% for CHES, with P_2O_5 content being the typical measure used to specify P content in fertilizers or commercial P sources. The Ca content was the highest in both final products recovered from CHES and BIOS due to the Ca^{2+} used in

the final precipitation step. Al and Fe have effectively and almost completely been removed as desired to below 1% in the CHES and BIOS final products.

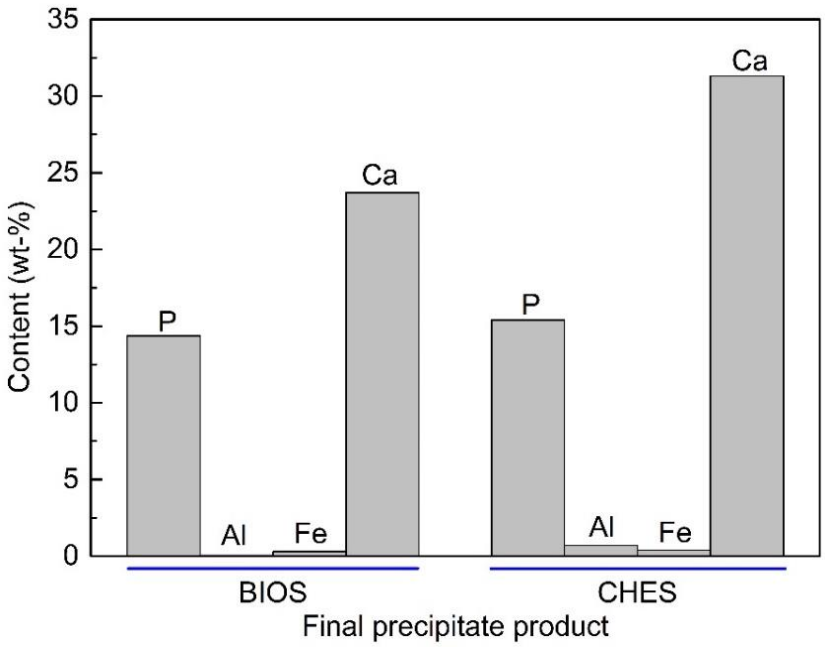

Fig. 7-14: Content of the main elements in the dried final product

A comparison of the mass ratio of relative metals to P in the input dried sludge and the final products is shown in Tab. 7-2. The mass ratio of metals to P in the final products has been significantly decreased compared to that in the input dried sludges. The mass ratio of Ca to P from input dried sludges is higher than that in final products which match closely the value of 2.15 of HAP as expected.

Tab. 7-2: Mass ratio of P to metals in input dried sludges and final products

Sample	Mass ratio of		
	Ca to P	Al to P	Fe to P
	g g^{-1}	g g^{-1}	g g^{-1}
Input BIOS	0.614	0.395	0.217
Final product (BIOS)	2.002	0.003	0.019
Input CHES	0.546	1.914	0.194
Final product (CHES)	2.091	0.043	0.023

Overall, the parameters optimized through lab experiments and simulations using the SLLE tool have been validated with pilot-plant experiments. The SLLE tool properly

describes all scales. Thus, the proposed process is validated and available for P recovery from the sludge of RWWTP.

7.2 Mass Balance and Cost Estimation

7.2.1 Mass Balance

To analyze material flows of phosphorus and impurities as a basis for the subsequent economic evaluation, mass balances for the relevant components have been evaluated. They may also serve as a foundation for scaling up to the industrial-scale process. The mass balances have been evaluated not only for each individual step but also for the entire P-recovery process for both CHES and BIOS. Reference is 1 kg of dried sludge input to pilot-scale process.

The changes in P and metals mass throughout the steps of the P-recovery process for BIOS and CHES are collected in Tabs. 7-3 and 7-4. Most of Al is removed at the final precipitation step for CHES and at the dissolution step for BIOS. Dissolution is the major step, where Fe is removed in CHES while it is removed in BIOS during the first precipitation as well as the dissolution steps. Ca is largely removed at the leaching step due to the formation of gypsum for both CHES and BIOS. Ca is again added in the final precipitation step. However, the removal of Ca in the leaching step is essential since If Ca would not be removed in the leaching step, the subsequent P-precipitates would not only be Al-P as desired but also Ca-P. This would increase the difficulty of impurity removal or cause P loss in the dissolution step. For the overall P-recovery process, more than 90% of Al and Fe in CHES and BIOS were removed.

Overall, the pilot batch trials of the proposed P-recovery process at the optimal parameters showed that the overall P recovery efficiency reached 65% for CHES and 67% for BIOS. Notably, washing the filter cake is essential to maximize P recovery and remove contaminants from pilot-scale products.

Tab. 7-3: P and metal mass at different steps of the P-recovery process on the pilot trial for 1kg of dried BIOS

BIOS	P	Al	Fe	Ca
	g	g	g	g
In 1kg of input dried sludge	45.01	17.79	9.80	27.08
In leached liquid with washing	40.51	16.90	9.41	2.44
In the first precipitate	37.67	15.72	4.42	2.26
In dissolved liquid	32.78	2.99	0.31	0.02
In final precipitate	30.15	0.14	0.29	60.34
Overall P recovery efficiency with washing, %	**67.00**			
Overall metal removal efficiency, %		99.00	97.00	
Loss from the leaching step	4.50	0.89	0.39	24.64
Loss from the first precipitation step	2.84	1.18	4.98	0.18
Loss from the dissolution step	4.89	12.73	4.11	2.24
Loss from the final-precipitation step	2.63	2.85	0.02	
Overall loss	14.86	17.65	9.51	27.06

For CHES, the Al content in the input sludge is very high due to polyaluminum chloride being used for P removal at RWWTPs. As discussed in the Chapter 6.4.4, the Al^{3+} ions are recovered in the solution after the final precipitation step, so that an Al-rich solution can be reused in the wastewater treatment at RWWTPs.

Tab. 7-4: P and metal mass at different steps of the P-recovery process on the pilot trial for 1kg of dried CHES

CHES	P	Al	Fe	Ca
	g	g	g	g
In 1kg of input dried sludge	59.09	113.40	11.54	32.50
In leached liquid with washing	53.18	107.73	10.96	3.90
In the first precipitate	48.39	89.42	10.52	0.86
In dissolved liquid	42.58	83.16	0.95	0.01
In final precipitate	38.75	1.66	0.90	81.06
Remaining Al-rich solution		81.50		
Overall P recovery efficiency with washing, %	**65.58**			
Overall metal removal efficiency, %		98.52	92.20	
Loss from the leaching step	5.91	5.67	0.58	28.60
Loss from the first precipitation step	4.79	18.31	0.44	3.04
Loss from the dissolution step	5.81	6.26	9.57	0.85
Loss from the final-precipitation step	3.83	81.50	0.05	
Overall loss	20.34	111.74	10.64	32.49

The input and output materials and auxiliaries of the pilot trials per 1 kg of dry sludge are detailed in Tabs. 7-5 and 7-6. The input chemicals and water are used to prepare the solutions for the different steps in the P-recovery process. H_2SO_4 is the chemical with the highest consumption, both for CHES and BIOS. The amount of chemicals and water consumed for CHES is roughly twice as high as for BIOS while only around 29% more P are recovered. These input data are basis for the following economic evaluation.

Tab. 7-5: Inputs and outputs from the pilot trials for each kg of dried BIOS used

BIOS	Input utilities				Output after each step		
	H_2SO_4	NaOH	$Ca(OH)_2$	Water (a)	Liquid	Wet solid	Dry solid
	molar	molar	g	L	L	kg	kg
Drying sludge					3.39 (b)		1.00
Leaching step	8.5			4.54	4.50	0.25	
Washing 1				1.00	0.91 (c)	0.28	
First precipitation step		5.31		5.31	5.00	0.58	
Dissolution step		0.62		4.40	4.58	0.18	
Washing 2		0.05		0.50	0.40	0.19	
Final precipitation step			88	2.00	6.62	0.35	
Total	**8.5**	**6.18**	**88**	**17.75**			

(a): volume of water used for preparing a 1.7M H_2SO_4 for leaching, 1M NaOH for first precipitation, 0.14M NaOH for dissolution, 4.4% $Ca(OH)_2$ slurry for final precipitation step, and for washing.

(b): volume of water evaporated after drying.

(c): this liquid is used together with water and H_2SO_4 to prepare the acid solution for the next leaching batch.

Tab. 7-6: Inputs and outputs from the pilot trials for each kg of dried CHES used

CHES	Input utilities				Output after each step		
	H_2SO_4	NaOH	$Ca(OH)_2$	Water (a)	Liquid	Wet solid	Dry solid
	molar	molar	g	L	L	kg	kg
Drying sludge					4.26 (b)		1.00
Leaching step	20			8.91	9.20	0.21	
Washing 1				1.00	0.90 (c)	0.28	
First precipitation step		7.51		7.51	7.12	0.81	
Dissolution step		4.05		9.00	9.13	0.17	
Washing 2		0.06		0.60	0.50	0.19	
Final precipitation step			156	2.00	11.45	0.43	
Total	**20**	**11.62**	**156**	**29.02**			

(a): volume of water used for preparing a 2.0M H_2SO_4 for leaching, 1M NaOH for first precipitation, 0.45M NaOH for dissolution, 7.8% $Ca(OH)_2$ slurry for final precipitation step, and for washing.

(b): volume of water evaporated after drying.

(c): this liquid is used together with water and H_2SO_4 to prepare the acid solution for the next leaching batch.

7.2.2 Cost Estimation

The cost estimation is performed to provide an overview of the costs of operating the proposed P-recovery process, based on the pilot experiments. Here, only the operating expenditure is evaluated since. Due to the simplicity of the equipment and the long time of operation expected, it can be assumed that the capital expenditure is negligible compared to the operating expenditure. The cost estimation is calculated based on the data in Tabs. 7-5 and 7-6. In addition, energy consumption for drying dewatered sludge, operating the mixing equipment, and chemical pumps has been estimated as shown in Tabs. 7-7 and 7-8.

The electrical energy consumption E is calculated according to

$$E = P_{rated}\, LF\, t \tag{7-1}$$

where, P_{rated} is the rated power of the motor, the parameter of which is shown on the device parameter table, LF the load factor, which accounts for the percentage of power actually being used compared to the rated power, t the operating time of the equipment.

The energy for drying sludge is calculated based on the total water content that needs to be evaporated. This includes the energy required for water and solids to reach the boiling point $\mathrm{T_b}$ and the energy required to evaporate water at ambient pressure. The initial temperature $\mathrm{T}_{initial}$ is assumed at 30°C. The dry mass (DM) contents in CHES and BIOS for pilot trials were approximately 20 and 24%, respectively. The dewatered sludges are assumed to be dried to a DM content of 95% or higher. The estimate of minimum energy consumption for evaporating water, Q is calculated according to

$$\mathrm{Q} = m_{\mathrm{H_2O}} \left(C_{\mathrm{p}}(\mathrm{T_b} - \mathrm{T}_{initial}) + \Delta H_{\mathrm{vap}}\right) + m_{solids}\, C_{p,solids}\, (\mathrm{T_b} - \mathrm{T}_{initial}), \tag{7-2}$$

where, $m_{\mathrm{H_2O}}$ and m_{solids} are the mass of water and solids, respectively, C_{p} and $C_{p,solids}$ are the specific heat of water and solids, ΔH_{vap} is the latent heat of vaporization of water.

The average energy consumption of the forced convection dryer for drying BIOS and CHES is 788 kWh t^{-1} of evaporated water. This compare well with the published research results of Bennamoun et al. on wastewater sludge drying methods who find a

range of 700 to 1400 kWh t^{-1} of evaporated water for convective drying technology (Bennamoun et al., 2013)

Tab. 7-7 and 7-8 show that the energy consumed during pilot experiments for CHES and BIOS results mainly from sludge drying. The sludge from RWWTP has been dewatered before being collected. Nevertheless, the dewatering efficiency is low, which leads to high moisture content in both types of sludge. To optimize energy demand, sludge dewatering methods and techniques could be optimized to increase dewatering efficiency at RWWTPs. Additionally, drying dewatered sludge at least partially with solar energy could reduce energy consumption further with these assumption. Pilot experiments with CHES and BIOS both indicated that the total energy consumption for mixing and pumping was much lower than that for sludge drying. The total energy consumption for the pilot process with CHES was higher than that for BIOS. However, since more phosphorus is recovered from CHES than from BIOS, the energy consumption per unit of recovered product is almost identical for CHES and BIOS.

From the required utilities shown in Tabs. 7-5 and 7-6 and energy in Tabs. 7-7 and 7-8, the total cost and revenues for the proposed process obtained per kg of dry sludge are evaluated and summarized in Tab. 7-9. The prices of chemicals, electricity, and water for industrial use were collected from suppliers in Vietnam, shown in the appendix in Tab. A 9-1. For revenue estimation, the mass of P recovered was converted to P_2O_5 and the selling price of P_2O_5 on the international market used, also included in Tab. A 9-1. In addition, for CHES, valuable by-products generated from the P-recovery process steps, such as dissolved Al in liquid after the final precipitation step can be recovered and reused at a wastewater treatment plant. Therefore, the value from reused dissolved Al is accounted for as revenue. The amount of dissolved Al obtained is converted to the equivalent value of PAC 30% Al_2O_3 currently used at RWWTP.

Tab. 7-7: Basic energy consumed to recover P from 1 kg dry BIOS by pilot trial

BIOS	Mixing		Pump		Drying	Energy used
	Motor power	Mixing time	Motor power	Pumping time	Mass of water	kWh
	W	h	W	h	kg	
Sludge drying					3.39	2.403
Leaching	25	1	45	0.17		0.037
Phase separation			45	0.17		0.009
First precipitation	25	1	45	0.33		0.044
Phase separation			45	0.67		0.033
Dissolution	25	1		0.17		0.014
Phase separation			45	0.17		0.009
Final precipitation	25	1	45	0.17		0.023
Phase separation			45	0.50		0.026
Total (kWh)						**2.598**

Tab. 7-8: Basic energy consumed to recover P from 1 kg dry CHES by pilot trial

CHES	Mixing		Pump		Drying	Energy used
	Motor power	Mixing time	Motor power	Pumping time	Mass of water	kWh
	W	h	W	h	kg	
Sludge drying					4.26	3.025
Leaching	25	1	45	0.33		0.044
Phase separation			45	0.33		0.017
First precipitation	25	1	45	0.50		0.053
Phase separation			45	0.67		0.033
Dissolution	25	1		0.33		0.014
Phase separation			45	0.33		0.017
Final precipitation	25	1	45	0.17		0.023
Phase separation			45	0.50		0.026
Total (kWh)						**3.253**

Currently, sludges from RWWTP at DONARUCO must be collected and treated. For each ton of dewatered sludge collected and treated, DONARUCO has to pay for the service about 600,000 VND, equivalent to 24.7 USD. Each ton of dried sludge for P recovery requires drying about 4.3 and 5.3 tons of dewatered sludge for BIOS and CHES, respectively. If dewatered sludges are used for P recovery, DONARUCO can thus save costs for current dewatered sludges treatment, which has to be accounted an benefit in Tab. 7-9.

Tab. 7-9 shows that chemicals are the most costly factor for both CHES and BIOS, especially for the leaching step. In the leaching step, the higher the metal content in the input dry sludge, the more H_2SO_4 is consumed to achieve the optimal equilibrium pH for P leaching. Since the input sludge has a high content of impurities such as metals Al, Fe, and Ca, a significant excess of chemical is required for the leaching.

Tab. 7-9: Operating cost and revenues for pilot trials per 1kg of dried sludge

STEP	Chemical		Energy		Water		Total	
	USD/kg of dry sludge		USD/kg of dry sludge		USD/kg of dry sludge		USD/kg of dry sludge	USD/kg of dry sludge
	BIOS	CHES	BIOS	CHES	BIOS	CHES	BIOS	CHES
Sludge drying			- 0.173	- 0.218			- 0.173	- 0.218
Leaching	- 0.279	- 0.659	- 0.003	- 0.004	- 0.002	- 0.004	- 0.284	- 0.667
First precipitation	- 0.152	- 0.219	- 0.006	- 0.006	- 0.003	- 0.004	- 0.161	- 0.229
Dissolution	- 0.019	- 0.125	- 0.002	- 0.002	- 0.002	- 0.005	- 0.023	- 0.132
Final precipitation	- 0.025	- 0.033	- 0.004	- 0.004	- 0.001	- 0.001	- 0.030	- 0.038
Overall cost	- 0.475	- 1.036	- 0.188	- 0.234	- 0.008	- 0.014	- 0.671	- 1.284
Revenue from recovered P-product							+ 0.200	+ 0.258
Revenue from reused Al solution							+ 0.000	+ 0.336
Avoided cost for dewatered sludge treatment							+ 0.109	+ 0.130
Total							**- 0.362**	**- 0.524**

The cost of H_2SO_4 used for P leaching from CHES is more than twice that for BIOS. For CHES and BIOS, the cost of energy is significantly lower than the cost of chemicals, and cost for the water is many times lower than the cost of energy and chemicals. Revenue from recovered P-products is equivalent to 30% of total costs for BIOS and about 20% for CHES. It is remarkable that the Al recovered from the P-recovery process for CHES generates higher revenue than the P-products obtained. Avoids costs from reduced sludge treatment costs are significant revenues to reduce the imbalance between costs and revenues.

The pilot experiments of the P-recovery process showed high P and Al recovery efficiency. However, the operating costs are still significantly higher than the recovered revenues. One direct optimization potential already mentioned above is direct solar drying of the sludge, which would almost half the imbalance between costs and revenues. Since a large fraction of chemicals used are utilized to deal with components that have been added in the WWTP process, further optimization may be possible by jointly considering WWTP and the P-recovery process. In the case of the DONARUCO, it is clear that P recovery from the sludges of RWWTP not only limits the loss of P and Al but also limits the amount of waste to be treated. Therefore, by applying the P-recovery process at RWWTP, DONARUCO can meet sustainable development and circular economy goals, which are required to be implemented step by step to limit waste by the Vietnamese Government.

In addition, the Vietnamese Government's environmental protection policies and regulations are becoming increasingly stringent. The Environmental Protection Law of Vietnam (Vietnamese Government, 2020) issued in 2020 also shows that waste treatment costs will be continuously adjusted to increase. Waste generators, therefore, need to find solutions to reduce the amount of waste to be treated if they do not want to pay higher costs for waste treatment in the future.

8 Conclusions

A general overview of existing P-recovery processes from organic waste streams, such as domestic wastewater treatment plants, shows that many processes follow identical general steps. Only the detailed technical solutions vary because they depend on the characteristics and composition of the input material used. The general structure is the basis for developing the P recovery process in this study. The simplest technical methods are selected that allow efficient removal of the impurities for case studied.

The large population and the development of agriculture create a large amount of waste, including many P-rich wastes in Southern Vietnam. Five typical wastes, namely sediment from catfish farming, manure from cattle and pig farming, as well as sludges from domestic and rubber latex-processing WWTPs were evaluated for P-recovery potential. Dewatered sludges from domestic and rubber latex-processing wastewater treatment plants were identified as highly suitable wastes for P recovery.

Since most existing studies address P-recovery from DWWTP but none from RWWTP, the goal was here to develop a suitable P-recovery process. BIOS and CHES from RWWTP in Dong Nai province were used to develop a P-recovery process suitable for Southern Vietnam. Sludge from RWWTP has a high P content and high metal content, such as Al, Ca, and Fe, especially for CHES. The flowchart of the proposed process is shown in Fig. 8-1. The wet chemical leaching method is used to leach P from sludge, which also results in the co-leaching of Al, Fe, and Ca. Removing these unwanted impurities is essential for the subsequent steps in the P-recovery process. Selective precipitation and dissolution methods are applied to remove these contaminant effectively dedicated pH conditions. The desired final P-product obtained from the final precipitation step are Ca-P salts, which can be used directly as a slow-release fertilizer in agriculture or as an ingredient of fertilizer.

The SLLE simulation tool has been shown to be very effective for developing the P-recovery process and for optimizing process parameters for different types of sludge. The results from lab experiments and simulations were used for finding the best parameters for each process step. The proposed process with these parameters has been then validated by pilot trials.

The overall efficiency of the P-recovery process reached about 67% for BIOS and 65% for CHES. The process fulfills the basic criteria in relation to the economic and technical conditions in Vietnam, which demand a simple yet effective and environmentally friendly process. Some of the output mass flows in the process can be reused to increase economic feasibility, such as the dissolved Al recovered for reuse in RWWTPs. Unfortunately, the total costs exceed the total revenues generated in the current process, primarily due to the high energy demand for dewatering the input sludge and the significant chemical consumption, especially for primary leaching. Improving sludge dewatering and incorporating at least partial solar drying can significantly reduce energy consumption. This approach is feasible given Vietnam's high average sunshine duration, ranging from approximately 1,600 to 2,600 hours per year (Riva Sanseverino et al., 2020).

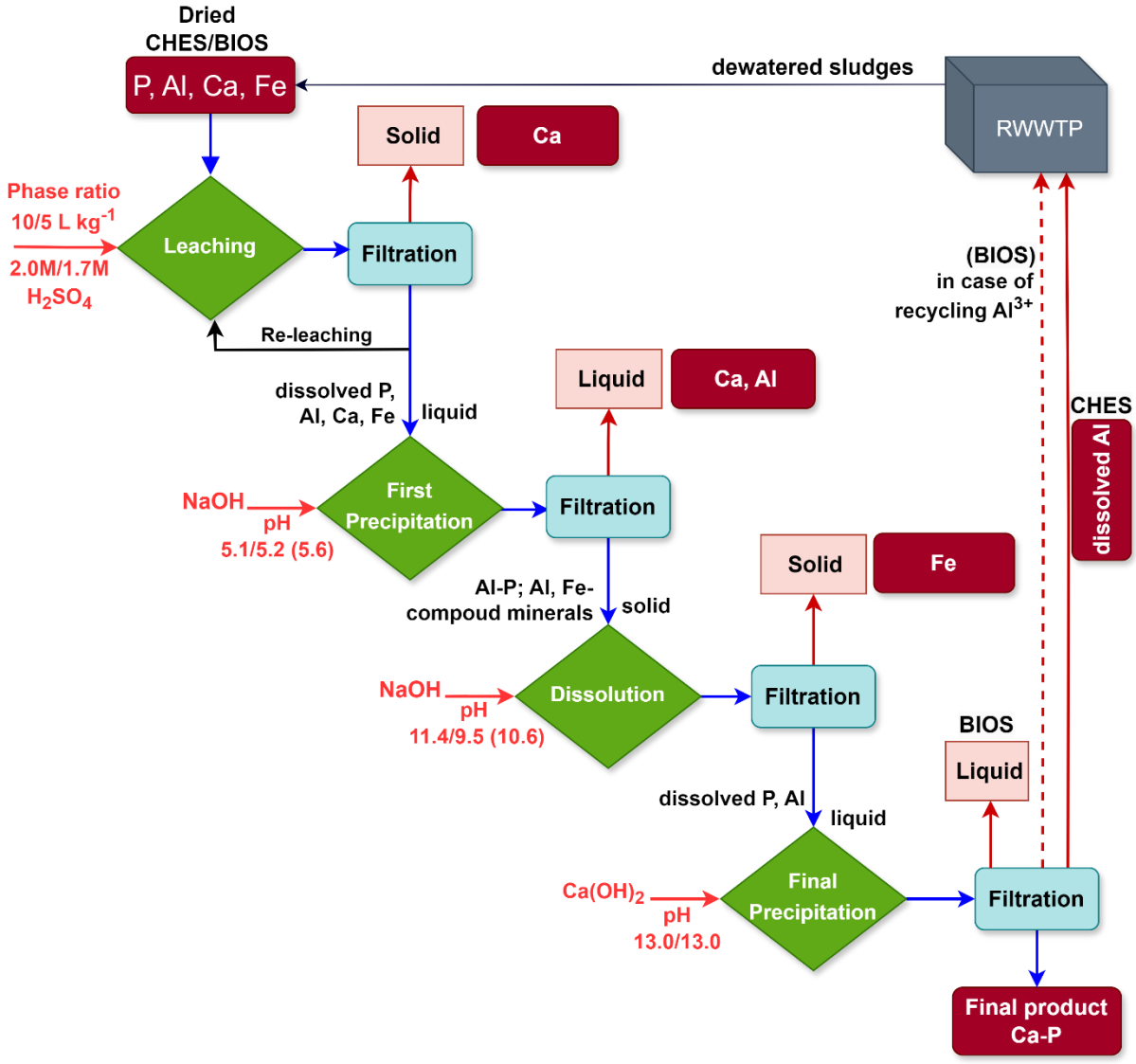

Fig. 8-1: Flowchart of developed P-recovery process, value indicated for CHES/BIOS

Overall, with the help of the SLLE simulation tool, the process can also be easily adapted to other WTTP sludges with varying compositions. A P-recovery process has been developed and validated to treat RWWTP sludges, which is suitable for application in Vietnam and allows for recovery of about 2400 t/a of P_2O_5 in Vietnam.

9 Appendix

9.1 List of Symbols

symbol	unit	description
K	-	equilibrium chemical constant
v	-	stoichiometric coefficient
I_s	-	saturation index
Q	$m^3\ d^{-1}$	flow rate
$\dot{m}$	$kg\ d^{-1}$	mass flow rate
S	$L\ person^{-1}\ d^{-1}$	water supply
C	$mg\ L^{-1}$	concentration of a substance
k_d	$g\ VSS\ g\ VSS\ d^{-1}$	endogenous decay coefficient
T	h	time
Y	$g\ VSS\ g\ BOD^{-1}$	biomass yield
q_w	$m^3\ t^{-1}$	water supply for rubber processing
W	$g\ kg^{-1}$	mass fraction
ρ	$kg\ m^{-3}$	density
a	-	activity of master species
N	-	number of species
P	person	people
R	-	ratio of volume
SS	$g\ m^{-3}$	suspended solids
Greek symbols		
γ	-	activity coefficient
μ	$Jmol^{-1}$	chemical potential
lower indices		
p		precipitating phases or species in chemical system
i		liquid phase species
m		master species
r		rural
u		urban
R, S		retention of solids
se		sediment

rp	rubber production
S	sludge

9.2 Pilot design and operating

Tank-unit for Main Steps of P-Recovery Process

The volume of tank 1 is calculated to suit the P leaching capacity for each batch for two types of studied sludge. The optimal phase ratios of liquid (H_2SO_4, liters) to solid (dry sludge, kg) for P leaching for CHES and BIOS are 5 L kg^{-1} and 10 L kg^{-1}, respectively. Subtracting 20% of the safe volume, the volume requirement for the P leaching process in tank 1 is met, even for the dissolution or precipitation steps where the volume requirement will increase due to the mixing of the two liquids (precipitation stage).

In tank 1, an overhead mixer with 2 agitator stages is used to stir the mixtures in all process steps, such as leaching, first precipitation, dissolution, and final precipitation step. A frequency converter attached to the motor is used to adjust the stirring speed as desired. During the leaching process, stirring significantly increases the contact between the solid sludge and the H_2SO_4 solution. In addition, due to the formation of gypsum precipitating from the P leaching process from Ca rich-sludge such as BIOS and CHES using H_2SO_4 agent, it can lead to pH differences in the leaching mixture if they are not stirred. And, therefore, it leads to a decrease in the P leaching efficiency if there is no stirring during the leaching process. Using an overhead mixer also has the disadvantage of increasing the volume of fine solids after leaching, which can cause problems in the following phase separation process. In this case, a solid-liquid separation was designed to overcome the problem of fine solid particles created by mixing. This is discussed in detail in the next section.

There are two pipelines to transfer liquid from other unit tanks to tank 1, including the pipeline system to transfer leached liquid from the temporary tank (tank 3) and the pipeline system to transfer chemical solutions (NaOH, $Ca(OH)_2$) from tank 4 for the precipitations and dissolution step. The specific liquids from these tanks are transferred to tank 1 in each specific operating case by a metering pump with a maximum capacity of 100 L h^{-1}. In addition, during the precipitation and the final precipitation step, the mixture from the bottom of tank 1 is continuously pumped back by the circulation pump

into the tank. The purpose of the circulating mixture is to ensure that there is no difference in equilibrium pH at any location in tank 1 at the end of the precipitation steps, especially at the bottom of the tank where mixing is limited.

Liquid and solid separation

Liquid-solid phase separation is an important step that is performed after each main step in the P-recovery process. Therefore, the products to be recovered after each phase separation are also different. In the phase separation step, immediately after the leaching and dissolution step, the recovered products are leached liquid and dissolved liquid, and the remaining residue solids are discarded. As for the phase separation after the precipitation steps, the products recovered are solid precipitates.

Due to the large fineness of the insoluble solids remaining in each major step of the P-recovery process, especially at the leaching and precipitation steps, liquid-solid separation by conventional single-stage filtration is very difficult. Trials with gravity filtration using a 300 µm pore-size filter plate showed that the liquid-solid separation efficiency was very low, with most of the fine particles easily passing through the filter. However, using a filter plate with a smaller pore size, for example, 10 µm, the filtration rate was extremely slow due to rapid clogging of the filter pores. Unsuccessful trials of liquid-solid separation after precipitation and dissolution step were also reported by using gravity single-stage filtration, with even worse results. In addition, the pilot operating procedure shows that the solid-liquid phase separation steps will only take place at tank 2, meaning that the phase separation filtration solution needs to be flexibly designed to be applicable to each specific case.

To eliminate the possibility of filter plate clogging and to suit each specific phase separation case, a multi-stage filter column is designed, which includes many filter columns with different corresponding filter pore sizes. These columns are nested together according to the principle of filter columns using large pore size filter plates on top to retain large particles first, then filter columns using filter plates with smaller pore sizes. Depending on each specific case, these filter columns will be used in combination with each other to separate liquid-solid phases. The structure and procedure of using multi-stage filtration for liquid-solid phase separation are shown in Fig. A 9-1. The multi-stage filter consists of 3 separate filter columns, each using a filter plate with a different pore

size. Filter columns 1, 2, and 3 use plates with pore sizes of 300, 10, and 1 µm, respectively.

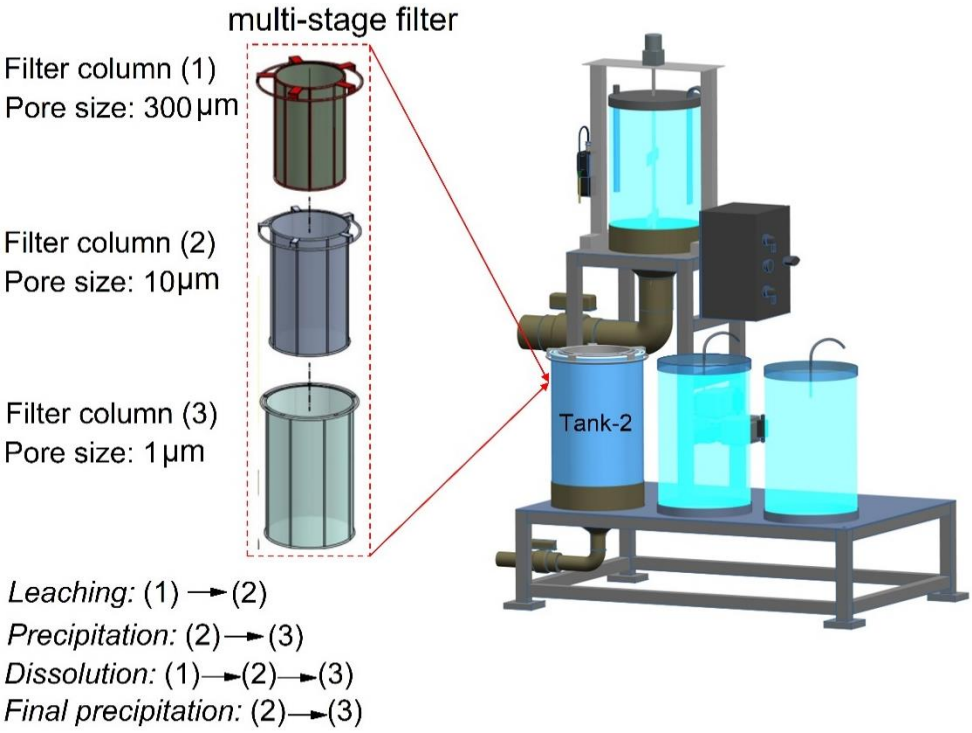

Fig. A 9-1: Structure of multi-stages filter column and the function of each filter column

For the separation of the liquid-solid phase after the leaching step, the liquid-solid mixture is transferred directly to the multi-stage filter column through the pipeline due to the difference in elevation between tank 1 and tank 2. Then, the mixture is filtered in order from filter column 1 to filter column 2. After the solid-liquid phase separation of the leaching step, the leached liquid is recovered. The remaining insoluble solids are washed with water at the multi-stage filtration column (tank 2) to further recover P and residual acid. This washing water is then reused to prepare the H_2SO_4 solution for the next leaching batch. In addition, washing the leached sludge with water also significantly reduces the acidity of the remaining solids after leaching - the substance that must be treated.

The separation of the liquid-solid phases after the precipitation steps are carried out through 2 filter columns in the order of filter column 2 to filter column 3. Correspondingly, the precipitates will be retained in both filter plates with pore sizes from 10 to 1 µm. The recovered precipitates retained on the multi-stage filters are carefully collected

and transferred to stainless steel trays. All three filter columns are used to separate the remaining solids after the dissolution step.

It should be noted that the liquid collected after the last filter column needs to be pumped back to the multi-stage filter column by the circulation pump until the filtration efficiency reaches the best efficiency, and then stops. Normally, at the beginning of each filtration process, fine particles often pass through the filter membrane, leading to a significant reduction in filtration efficiency. Only when the structure of the filtered solid layer is stabilized, the filtration efficiency will be increased.

Precipitates Filtration on pilot operating

At the beginning of filtration, the precipitate mixture was filtered through a 10 µm pore-size filter plate. A pump was used to circulate the mixture back to the filter column until the precipitate layer stabilized on the filter plate and the filtered liquid became clear. The precipitates from pilot trials were recovered after filtration by using 10 µm pore-size filter plate, are shown in Fig. A 9-2. Then, a 1 µm pore-size filter was used to continue filtering once more. This multi-stage filtration process increased the filtration rate (compared to if a 1 µm pore-size filter was used at the same time from the beginning) and maximized the recovery of precipitate particles in the mixture.

Fig. A 9-2: The thick and stable precipitate layer in the 10 µm pore-size filter plate

Pilot Setting up

The overall layout of the pilot is shown in Fig. A 9-3. The pilot is designed with basic dimensions of 800 x 1200 x 1800mm. The entire pilot frame, as well as the floor where the tank units are placed, are made of stainless steel and painted with anti-corrosion paint. The pilot is placed on four wheels with adjustable locks for easy movement in the laboratory at IUH.

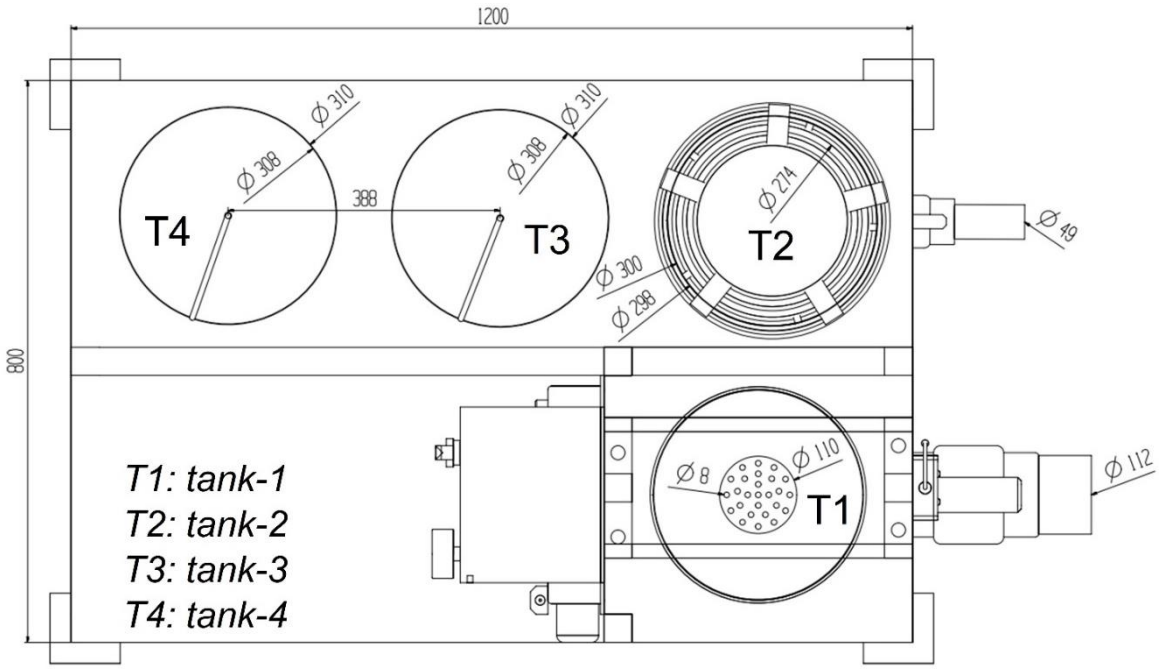

Fig. A 9-3: General layout of pilot units

The details of the pilot parts in order of installation are shown in Fig. A 9-4.

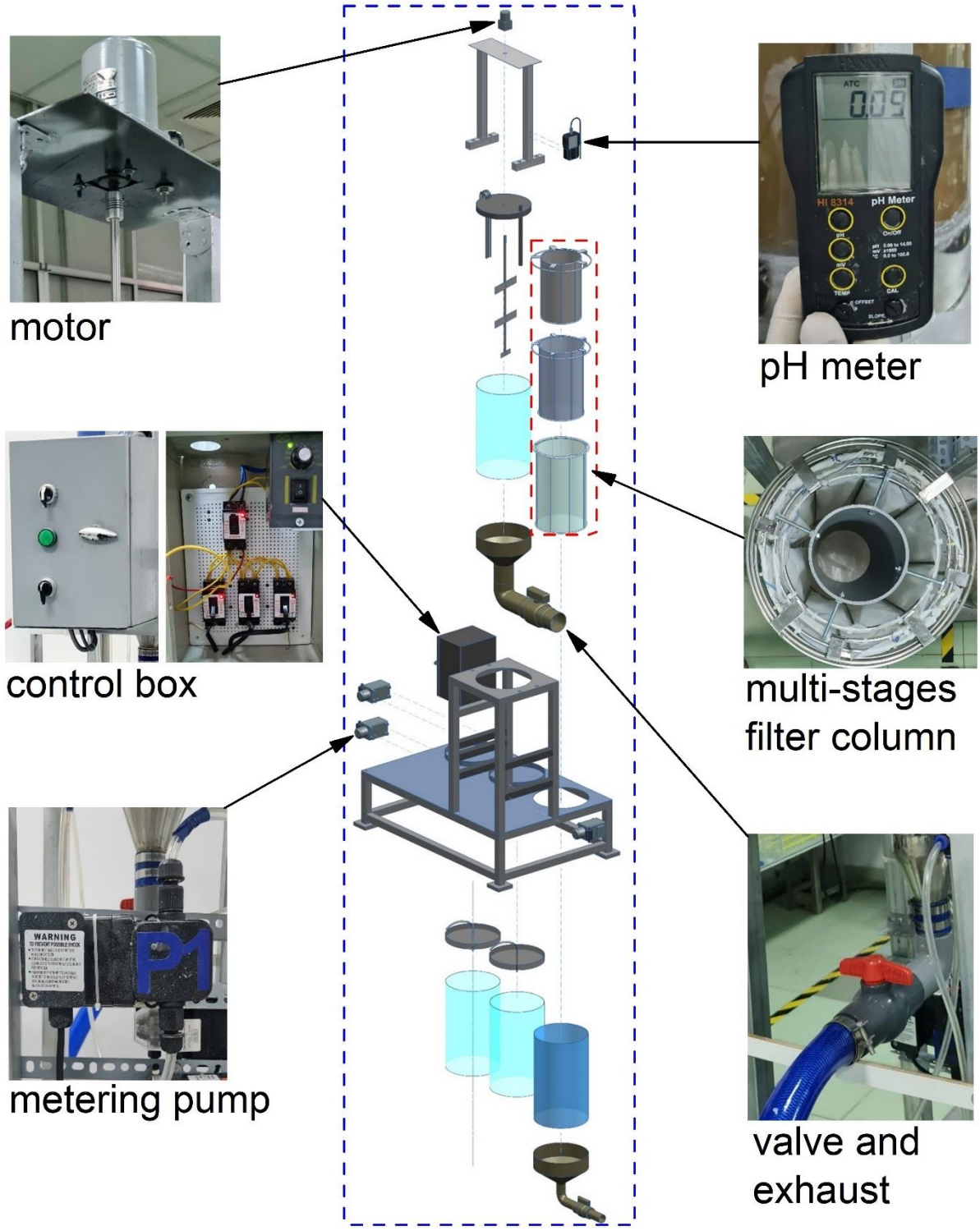

Fig. A 9-4: Pilot parts in order of installation

The pilot is designed and operated in batches, so the main stages of the P-recovery process take place mainly in 2 tanks, namely the reaction tank: Tank 1 and the multi-stage filter column for liquid-solid separation: Tank 2. Therefore, the area requirement

is very low and the pilot structure becomes much simpler. The mixing system, support, and cover on Tank 1 are designed to be quickly removed using a 1-step release lock in case of loading input dried sludge material into the tank or for maintenance. In addition, to limit the emission of toxic vapors into the environment during the leaching process, especially acid vapors, a gas collection system was also installed. The toxic vapors were led directly into the bottle of alkaline solution $Ca(OH)_2$, as shown in Fig. A 9-5.

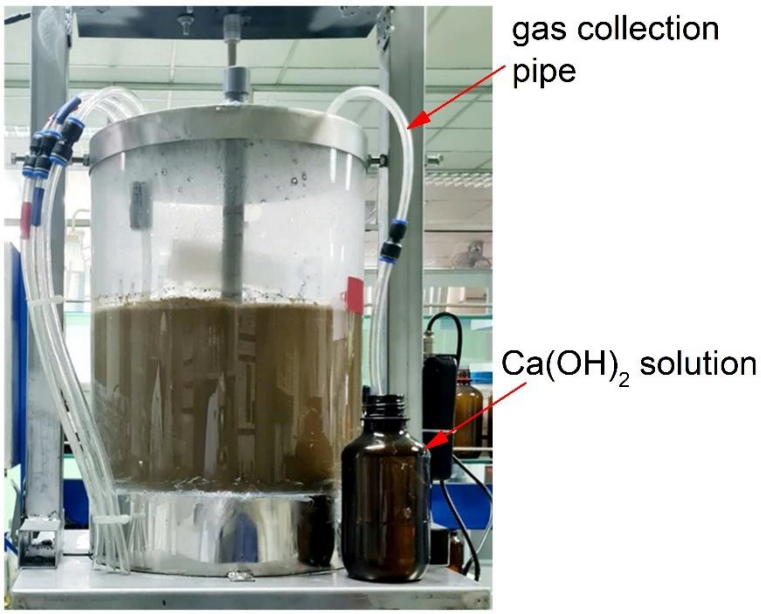

Fig. A 9-5: Generated gas collection pipe from leaching step

The flexible pipe system and control valve are connected from the bottom of Tank 1 to transfer the mixture after each process to Tank 2 based on the difference in elevation between the two tanks. This has reduced the use of pumps. The units for sludge preparation, such as the forced-convection oven and the crusher machine, are located directly in the laboratory together with the other pilot units for operating.

The images of the input dried sludges and products through the steps of the P-recovery process are shown in Fig A 9-6. The precipitate was dried to constant mass at 100°C and collected as the final precipitate. The mass ratio of the final precipitates and the input dried sludge used was approximately 18.9% for BIOS and and 25.1% for CHES.

Fig. A 9-6: Images of input dried sludges and products from the P-recovery process

Tab. A 9-1: Price of categories for cost estimation

Category	Unit	Price	Reference
H_2SO_4 98%	USD/L	0.588	(HPDON, 2024)
HCl 37%	USD/L	0.161	(Vu Hoang Chemicals, 2024)
HNO_3 65%	USD/L	0.656	(MINACHEM, 2024)
NaOH 99%	USD/kg	0.722	(HPDON, 2024)
$Ca(OH)_2$ 93%	USD/kg	0.206	(HPDON, 2024)
Electricity	USD/kWh	0.072	(EVN, 2024)
Water supply	USD/m^3	0.500	(SAWACO, 2024)
PAC (30% Al_2O_3)	USD/kg	0.577	(HANTECO VIETNAM, 2014)
P_2O_5 68%	USD/kg	1.973	(Alibaba, 2024)

9.3 Collected data for P-reserves calculation

Tab. A 9-2: Annual pig production in Southern Vietnam from 2015 to 2018

Province/City	Annual pig production			
	2015	2016	2017	2018
	Thousand head	Thousand head	Thousand head	Thousand head
Binh Phuoc	456.05	504.87	504.48	527.66
Tay Ninh	474.02	458.15	431.55	398.56
Binh Duong	956.36	1,107.73	1,002.38	1,032.57
Dong Nai	2,482.95	3,050.63	2,942.39	2,993.14
Ba Ria - Vung Tau	706.90	738.20	714.82	728.61
Ho Chi Minh	586.75	630.52	612.78	626.95
Long An	449.89	461.10	416.92	349.96
Tien Giang	1,151.64	1,133.38	1,103.28	1,150.04
Ben Tre	979.46	1,028.77	976.12	984.28
Tra Vinh	548.32	632.24	603.16	576.53
Vinh Long	632.05	665.60	598.81	591.78
Dong Thap	343.89	444.09	395.86	411.13
An Giang	182.42	193.54	157.65	158.14
Kien Giang	468.70	587.58	527.88	529.99
Can Tho	195.77	223.42	212.13	223.96
Hau Giang	245.18	289.32	289.15	298.99
Soc Trang	496.81	601.00	544.70	500.24
Bac Lieu	459.41	351.84	366.58	396.15
Ca Mau	205.75	214.32	218.38	209.35
TOTAL	12,022.32	13,316.30	12,619.02	12,688.03

Tab. A 9-3: Cattle in Southern Vietnam from 2015 to 2018

Province/City	Cattle farming			
	2015	2016	2017	2018
	Thousand head	Thousand head	Thousand head	Thousand head
Binh Phuoc	28.00	28.50	29.80	30.42
Tay Ninh	86.10	89.50	95.40	82.23
Binh Duong	22.40	23.20	24.00	23.42
Dong Nai	68.40	71.00	75.30	70.00
Ba Ria - Vung Tau	36.60	37.50	40.00	32.77
Ho Chi Minh	125.60	127.70	125.00	123.77
Long An	86.00	90.30	95.80	80.50
Tien Giang	80.30	83.70	86.50	85.50
Ben Tre	155.60	162.70	170.20	174.38
Tra Vinh	141.00	148.20	155.70	156.84
Vinh Long	60.00	61.60	64.50	66.79
Dong Thap	23.20	24.40	24.90	20.20
An Giang	100.70	96.00	81.50	63.63
Kien Giang	10.10	10.30	11.10	1.74
Can Tho	3.60	3.90	4.10	2.51
Hau Giang	1.60	1.70	1.80	2.21
Soc Trang	25.50	27.60	29.10	21.02
Bac Lieu	1.20	1.10	1.00	0.10
Ca Mau	0.30	0.40	0.50	0.35
TOTAL	1056.20	1089.30	1116.20	1038.38

Tab. A 9-4: Rubber-latex production in Southern Vietnam from 2015 to 2018

Year	Area	Harvesting area	Production of latex
	ha	ha	tons
2015	546,100	395,400	728,800
2016	543,000	404,200	748,000
2017	548,900	417,200	777,200
2018	566,464	430,550	802,070

Tab. A 9-5: Catfish farming area in Southern Vietnam from 2015 to 2018

Province/City	Catfish farming area			
	2015	2016	2017	2018
	ha	ha	ha	ha
Tien Giang	111	167	164	93
Ben Tre	730	760	769	770
Tra Vinh	10	41	38	65
Vinh Long	444	458	458	468
Dong Thap	2,071	2,033	2,465	2,450
An Giang	1,233	1,262	1,368	1,696
Kien Giang	2	2	3	3
Can Tho	837	698	733	750
Hau Giang	114	95	103	119
Soc Trang	71	35	66	94
TOTAL	5,623	5,551	6,167	6,508

Tab. A 9-6: Population in Southern Vietnam from 2015 to 2018

Province/City	2015		2016		2017		2018	
	Urban	Rural	Urban	Rural	Urban	Rural	Urban	Rural
	thousand		thousand		thousand		thousand	
Binh Phuoc	209.9	734.5	189.0	767.4	193.1	775.8	201.1	778.5
Tay Ninh	246.6	864.9	249.7	869.1	252.8	873.4	257.3	861.5
Binh Duong	1,485.8	444.6	1,527.0	468.8	1,577.9	493.1	1,669.7	471.0
Dong Nai	1,006.4	1,891.2	1,037.2	1,924.6	1,069.0	1,958.3	1,114.1	1,980.5
Ba Ria - Vung Tau	550.1	529.0	560.8	529.5	571.7	529.9	591.3	524.3
Ho Chi Minh	6,632.8	1,495.1	6,733.1	1,553.9	6,825.3	1,619.3	7,240.8	1,483.0
Long An	267.5	1216.5	268.7	1221.7	269.8	1227	271.4	1236.5
Tien Giang	266.1	1462	269.8	1470.3	271.4	1480.4	264.5	1498.8
Ben Tre	131.1	1132.6	133.1	1132.1	135.1	1131.6	139.5	1128.9
Tra Vinh	183.3	851.3	186.3	854.2	189.2	856.4	189.2	862.0
Vinh Long	176.3	868.8	177.5	871.1	178.2	872.0	179.6	876.8
Dong Thap	299.3	1,385.0	299.8	1,387.5	300.3	1,390.0	304.9	1,388.8
An Giang	653.2	1,505.1	664.1	1,495.8	664.7	1,497.0	692.7	1472.0
Kien Giang	485.2	1,275.8	506.3	1,270.4	528.4	1,264.2	540.1	1,260.1
Can Tho	833.0	415.0	844.7	417.9	853.6	419.2	881.8	396.1
Hau Giang	188.7	581.8	191.4	581.1	194.2	580.4	202.0	574.9
Soc Trang	401.1	909.6	401.6	910.9	402.2	912.1	422.1	896.8
Bac Lieu	232.5	649.5	233.6	652.6	261.9	632.4	268.4	626.4
Ca Mau	275.8	943.1	277.0	945.6	278.2	948.1	294.4	932.3

9.4 Sample analysis

Tab. A 9-7: P leaching results at different sludge particle sizes and leaching time using phase ratio 20 mL g^{-1} and 1M H_2SO_4, for CHES

	Element concentrations in leach liquid after leaching								
Particle size	30 mins.	60 mins.	90 mins.	120 mins.	150 mins.	180 mins.	210 mins.	240 mins.	270 mins.
mm	mol L^{-1}	mol L^{-1}	mol L^{-1}	mol L^{-1}	mol L^{-1}	mol L^{-1}	mol L^{-1}	mol L^{-1}	mol L^{-1}
< 1	0.0764	0.0773	0.0790	0.0790	0.0790	0.0790	0.0773	0.0764	0.0737
1 to 2.5	0.0737	0.0755	0.0764	0.0773	0.0781	0.0773	0.0764	0.0746	0.0728
2.5 to 5	0.0675	0.0710	0.0719	0.0737	0.0746	0.0755	0.0746	0.0728	0.0728
> 5	0.0604	0.0639	0.0666	0.0702	0.0746	0.0746	0.0737	0.0737	0.0710

Tab. A 9-8: Al leaching results at different particle sizes and leaching time using phase ratio 20 mL g^{-1} and 1M H_2SO_4, for CHES

Particle size	Element concentrations in leach liquid after leaching								
	30 min	60 min	90 min	120 min	150 min	180 min	210 min	240 min	270 min
mm	mol L^{-1}	mol L^{-1}	mol L^{-1}	mol L^{-1}	mol L^{-1}	mol L^{-1}	mol L^{-1}	mol L^{-1}	mol L^{-1}
< 1	0.1993	0.2056	0.2056	0.2056	0.2056	0.2014	0.2056	0.1993	0.1951
1 to 2.5	0.1888	0.1993	0.2014	0.2035	0.2056	0.2035	0.2035	0.1993	0.1951
2.5 to 5	0.1783	0.1867	0.1951	0.1993	0.2056	0.2056	0.2056	0.1993	0.1930
> 5	0.1699	0.1741	0.1846	0.1930	0.1993	0.2014	0.2035	0.2014	0.1909

Tab. A 9-9: Ca leaching results at different particle sizes and leaching time using phase ratio 20 mL g^{-1} and 1M H_2SO_4, for CHES

Particle size	Element concentrations in leach liquid after leaching								
	30 min	60 min	90 min	120 min	150 min	180 min	210 min	240 min	270 min
mm	mol L^{-1}	mol L^{-1}	mol L^{-1}	mol L^{-1}	mol L^{-1}	mol L^{-1}	mol L^{-1}	mol L^{-1}	mol L^{-1}
< 1	0.0120	0.0128	0.0132	0.0132	0.0132	0.0132	0.012	0.0112	0.0096
1 to 2.5	0.0116	0.0128	0.0128	0.0132	0.0132	0.0128	0.0124	0.0112	0.0096
2.5 to 5	0.0104	0.0124	0.0124	0.0132	0.0132	0.0132	0.0120	0.0112	0.0096
> 5	0.0092	0.0104	0.0112	0.0124	0.0124	0.0128	0.0116	0.0112	0.0096

Tab. A 9-10: Fe leaching results at different particle sizes and leaching time using phase ratio 20 mL g^{-1} and 1M H_2SO_4, for CHES

Particle size	Element concentrations in leach liquid after leaching								
	30 min	60 min	90 min	120 min	150 min	180 min	210 min	240 min	270 min
mm	mol L^{-1}	mol L^{-1}	mol L^{-1}	mol L^{-1}	mol L^{-1}	mol L^{-1}	mol L^{-1}	mol L^{-1}	mol L^{-1}
< 1	0.0041	0.0045	0.0047	0.0048	0.0047	0.0047	0.0048	0.0045	0.0043
1 to 2.5	0.0039	0.0043	0.0047	0.0047	0.0047	0.0047	0.0047	0.0046	0.0046
2.5 to 5	0.0037	0.0042	0.0047	0.0048	0.0048	0.0048	0.0047	0.0047	0.0043
> 5	0.0034	0.0037	0.0039	0.0040	0.0041	0.0042	0.0042	0.0043	0.0043

Tab. A 9-11: P leaching results at different particle sizes and leaching time using phase ratio 20 mL $g^{-1}$and 1M H_2SO_4, for BIOS

	Element concentrations in leach liquid after leaching								
Particle size	30 min	60 min	90 min	120 min	150 min	180 min	210 min	240 min	270 min
mm	mol L^{-1}	mol L^{-1}	mol L^{-1}	mol L^{-1}	mol L^{-1}	mol L^{-1}	mol L^{-1}	mol L^{-1}	mol L^{-1}
< 1	0.0489	0.0523	0.0534	0.0539	0.0534	0.0534	0.0539	0.0539	0.0528
1 to 2.5	0.0484	0.0528	0.0534	0.0528	0.0545	0.0528	0.0528	0.0523	0.0523
2.5 to 5	0.0473	0.0517	0.0523	0.0528	0.0528	0.0528	0.0523	0.0528	0.0528
> 5	0.0439	0.0461	0.0495	0.0512	0.0512	0.0523	0.0523	0.0523	0.0523

Tab. A 9-12: Al leaching results at different particle sizes and leaching time using phase ratio 20 mL g^{-1} and 1M H_2SO_4, for BIOS

	Element concentrations in leach liquid after leaching								
2	30 min	60 min	90 min	120 min	150 min	180 min	210 min	240 min	270 min
mm	mol L^{-1}	mol L^{-1}	mol L^{-1}	mol L^{-1}	mol L^{-1}	mol L^{-1}	mol L^{-1}	mol L^{-1}	mol L^{-1}
< 1	0.0335	0.0342	0.0345	0.0345	0.0345	0.0349	0.0349	0.0349	0.0349
1 to 2.5	0.0320	0.0335	0.0342	0.0345	0.0342	0.0349	0.0349	0.0345	0.0338
2.5 to 5	0.0299	0.0317	0.0335	0.0338	0.0342	0.0342	0.0342	0.0345	0.0335
> 5	0.0278	0.0292	0.0310	0.0328	0.0338	0.0342	0.0338	0.0342	0.0335

Tab. A 9-13: Ca leaching results at different particle sizes and leaching time using phase ratio 20 mL g^{-1} and 1M H_2SO_4, for BIOS

2	Element concentrations in leach liquid after leaching								
	30 min	60 min	90 min	120 min	150 min	180 min	210 min	240 min	270 min
mm	mol L^{-1}	mol L^{-1}	mol L^{-1}	mol L^{-1}	mol L^{-1}	mol L^{-1}	mol L^{-1}	mol L^{-1}	mol L^{-1}
< 1	0.0179	0.0196	0.0196	0.0196	0.0196	0.0196	0.0186	0.0179	0.0175
1 to 2.5	0.0172	0.0196	0.0196	0.0193	0.0193	0.0196	0.0186	0.0179	0.0175
2.5 to 5	0.0172	0.0186	0.0193	0.0189	0.0189	0.0189	0.0189	0.0175	0.0172
> 5	0.0144	0.0165	0.0179	0.0186	0.0189	0.0189	0.0189	0.0182	0.0179

Tab. A 9-14: Fe leaching results at different particle sizes and leaching time using phase ratio 20 mL g^{-1} and 1M H_2SO_4, for BIOS

Particle size	Element concentrations in leach liquid after leaching								
	30 min	60 min	90 min	120 min	150 min	180 min	210 min	240 min	270 min
mm	mol L^{-1}	mol L^{-1}	mol L^{-1}	mol L^{-1}	mol L^{-1}	mol L^{-1}	mol L^{-1}	mol L^{-1}	mol L^{-1}
< 1	0.0087	0.0090	0.0090	0.0090	0.0090	0.0089	0.0089	0.0089	0.0089
1 to 2.5	0.0086	0.0088	0.0088	0.0090	0.0090	0.0088	0.0089	0.0089	0.0089
2.5 to 5	0.0086	0.0086	0.0087	0.0087	0.0089	0.0090	0.0089	0.0088	0.0090
> 5	0.0082	0.0085	0.0085	0.0086	0.0086	0.0086	0.0085	0.0087	0.0086

Tab. A 9-15: Experimental results on P leaching at different phase ratios and leaching time by using 1M H_2SO_4, for CHES

Phase ratio mL g^{-1}	Input P concentration mol L^{-1}	P concentration after leaching mol L^{-1}				
		60 min	90 min	120 min	150 min	180 min
5.02	0.3540	0	0	0	0	0
5.99	0.2966	0	0	0	0	0
6.99	0.2542	0	0	0	0	0
8.01	0.2218	0	0	0	0	0
8.96	0.1983	0.0139	0.0169	0.0169	0.0184	0.0169
9.99	0.1779	0.0169	0.0190	0.0189	0.0171	0.0174
10.99	0.1617	0.0178	0.0186	0.0186	0.0181	0.0186
11.99	0.1482	0.0181	0.0193	0.0170	0.0185	0.0178
12.94	0.1373	0.0181	0.0206	0.0207	0.0199	0.0172
13.86	0.1282	0.0436	0.0429	0.0429	0.0449	0.0429
14.93	0.1190	0.0631	0.0631	0.0612	0.0637	0.0607
16.03	0.1108	0.0643	0.0632	0.0626	0.0620	0.0637
17.17	0.1035	0.0631	0.0652	0.0631	0.0626	0.0637
17.92	0.0992	0.0636	0.0650	0.0655	0.0650	0.0645
18.91	0.0940	0.0682	0.0673	0.0667	0.0682	0.0667
20.01	0.0888	0.0696	0.0713	0.0699	0.0718	0.0720
20.96	0.0848	0.0742	0.0732	0.0750	0.0762	0.0757
21.99	0.0808	0.0760	0.0768	0.0755	0.0764	0.0751
22.95	0.0774	0.0739	0.0731	0.0739	0.0743	0.0724
23.92	0.0743	0.0702	0.0714	0.0698	0.0709	0.0698
24.9	0.0714	0.0682	0.0682	0.0671	0.0682	0.0678
29.9	0.0594	0.0561	0.0555	0.0564	0.0555	0.0555

Tab. A 9-16: Experimental results on Ca leaching at different phase ratios and leaching time by using 1M H_2SO_4, for CHES

Phase ratio mL g^{-1}	Input Ca concentration mol L^{-1}	Ca concentration after leaching mol L^{-1}				
		60 min	90 min	120 min	150 min	180 min
5.02	0.1602	0.0070	0.0070	0.0073	0.0065	0.0070
5.99	0.1343	0.0094	0.0094	0.0094	0.0094	0.0094
6.99	0.1151	0.0092	0.0092	0.0092	0.0092	0.0092
8.01	0.1004	0.0090	0.0090	0.0090	0.0090	0.0090
8.96	0.0898	0.0087	0.0087	0.0087	0.0087	0.0087
9.99	0.0805	0.0086	0.0087	0.0084	0.0083	0.0087
10.99	0.0732	0.0092	0.0092	0.0092	0.0092	0.0092
11.99	0.0671	0.0090	0.0090	0.0090	0.0090	0.0090
12.94	0.0622	0.0090	0.0090	0.0090	0.0090	0.0090
13.86	0.0580	0.0087	0.0087	0.0087	0.0087	0.0087
14.93	0.0539	0.0093	0.0096	0.0098	0.0100	0.0098
16.03	0.0502	0.0090	0.0095	0.0093	0.0090	0.0093
17.17	0.0468	0.0103	0.0112	0.0101	0.0103	0.0105
17.92	0.0449	0.0114	0.0119	0.0119	0.0121	0.0123
18.91	0.0425	0.0121	0.0128	0.0125	0.0123	0.0121
20.01	0.0402	0.0129	0.0126	0.0133	0.0130	0.0135
20.96	0.0384	0.0136	0.0138	0.0138	0.0136	0.0134
21.99	0.0366	0.0140	0.0142	0.0137	0.0137	0.0143
22.95	0.0350	0.0147	0.0147	0.0147	0.0149	0.0150
23.92	0.0336	0.0152	0.0151	0.0153	0.0156	0.0151
24.90	0.0323	0.0156	0.0156	0.0152	0.0155	0.0155
29.90	0.0269	0.0154	0.0152	0.0157	0.0156	0.0153

Tab. A 9-17: Experimental results on Al leaching at different phase ratios and leaching time by using 1M H_2SO_4, for CHES

Phase ratio mL g^{-1}	Input Al concentration mol L^{-1}	Al concentration after leaching mol L^{-1}				
		60 min	90 min	120 min	150 min	180 min
5.02	0.8364	0.2313	0.2283	0.2339	0.2339	0.2295
5.99	0.7009	0.2103	0.2173	0.2138	0.2033	0.2068
6.99	0.6006	0.2492	0.2432	0.2432	0.2432	0.2342
8.01	0.5242	0.2490	0.2385	0.2411	0.2516	0.2542
8.96	0.4686	0.2366	0.2413	0.2530	0.2460	0.2484
9.99	0.4203	0.2375	0.2373	0.2343	0.2434	0.2405
10.99	0.3820	0.2254	0.2177	0.2235	0.2197	0.2197
11.99	0.3502	0.2189	0.2101	0.2154	0.2241	0.2171
12.94	0.3245	0.2937	0.2839	0.2856	0.2839	0.2937
13.86	0.3029	0.2787	0.2832	0.2772	0.2802	0.2802
14.93	0.2812	0.2621	0.2593	0.2619	0.2593	0.2660
16.03	0.2619	0.2462	0.2488	0.2462	0.2436	0.2462
17.17	0.2445	0.2274	0.2274	0.2323	0.2335	0.2311
17.92	0.2343	0.2273	0.2238	0.2249	0.2273	0.2249
18.91	0.2220	0.2120	0.2142	0.2131	0.2142	0.2131
20.01	0.2098	0.2085	0.2092	0.2060	0.2069	0.2026
20.96	0.2003	0.1965	0.1965	0.1949	0.1969	0.1952
21.99	0.1909	0.1871	0.1852	0.1852	0.1852	0.1861
22.95	0.1829	0.1774	0.1756	0.1738	0.1765	0.1765
23.92	0.1755	0.1702	0.1676	0.1685	0.1694	0.1694
24.90	0.1686	0.1652	0.1635	0.1635	0.1619	0.1610
29.90	0.1404	0.1355	0.1355	0.1334	0.1341	0.1362

Tab. A 9-18: Experimental results on Fe leaching at different phase ratios and leaching time by using 1M H_2SO_4, for CHES

Phase ratio mL g^{-1}	Input Fe concentration mol L^{-1}	Fe concentration after leaching mol L^{-1}				
		60 min	90 min	120 min	150 min	180 min
5.02	0.0418	0	0	0	0	0
5.99	0.0350	0	0	0	0	0
6.99	0.0300	0	0	0	0	0
8.01	0.0262	0	0	0	0	0
8.96	0.0234	0	0	0	0	0
9.99	0.0210	0	0	0	0	0
10.99	0.0191	0	0	0	0	0
11.99	0.0175	0	0	0	0	0
12.94	0.0162	0	0	0	0	0
13.86	0.0151	0	0	0	0	0
14.93	0.0140	0.0001	0.0001	0.0001	0.0002	0.0002
16.03	0.0131	0.0007	0.0005	0.0005	0.0006	0.0008
17.17	0.0122	0.0009	0.0006	0.0007	0.0009	0.0005
17.92	0.0117	0.0017	0.0017	0.0017	0.0015	0.0017
18.91	0.0111	0.0032	0.0031	0.0033	0.0033	0.0033
20.01	0.0105	0.0043	0.0046	0.0045	0.0041	0.0043
20.96	0.0100	0.0061	0.0062	0.0062	0.0062	0.0063
21.99	0.0095	0.0088	0.0089	0.0088	0.0088	0.0089
22.95	0.0091	0.0087	0.0086	0.0087	0.0087	0.0088
23.92	0.0088	0.0085	0.0084	0.0084	0.0084	0.0084
24.9	0.0084	0.0081	0.0080	0.0080	0.0080	0.0081
29.9	0.0070	0.0067	0.0067	0.0067	0.0067	0.0067

Tab. A 9-19: Experimental results on P leaching at different phase ratios and leaching time by using 1M H_2SO_4, for BIOS

Phase ratio mL g^{-1}	Input P concentration mol L^{-1}	P concentration after leaching mol L^{-1}				
		60 min	90 min	120 min	150 min	180 min
5.03	0.2210	0.095	0.0972	0.0972	0.0983	0.1006
5.99	0.1856	0.0965	0.1012	0.0974	0.0993	0.0956
6.97	0.1595	0.1077	0.1069	0.1013	0.1077	0.1045
8.05	0.1381	0.1029	0.1015	0.0953	0.1008	0.0994
8.96	0.1241	0.0999	0.1024	0.1018	0.1005	0.1024
9.96	0.1116	0.0977	0.1010	0.0993	0.1021	0.1016
10.98	0.1013	0.0912	0.0932	0.0932	0.0912	0.0902
11.98	0.0928	0.0886	0.0882	0.0882	0.0891	0.0886
12.95	0.0859	0.0816	0.0825	0.0825	0.0816	0.0812
13.92	0.0799	0.0755	0.0759	0.0767	0.0771	0.0771
14.93	0.0745	0.0723	0.0723	0.0719	0.0726	0.0730
15.97	0.0696	0.0672	0.0668	0.0668	0.0661	0.0665
16.99	0.0654	0.0621	0.0628	0.0628	0.0631	0.0634
17.99	0.0618	0.0593	0.0593	0.0603	0.0590	0.0603
18.97	0.0586	0.0560	0.0565	0.0563	0.0563	0.0565
20.01	0.0556	0.0539	0.0537	0.0539	0.0539	0.0539
20.96	0.0530	0.0511	0.0509	0.0517	0.0509	0.0511
21.99	0.0506	0.0491	0.0493	0.0488	0.0493	0.0491
22.95	0.0484	0.0469	0.0467	0.0467	0.0472	0.0469
23.92	0.0465	0.0451	0.0446	0.0456	0.0451	0.0451
24.96	0.0445	0.0432	0.0436	0.0432	0.0434	0.0427
29.93	0.0371	0.0360	0.0360	0.0364	0.0362	0.0358

Tab. A 9-20: Experimental results on Ca leaching at different phase ratios and leaching time by using 1M H_2SO_4, for BIOS

Phase ratio mL g^{-1}	Input Ca concentration mol L^{-1}	Ca concentration after leaching mol L^{-1}				
		60 min	90 min	120 min	150 min	180 min
5.03	0.1393	0.0104	0.0098	0.0098	0.0098	0.0091
5.99	0.1169	0.0123	0.014	0.0134	0.0129	0.0134
6.97	0.1005	0.0141	0.0141	0.0146	0.0146	0.0141
8.05	0.0870	0.0152	0.0152	0.0148	0.0144	0.0152
8.96	0.0782	0.0156	0.016	0.0156	0.0152	0.0149
9.96	0.0703	0.0158	0.0158	0.0162	0.0158	0.0162
10.98	0.0638	0.0169	0.0172	0.0166	0.016	0.0169
11.98	0.0585	0.0170	0.0170	0.0161	0.0161	0.0161
12.95	0.0541	0.0168	0.0173	0.0176	0.0173	0.0168
13.92	0.0503	0.0171	0.0171	0.0169	0.0163	0.0169
14.93	0.0469	0.0159	0.0164	0.0159	0.0155	0.0164
15.97	0.0439	0.0167	0.0165	0.0173	0.0156	0.0165
16.99	0.0412	0.0171	0.0165	0.0169	0.0159	0.0165
17.99	0.0389	0.0161	0.0161	0.0159	0.0158	0.0165
18.97	0.0369	0.0159	0.0157	0.0148	0.0164	0.0159
20.01	0.0350	0.0168	0.0158	0.0165	0.0172	0.0179
20.96	0.0334	0.0182	0.0180	0.0180	0.0182	0.0180
21.99	0.0319	0.0175	0.0177	0.0179	0.0174	0.0177
22.95	0.0305	0.0174	0.0174	0.0175	0.0168	0.0171
23.92	0.0293	0.0176	0.0171	0.0176	0.0177	0.0168
24.96	0.0281	0.0173	0.0170	0.0171	0.0176	0.0170
29.93	0.0234	0.0170	0.0173	0.0173	0.0176	0.0171

Tab. A 9-21: Experimental results on Al leaching at different phase ratios and leaching time by using 1M H_2SO_4, for BIOS

Phase ratio mL g^{-1}	Input Al concentration mol L^{-1}	Al concentration after leaching mol L^{-1}				
		60 min	90 min	120 min	150 min	180 min
5.03	0.1417	0.1332	0.1332	0.1339	0.1332	0.1346
5.99	0.1190	0.1142	0.1119	0.1131	0.1107	0.1125
6.97	0.1023	0.0967	0.0982	0.0967	0.0977	0.0972
8.05	0.0886	0.0864	0.0855	0.0855	0.0868	0.0859
8.96	0.0796	0.0764	0.0768	0.078	0.0764	0.0768
9.96	0.0716	0.0695	0.0698	0.0687	0.0695	0.0691
10.98	0.0649	0.0626	0.0636	0.0626	0.0633	0.0630
11.98	0.0595	0.0571	0.0577	0.058	0.0577	0.0574
12.95	0.0550	0.0539	0.0536	0.0531	0.0536	0.0534
13.92	0.0512	0.0494	0.0494	0.0497	0.0502	0.0502
14.93	0.0477	0.0467	0.0463	0.0465	0.0463	0.0465
15.97	0.0446	0.0424	0.0428	0.0426	0.0421	0.0428
16.99	0.0420	0.0401	0.0399	0.0410	0.0399	0.0407
17.99	0.0396	0.0376	0.0374	0.0378	0.0382	0.0382
18.97	0.0376	0.0361	0.0361	0.0367	0.0368	0.0368
20.01	0.0356	0.0344	0.0345	0.0345	0.0344	0.0345
20.96	0.0340	0.0332	0.0326	0.0328	0.0326	0.0328
21.99	0.0324	0.0316	0.0314	0.0313	0.0314	0.0316
22.95	0.0311	0.0303	0.0299	0.0302	0.0305	0.0303
23.92	0.0298	0.0291	0.0288	0.0289	0.0291	0.0289
24.96	0.0286	0.0277	0.0280	0.0280	0.0279	0.0277
29.93	0.0238	0.0233	0.0231	0.0228	0.0232	0.0231

Tab. A 9-22: Experimental results on Fe leaching at different phase ratios and leaching time by using 1M H_2SO_4, for BIOS

Phase ratio	Input Fe concentration	Fe concentration after leaching				
mL g^{-1}	mol L^{-1}	mol L^{-1}	mol L^{-1}	mol L^{-1}	mol L^{-1}	mol L^{-1}
		60 min	90 min	120 min	150 min	180 min
5.03	0.0364	0.0011	0.0015	0.0011	0.0011	0.0013
5.99	0.0306	0.0044	0.0043	0.0043	0.0026	0.0026
6.97	0.0263	0.0112	0.0104	0.0113	0.0105	0.0107
8.05	0.0228	0.0111	0.0106	0.0114	0.0112	0.0106
8.96	0.0204	0.0145	0.0147	0.0145	0.0138	0.0139
9.96	0.0184	0.0163	0.0160	0.0157	0.0158	0.0161
10.98	0.0167	0.0149	0.0147	0.0151	0.0151	0.0146
11.98	0.0153	0.0142	0.0141	0.0143	0.0144	0.0138
12.95	0.0141	0.0132	0.0133	0.0132	0.0133	0.0128
13.92	0.0132	0.0121	0.0120	0.0124	0.0121	0.0121
14.93	0.0123	0.0114	0.0115	0.0113	0.0116	0.0115
15.97	0.0115	0.0110	0.0109	0.0108	0.0108	0.0107
16.99	0.0108	0.0101	0.0102	0.0104	0.0103	0.0104
17.99	0.0102	0.0096	0.0095	0.0097	0.0098	0.0095
18.97	0.0097	0.0092	0.0091	0.0091	0.0093	0.0094
20.01	0.0092	0.0086	0.0089	0.0085	0.0086	0.0089
20.96	0.0087	0.0082	0.0083	0.0082	0.0083	0.0082
21.99	0.0083	0.0079	0.0081	0.0078	0.0079	0.0078
22.95	0.0080	0.0074	0.0076	0.0077	0.0076	0.0076
23.92	0.0077	0.0072	0.0072	0.0073	0.0074	0.0073
24.96	0.0073	0.0069	0.0068	0.0068	0.0068	0.0070
29.93	0.0061	0.0058	0.0057	0.0057	0.0058	0.0059

Tab. A 9-23: The experimental results on first precipitation step for P, Al at different pHs, for CHES

Equilibrium pH	Dissolved element concentration in liquid after precipitation	
	P	Al
	mol L^{-1}	mol L^{-1}
2.27–2.40	0.1532	0.0379
2.80–3.00	0.0782–0.0878	0.036–0.0375
3.00–3.40	0.0215–0.0327	0.0352–0.038
3.60–3.90	0.0016	0.0348–0.0361
4.00–4.30	0.0016	0.0349
4.50–4.80	0.0016	0.0306–0.0314
4.98–5.36	0.0016	0.0107
5.66–5.90	0.0016	0.0008
6.05–6.55	0.0016	0.0008
6.54–6.80	0.0016	0.0008
7.34–7.60	0.0160	0.0008
7.75–7.96	0.0207	0.0004
8.12–8.30	0.0303–0.0399	0.0004
8.65–8.94	0.0766–0.0766	0.0004
9.09–9.50	0.1101	0.0008
9.73–9.93	0.1213	0.0031
10.49–10.68	0.1314–0.1376	0.0042–0.0062
10.85–11.14	0.1309–0.1436	0.0111–0.0144
11.30–11.50	0.1389–0.1452	0.0324–0.0369
11.79–11.96	0.1436–0.1468	0.0326–0.0379
12.27–12.55	0.1420–0.1548	0.0383

Tab. A 9-24: The experimental results on first precipitation step for Ca, Fe at different pHs, for CHES

Equilibrium pH	Dissolved element concentration in liquid after precipitation	
	Ca	Fe
	mol L^{-1}	mol L^{-1}
2.27–2.40	0.0092	0.0163
2.80–3.00	0.0081	0.0042–0.0062
3.00–3.40	0.0078	0.0010–0.0034
3.60–3.90	0.0072–0.0075	0.0002–0.0006
4.00–4.30	0.0070	0.0004
4.50–4.80	0.0069	0.0004
4.98–5.36	0.0064–0.0068	0.0002
5.66–5.90	0.0055–0.0063	0.0004
6.05–6.55	0.0049–0.0056	0.0002
6.54–6.80	0.0042–0.0048	0.0002
7.34–7.60	0.0036–0.0042	0.0004
7.75–7.96	0.0026–0.0029	0.0002
8.12–8.30	0.0011–0.0020	0.0004
8.65–8.94	0.0004–0.0010	0.0004
9.09–9.50	0.0007	0.0004
9.73–9.93	0.0006	0.0004
10.49–10.68	0.0005	0.0004
10.85–11.14	0.0007	0.0002–0.0010
11.30–11.50	0.0001	0.0006
11.79–11.96	0.0001	0.0006
12.27–12.55	0.0002	0.0006

Tab. A 9-25: The experimental results on first precipitation step for P, Al at different pHs, for BIOS

Equilibrium pH	Dissolved element concentration in liquid after precipitation	
	P	Al
	mol L^{-1}	mol L^{-1}
0.90–1.10	0.1850	0.1314–0.1320
1.50–1.51	0.1830	0.1279
1.90–2.10	0.1790	0.1206–0.1311
2.30–2.70	0.1472	0.1152–0.1284
2.80–3.00	0.0511–0.0577	0.1097–0.1191
3.20–3.60	0.0294–0.0396	0.1113–0.1140
3.79–3.99	0.0259–0.0330	0.1090
4.19–4.50	0.0211–0.0329	0.1061
4.69–4.96	0.0130–0.0249	0.1022
5.10–5.46	0.0115–0.0195	0.0705
5.61–5.95	0.0100–0.0176	0.0067
6.30–6.55	0.0094–0.0133	0
6.74–7.17	0.0072–0.0150	0
7.14–7.60	0.0001–0.0139	0
7.76–7.97	0.0080	0
8.20–8.54	0.0080	0
8.66–8.85	0.0099–0.0259	0
9.31–9.70	0.1432	0.0027
9.92–10.35	0.1571	0.0114–0.0175
10.55–11.02	0.1626–0.1695	0.0332–0.0436
11.01–11.23	0.1810	0.1150–0.1273
11.69–12.15	0.1929	0.1319

Tab. A 9-26: The experimental results on first precipitation step for Ca, Fe at different pHs, for BIOS

Equilibrium pH	Dissolved element concentration in liquid after precipitation	
	Ca	Fe
	mol L^{-1}	mol L^{-1}
0.90–1.10	0.0101	0.0332
1.50–1.51	0.0098–0.0101	0.0311
1.90–2.10	0.0090	0.0292–0.0312
2.30–2.70	0.0080	0.0181–0.0195
2.80–3.00	0.0072–0.0082	0.0111–0.0130
3.20–3.60	0.0072–0.0079	0.0091–0.0112
3.79–3.99	0.0070–0.0076	0.0066–0.0098
4.19–4.50	0.0060–0.0068	0.0045
4.69–4.96	0.0063	0.0014–0.0035
5.10–5.46	0.0056	0.0010
5.61–5.95	0.0041–0.0049	0.0007
6.30–6.55	0.0025–0.0034	0.0010
6.74–7.17	0.0015–0.0030	0.0007–0.0014
7.14–7.60	0.0014–0.0019	0.0007
7.76–7.97	0.001–0.0017	0.0007
8.20–8.54	0.0008	0.0007
8.66–8.85	0.0005	0.0009–0.0014
9.31–9.70	0	0.0012–0.0017
9.92–10.35	0.0001	0.0021
10.55–11.02	0	0.0024
11.01–11.23	0	0.0024
11.69–12.15	0	0.0021

9.5 Simulation data

Tab. A 9-27: Input data for leaching simulations, for CHES

Component	Phase ratio 5	Phase ratio 6	Phase ratio 7	Phase ratio 8	Phase ratio 9	Phase ratio 10
	mol L^{-1}	mol L^{-1}	mol L^{-1}	mol L^{-1}	mol L^{-1}	mol L^{-1}
H^+	2.00E-07	1.67E-07	1.43E-07	1.25E-07	1.11E-07	1.00E-07
Al	8.40E-01	7.00E-01	6.00E-01	5.25E-01	4.67E-01	4.20E-01
Ca	1.61E-01	1.34E-01	1.15E-01	1.01E-01	8.94E-02	8.04E-02
SO_4^{2-}	varied	varied	varied	varied	varied	varied
CO_3^{2-}	3.33E-09	2.78E-09	2.38E-09	2.08E-09	1.85E-09	1.67E-09
Cr^{3+}	6.42E-04	5.35E-04	4.59E-04	4.01E-04	3.57E-04	3.21E-04
Cu	4.50E-04	3.75E-04	3.22E-04	2.81E-04	2.50E-04	2.25E-04
Fe^{2+}	1.43E-05	1.19E-05	1.02E-05	8.95E-06	7.96E-06	7.16E-06
Fe	4.20E-02	3.50E-02	3.00E-02	2.63E-02	2.34E-02	2.10E-02
K	4.28E-02	3.56E-02	3.05E-02	2.67E-02	2.38E-02	2.14E-02
Mg	1.27E-01	1.06E-01	9.06E-02	7.93E-02	7.05E-02	6.34E-02
Mn	1.46E-03	1.21E-03	1.04E-03	9.10E-04	8.09E-04	7.28E-04
Na	9.05E-02	7.54E-02	6.47E-02	5.66E-02	5.03E-02	4.53E-02
PO_4^{3-}	1.16E-01	9.67E-02	8.29E-02	7.25E-02	6.44E-02	5.80E-02
Zn	4.41E-03	3.67E-03	3.15E-03	2.75E-03	2.45E-03	2.20E-03

Tab. A 9-28: Input data for leaching simulations, for CHES (cont.)

Component	Phase ratio 11	Phase ratio 12	Phase ratio 13	Phase ratio 14	Phase ratio 15	Phase ratio 16
	mol L^{-1}	mol L^{-1}	mol L^{-1}	mol L^{-1}	mol L^{-1}	mol L^{-1}
H^+	9.09E-08	8.33E-08	7.69E-08	7.14E-08	6.67E-08	6.25E-08
Al	3.82E-01	3.50E-01	3.23E-01	3.00E-01	2.80E-01	2.63E-01
Ca	7.31E-02	6.70E-02	6.19E-02	5.74E-02	5.36E-02	5.03E-02
SO_4^{2-}	varied	varied	varied	varied	varied	varied
CO_3^{2-}	1.52E-09	1.39E-09	1.28E-09	1.19E-09	1.11E-09	1.04E-09
Cr^{3+}	2.92E-04	2.68E-04	2.47E-04	2.29E-04	2.14E-04	2.01E-04
Cu	2.05E-04	1.88E-04	1.73E-04	1.61E-04	1.50E-04	1.41E-04
Fe^{2+}	6.51E-06	5.97E-06	5.51E-06	5.12E-06	4.78E-06	4.48E-06
Fe	1.91E-02	1.75E-02	1.62E-02	1.50E-02	1.40E-02	1.31E-02
K	1.94E-02	1.78E-02	1.64E-02	1.53E-02	1.43E-02	1.34E-02
Mg	5.77E-02	5.29E-02	4.88E-02	4.53E-02	4.23E-02	3.97E-02
Mn	6.62E-04	6.07E-04	5.60E-04	5.20E-04	4.85E-04	4.55E-04
Na	4.11E-02	3.77E-02	3.48E-02	3.23E-02	3.02E-02	2.83E-02
PO_4^{3-}	5.27E-02	4.83E-02	4.46E-02	4.14E-02	3.87E-02	3.63E-02
Zn	2.00E-03	1.84E-03	1.69E-03	1.57E-03	1.47E-03	1.38E-03

Tab. A 9-29: Input data for leaching simulations, for CHES (cont.)

Component	Phase ratio 17	Phase ratio 18	Phase ratio 19	Phase ratio 20	Phase ratio 21
	mol L^{-1}	mol L^{-1}	mol L^{-1}	mol L^{-1}	mol L^{-1}
H^+	5.88E-08	5.56E-08	5.26E-08	5.00E-08	4.76E-08
Al	2.47E-01	2.33E-01	2.21E-01	2.10E-01	2.00E-01
Ca	4.73E-02	4.47E-02	4.23E-02	4.02E-02	3.83E-02
SO_4^{2-}	varied	varied	varied	varied	varied
CO_3^{2-}	9.80E-10	9.26E-10	8.77E-10	8.33E-10	7.94E-10
Cr^{3+}	1.89E-04	1.78E-04	1.69E-04	1.61E-04	1.53E-04
Cu	1.32E-04	1.25E-04	1.18E-04	1.13E-04	1.07E-04
Fe^{2+}	4.21E-06	3.98E-06	3.77E-06	3.58E-06	3.41E-06
Fe	1.24E-02	1.17E-02	1.11E-02	1.05E-02	1.00E-02
K	1.26E-02	1.19E-02	1.13E-02	1.07E-02	1.02E-02
Mg	3.73E-02	3.52E-02	3.34E-02	3.17E-02	3.02E-02
Mn	4.28E-04	4.05E-04	3.83E-04	3.64E-04	3.47E-04
Na	2.66E-02	2.51E-02	2.38E-02	2.26E-02	2.16E-02
PO_4^{3-}	3.41E-02	3.22E-02	3.05E-02	2.90E-02	2.76E-02
Zn	1.30E-03	1.22E-03	1.16E-03	1.10E-03	1.05E-03

Tab. A 9-30: Input data for leaching simulations, for BIOS

Component	Phase ratio 5	Phase ratio 6	Phase ratio 7	Phase ratio 8	Phase ratio 9	Phase ratio 10
	mol L^{-1}	mol L^{-1}	mol L^{-1}	mol L^{-1}	mol L^{-1}	mol L^{-1}
H^+	2.00E-07	1.67E-07	1.43E-07	1.25E-07	1.11E-07	1.00E-07
Al	1.43E-01	1.19E-01	1.02E-01	8.92E-02	7.93E-02	7.13E-02
Ca	1.40E-01	1.17E-01	1.00E-01	8.76E-02	7.78E-02	7.01E-02
SO_4^{2-}	varied	varied	varied	varied	varied	varied
CO_3^{2-}	3.33E-09	2.78E-09	2.38E-09	2.08E-09	1.85E-09	1.67E-09
Cr^{3+}	5.38E-05	4.49E-05	3.85E-05	3.37E-05	2.99E-05	2.69E-05
Cu	4.09E-04	3.41E-04	2.92E-04	2.56E-04	2.27E-04	2.05E-04
Fe^{2+}	1.43E-05	1.19E-05	1.02E-05	8.95E-06	7.96E-06	7.16E-06
Fe	3.67E-02	3.06E-02	2.62E-02	2.30E-02	2.04E-02	1.84E-02
K	4.46E-02	3.72E-02	3.19E-02	2.79E-02	2.48E-02	2.23E-02
Mg	9.06E-02	7.55E-02	6.47E-02	5.66E-02	5.03E-02	4.53E-02
Mn	2.26E-03	1.88E-03	1.61E-03	1.41E-03	1.25E-03	1.13E-03
Na	7.92E-02	6.60E-02	5.66E-02	4.95E-02	4.40E-02	3.96E-02
PO_4^{3-}	7.26E-02	6.05E-02	5.18E-02	4.54E-02	4.03E-02	3.63E-02
Zn	4.47E-03	3.72E-03	3.19E-03	2.79E-03	2.48E-03	2.23E-03

Tab. A 9-31: Input data for leaching simulations, for BIOS (cont.)

Component	Phase ratio 11	Phase ratio 12	Phase ratio 13	Phase ratio 14	Phase ratio 15	Phase ratio 16
	mol L^{-1}	mol L^{-1}	mol L^{-1}	mol L^{-1}	mol L^{-1}	mol L^{-1}
H^+	9.09E-08	8.33E-08	7.69E-08	7.14E-08	6.67E-08	6.25E-08
Al	6.49E-02	5.95E-02	5.49E-02	5.10E-02	4.76E-02	4.46E-02
Ca	6.37E-02	5.84E-02	5.39E-02	5.00E-02	4.67E-02	4.38E-02
SO_4^{2-}	varied	varied	varied	varied	varied	varied
CO_3^{2-}	1.52E-09	1.39E-09	1.28E-09	1.19E-09	1.11E-09	1.04E-09
Cr^{3+}	2.45E-05	2.24E-05	2.07E-05	1.92E-05	1.79E-05	1.68E-05
Cu	1.86E-04	1.70E-04	1.57E-04	1.46E-04	1.36E-04	1.28E-04
Fe^{2+}	6.51E-06	5.97E-06	5.51E-06	5.12E-06	4.78E-06	4.48E-06
Fe	1.67E-02	1.53E-02	1.41E-02	1.31E-02	1.22E-02	1.15E-02
K	2.03E-02	1.86E-02	1.72E-02	1.59E-02	1.49E-02	1.39E-02
Mg	4.12E-02	3.77E-02	3.48E-02	3.24E-02	3.02E-02	2.83E-02
Mn	1.03E-03	9.41E-04	8.68E-04	8.06E-04	7.52E-04	7.05E-04
Na	3.60E-02	3.30E-02	3.05E-02	2.83E-02	2.64E-02	2.47E-02
PO_4^{3-}	3.30E-02	3.02E-02	2.79E-02	2.59E-02	2.42E-02	2.27E-02
Zn	2.03E-03	1.86E-03	1.72E-03	1.60E-03	1.49E-03	1.40E-03

Tab. A 9-32: Input data for leaching simulations, for BIOS (cont.)

Component	Phase ratio 17	Phase ratio 18	Phase ratio 19	Phase ratio 20	Phase ratio 21
	mol L^{-1}	mol L^{-1}	mol L^{-1}	mol L^{-1}	mol L^{-1}
H^+	5.88E-08	5.56E-08	5.26E-08	5.00E-08	4.76E-08
Al	4.20E-02	3.96E-02	3.75E-02	3.57E-02	3.40E-02
Ca	4.12E-02	3.89E-02	3.69E-02	3.50E-02	3.34E-02
SO_4^{2-}	varied	varied	varied	varied	varied
CO_3^{2-}	9.80E-10	9.26E-10	8.77E-10	8.33E-10	7.94E-10
Cr^{3+}	1.58E-05	1.50E-05	1.42E-05	1.35E-05	1.28E-05
Cu	1.20E-04	1.14E-04	1.08E-04	1.02E-04	9.74E-05
Fe^{2+}	4.21E-06	3.98E-06	3.77E-06	3.58E-06	3.41E-06
Fe	1.08E-02	1.02E-02	9.67E-03	9.18E-03	8.75E-03
K	1.31E-02	1.24E-02	1.17E-02	1.12E-02	1.06E-02
Mg	2.66E-02	2.52E-02	2.38E-02	2.26E-02	2.16E-02
Mn	6.64E-04	6.27E-04	5.94E-04	5.64E-04	5.37E-04
Na	2.33E-02	2.20E-02	2.08E-02	1.98E-02	1.89E-02
PO_4^{3-}	2.13E-02	2.02E-02	1.91E-02	1.81E-02	1.73E-02
Zn	1.31E-03	1.24E-03	1.18E-03	1.12E-03	1.06E-03

Tab. A 9-33: Input data for first precipitation and dissolution simulations

Component	First precipitation		Dissolution	
	CHES	BIOS	CHES	BIOS
	mol L^{-1}	mol L^{-1}	mol L^{-1}	mol L^{-1}
H^+	5.23E-01	8.71E-01	1.00E-06	1.00E-06
Al	4.20E-01	1.41E-01	3.06E-01	6.95E-02
Ca	1.17E-02	1.38E-02	2.80E-03	4.70E-03
SO_4^{2-}	1.90E+00	1.36E+00	1.00E-06	1.00E-06
CO_3^{2-}	0.00E+00	1.00E-06	1.00E-06	1.00E-06
Cr^{3+}	3.00E-04	1.00E-06	3.00E-04	1.00E-06
Cu	1.00E-04	1.00E-06	1.00E-06	1.00E-06
Fe^{2+}	0.00E+00	1.00E-06	1.00E-06	1.00E-06
Fe	2.10E-02	3.60E-02	2.10E-02	3.60E-02
K	2.14E-02	4.46E-02	1.00E-06	1.00E-06
Mg	1.37E-02	2.99E-02	1.00E-06	1.00E-06
Mn	7.00E-04	2.30E-03	7.00E-04	2.20E-03
Na	varied	varied	varied	varied
PO_4^{3-}	5.69E-02	7.17E-02	5.69E-02	7.17E-02
Zn	4.00E-04	1.30E-03	1.00E-06	1.00E-06

Tab. A 9-34: Input data for final precipitation simulations

Component	CHES	BIOS
	mol L^{-1}	mol L^{-1}
H^+	1.00E-06	1.00E-06
Al	3.06E-01	4.20E-03
Ca	varied	varied
SO_4^{2-}	1.00E-06	1.00E-06
CO_3^{2-}	1.00E-06	1.00E-06
Cr^{3+}	1.00E-06	1.00E-06
Cu	1.00E-06	1.00E-06
Fe^{2+}	1.00E-06	1.00E-06
Fe	2.10E-03	3.60E-03
K	1.00E-06	1.00E-06
Mg	1.00E-06	1.00E-06
Mn	2.20E-06	2.20E-06
Na	4.23E-01	1.34E-01
PO_4^{3-}	5.40E-02	6.54E-02
Zn	1.00E-06	1.00E-06

9.6 References

Alam, Md. Z., Fakhru'l-Razi, A., & Molla, A. H. (2003). Biosolids accumulation and biodegradation of domestic wastewater treatment plant sludge by developed liquid state bioconversion process using a batch fermenter. *Water Research*, *37*(15), 3569–3578. https://doi.org/10.1016/S0043-1354(03)00260-4

Ali, T. U., & Kim, D.-J. (2016). Phosphorus extraction and sludge dissolution by acid and alkali treatments of polyaluminum chloride (PAC) treated wastewater sludge. *Bioresource Technology*, *217*, 233–238. https://doi.org/10.1016/j.biortech.2016.02.017

Alibaba, A. (2024). *P2O5≥68%—Buy Shmp Product on Alibaba.com*. Www.Alibaba.Com. https://www.alibaba.com/product-detail/SHMP-P2O5-68-_1601234725608.html

Aqion. (2024). *Activity Coefficients (Activity Models)*. https://www.aqion.de/site/101#fn:lg

Bednarz, A., Rüngeler, B., & Pfennig, A. (2014). Use of Cascaded Option Trees in Chemical-Engineering Process Development. *Chemie Ingenieur Technik*, *86*(5), 611–620. https://doi.org/10.1002/cite.201300115

Bennamoun, L., Arlabosse, P., & Léonard, A. (2013). Review on fundamental aspect of application of drying process to wastewater sludge. *Renewable and Sustainable Energy Reviews*, *28*, 29–43. https://doi.org/10.1016/j.rser.2013.07.043

Berg, U., Ehbrecht, A., Röhm, E., Weidler, P. G., & Nüesch, R. (2007). Impact of calcite on phosphorus removal and recovery from wastewater using CSH-filled fixed bed filters. *J. Residuals Sci. Technol*, *4*(2), 73–81.

Bianchini, A., & Rossi, J. (2020). An Integrated Industry-Based Methodology to Unlock Full-Scale Implementation of Phosphorus Recovery Technology. *Sustainability*, *12*(24), Article 24. https://doi.org/10.3390/su122410632

Biswas, B. K., Inoue, K., Harada, H., Ohto, K., & Kawakita, H. (2009). Leaching of phosphorus from incinerated sewage sludge ash by means of acid extraction followed by adsorption on orange waste gel. *Journal of Environmental Sciences*, *21*(12), 1753–1760. https://doi.org/10.1016/S1001-0742(08)62484-5

Blöcher, C., Niewersch, C., & Melin, T. (2012). Phosphorus recovery from sewage sludge with a hybrid process of low pressure wet oxidation and nanofiltration. *Water Research*, *46*(6), 2009–2019.

Blöcher, C., Niewersch, C., Schröder, H., Gebhardt, W., & Melin, T. (2009). Optimierte Phosphor-Rückgewinnung aus Klärschlämmen durch ein Hybridverfahren aus Niederdruck-Nassoxidation und Nanofiltration (Verbundprojekt PHOXNAN). *Final Report of BMBF Project 02WA0796/97/98*. https://phosphorrecycling.de/de/publikationen-mainmenu-59/schlusspraesentation/49-/PHOXNAN_Bloecher%20et%20al.pdf

Bosma, R., Anh, P. T., & Potting, J. (2011). Life cycle assessment of intensive striped catfish farming in the Mekong Delta for screening hotspots as input to environmental policy and research agenda. *The International Journal of Life Cycle Assessment*, *16*(9), 903. https://doi.org/10.1007/s11367-011-0324-4

BSI, PAS 100:2018 Specification for composted materials. London: The British Standards Institution (2018).

Butusov, M., & Jernelöv, A. (2013). The Role of Phosphorus in the Origin of Life and in Evolution. In M. Butusov & A. Jernelöv, *Phosphorus* (Vol. 9, pp. 1–12). Springer New York. https://doi.org/10.1007/978-1-4614-6803-5_1

Carrasco, L., Chacón-m de Lara, F., Martín de las Mulas, J., Gómez-Villamandos, J. C., Sierra, M. A., Villeda, C. J., & Wilkinson, P. J. (1997). Ultrastructural changes related to the lymph node haemorrhages in acute African swine fever. *Research in Veterinary Science*, *62*(3), 199–204. https://doi.org/10.1016/S0034-5288(97)90190-9

Carrayrou, J., Mosé, R., & Behra, P. (2002). New efficient algorithm for solving thermodynamic chemistry. *AIChE Journal*, *48*(4), 894–904. https://doi.org/10.1002/aic.690480423

CCME, PN 1340 Guidelines for compost quality. Winnipeg: Canadian Council of Ministers of the Environment (2005). https://ccme.ca/en/res/compostgdlns_1340_e.pdf

Chi, R., Xiao, C., & Gao, H. (2006). Bioleaching of phosphorus from rock phosphate containing pyrites by Acidithiobacillus ferrooxidans. *Minerals Engineering*, *19*(9), 979–981.

Cordell, D., Rosemarin, A., Schröder, J. J., & Smit, A. L. (2011). Towards global phosphorus security: A systems framework for phosphorus recovery and reuse options. *Chemosphere*, *84*(6), 747–758. https://doi.org/10.1016/j.chemosphere.2011.02.032

De Ruiter, R. (2014). The EcoPhos technology to close the P cycle and to safeguard the world's food chain. *Abwasser–Phosphor–Dünger-Workshop Inclusive Fachgespräch Zum UFOPLAN-Projekt Klärschlammaschemonitoring, Berlin*, 28–29.

Dittrich, C., Rath, W., Montag, D., & Pinnekamp, J. (2009). Phosphorus recovery from sewage sludge ash by a wet-chemical process. *Proceedings of the International Conference on Nutrient Recovery, Vancouver, BC, Canadá. IWA Publishing*, 645–658. https://iwaponline.com/ebooks/book-pdf/141854/wio9781780401805.pdf#page=659

Dixon, L. K., Islam, M., Nash, R., & Reis, A. L. (2019). African swine fever virus evasion of host defences. *Virus Research*, *266*, 25–33. https://doi.org/10.1016/j.virusres.2019.04.002

Dixon, L. K., Sun, H., & Roberts, H. (2019). African swine fever. *Antiviral Research*, *165*, 34–41. https://doi.org/10.1016/j.antiviral.2019.02.018

DNP. (2024). *Nutrient Platform | NWP*. https://www.netherlandswaterpartnership.com/our-themes/water-agrifood/nutrient-platform

Donatello, S., Freeman-Pask, A., Tyrer, M., & Cheeseman, C. R. (2010). Effect of milling and acid washing on the pozzolanic activity of incinerator sewage sludge ash. *Cement and Concrete Composites*, *32*(1), 54–61. https://doi.org/10.1016/j.cemconcomp.2009.09.002

Donatello, S., Tong, D., & Cheeseman, C. R. (2010). Production of technical grade phosphoric acid from incinerator sewage sludge ash (ISSA). *Waste Management*, *30*(8), 1634–1642. https://doi.org/10.1016/j.wasman.2010.04.009

Egle, L., Rechberger, H., & Zessner, M. (2015). Overview and description of technologies for recovering phosphorus from municipal wastewater. *Resources, Conservation and Recycling*, *105*, 325–346. https://doi.org/10.1016/j.resconrec.2015.09.016

Ehrlich, H. L. (2001). Past, present and future of biohydrometallurgy. *Hydrometallurgy*, *59*(2–3), 127–134.

ESPP. (2024). *European Sustainable Phosphorus Platform—Home*. https://www.phosphorusplatform.eu/

Esteve, C., Elena, G. B., & Carmen, A. (1993). Virulence of Aeromonas hydrophila and some other bacteria isolated from European eels Anguilla anguilla reared in fresh water. *Diseases of Aquatic Organisms*, *16*(1), 5.

EU, Regulation EU 2019/1009: Rules on the making available on the market of EU fertilizing products. Brussels: European Union (2019). https://eur-lex.europa.eu/eli/reg/2019/1009/oj

European Commission. (2023). *European Critical Raw Materials Act—European Commission*. https://commission.europa.eu/strategy-and-policy/priorities-2019-2024/european-green-deal/green-deal-industrial-plan/european-critical-raw-materials-act_en

EVN, V. E. (2024). *Average retail electricity price*. https://www.evn.com.vn/c3/evn-va-khach-hang/Bieu-gia-ban-le-dien-9-79.aspx

FAO. (2023). *FAOSTAT*. https://www.fao.org/faostat/en/#data

FAOSTAT. (2022). *Fertilizers by Nutrient*. FAO. https://doi.org/10.4060/cd1485en

Fraikin, L., Herbreteau, B., Salmon, T., Nicol, F., Crine, M., & Léonard, A. (2015). Use of an Experimental Design to Characterize the Convective Drying Behavior of Different Sludges. *Drying Technology*, *33*(11), 1302–1308. https://doi.org/10.1080/07373937.2015.1026979

Franz, M. (2008). Phosphate fertilizer from sewage sludge ash (SSA). *Waste Management*, *28*(10), 1809–1818.

García-Albacete, M., Martín, A., & Cartagena, M. C. (2012). Fractionation of phosphorus biowastes: Characterisation and environmental risk. *Waste Management*, *32*(6), 1061–1068. https://doi.org/10.1016/j.wasman.2012.02.003

General Statistic, O. (2018). *Statistical Yearbook of Vietnam 2017*. Statistical Publishing House.

General Statistic, O. (2019). *Statistical Yearbook of Vietnam 2018*. Statistical Publishing House.

Gon Kim, J., Hyun Kim, J., Moon, H.-S., Chon, C.-M., & Sung Ahn, J. (2002). Removal capacity of water plant alum sludge for phosphorus in aqueous solutions. *Chemical Speciation & Bioavailability*, *14*(1–4), 67–73. https://doi.org/10.3184/095422902782775344

González Medeiros, J. J., Pérez Cid, B., & Fernández Gómez, E. (2005). Analytical phosphorus fractionation in sewage sludge and sediment samples. *Analytical and*

Bioanalytical Chemistry, *381*(4), 873–878. https://doi.org/10.1007/s00216-004-2989-z

GSO. (2024). *General Statistics Office of Vietnam*. https://www.gso.gov.vn/en/homepage/

Günther, L., Dockhorn, T., Dichtl, N., Müller, J., Urban, I., Phan, L. C., Weichgrebe, D., Rosenwinkel, K. H., & Bayerle, N. (2008). Technical and scientific monitoring of the large-scale seaborne technology at the WWTP Gifhorn. *Water Practice and Technology*, *3*(1), wpt2008006.

Guong, V. T., & Hoa, N. M. (2012). Aquaculture and Agricultural Production in the Mekong Delta and its Effects on Nutrient Pollution of Soil and Water. In F. G. Renaud & C. Kuenzer (Eds.), *The Mekong Delta System* (pp. 363–393). Springer Netherlands. https://doi.org/10.1007/978-94-007-3962-8_14

HANTECO VIETNAM. (2014, May 28). *PAC (Poly Aluminium Chloride) price*. Hóa chất trợ lắng PAC - Keo tụ PAC (Poly Aluminium Chloride) | KIDOPOOL. https://kidopool.vn:443/hoa-chat-pac.html?gclid=Cj0KCQjw9fqnBhDSARIsAHlcQYSM6wBT3NTkv2T7yPfXU7iaPqmQpPg-_MTSAeODmr6xdwjdksgb73kaAqRBEALw_wcB

Ho, T. T., Nontawith, A., Prapansak, S., & Songsri, M. (2008). Identification and antibiotic sensitivity test of the bacteria isolated from Tra catfish (Pangasianodon hypophthalmus [Sauvage, 1878]) cultured in pond in Vietnam. *Agriculture and Natural Resources*, *42*(5), 6.

Horizontal. (2006). *Cluster 6: Inorganic parameters*. https://horizontal.ecn.nl/consultation-of-phase-ii/inorganic-parameters/index.html

Houssaine Moutiy, E., Tran, L.-H., Mueller, K. K., Coudert, L., & Blais, J.-F. (2020). Optimized indium solubilization from LCD panels using H2SO4 leaching. *Waste Management*, *114*, 53–61. https://doi.org/10.1016/j.wasman.2020.07.002

HPDON. (2024). *Industrial chemical prices*. https://hoaphatdongnai.com

Hwang, E.-J., & Cheon, H.-C. (2009). High-rate phosphorous removal by PAC (poly aluminum chloride) coagulation of A2O effluent. *Journal of Korean Society of Environmental Engineers*, *31*(8), 673–678.

IndexMundi, I. (2024). *Rock Phosphate—Monthly Price—Commodity Prices—Price Charts, Data, and News—IndexMundi*. https://www.indexmundi.com/commodities/?commodity=rock-phosphate&months=120

Inocre. (2013). *Inocre process*. https://www.fritzmeier-umwelttechnik.com/en/404-error

Interreg North-West Europe. (2020). *Phos4you project*. https://vb.nweurope.eu/projects/project-search/

James PM, S., Kettner, A. J., Overeem, I., WH Hutton, E., T. Hannon, M., Brakenridge, G. R., & R.J., N. (2009). Sinking deltas due to human activities | Nature Geoscience. *Nature Geoscience*, *2*(10), 681–686.

Jupp, A., Beijer, S., C. Narain, G., Schipper, W., & Chris Slootweg, J. (2021). Phosphorus recovery and recycling – closing the loop. *Chemical Society Reviews*, *50*(1), 87–101. https://doi.org/10.1039/D0CS01150A

Khoi C. M., Nha H. H., & Nhien C. T. (2012). Accumulation of nitrogen, inorganic and organic phosphorus in water and sediment of intensive catfish farming in the Mekong Delta. *CTU Journal of Science*, *22a*, Article 22a.

Lam Minh, T., Nguyen Thanh, H., & Nguyen Phuoc, D. (2015). *Domestic and industrial wastewater treatment: Calculation and engineering design* (5th edition, with corrections and additions). Viet Nam National University Ho Chi Minh City Publishing House.

Levlin, E., & Hultman, B. (2004). *Phosphorus recovery from sewage sludge-Ideas for further studies to improve leaching*. https://energiomiljo.org/kth/Polishproject/rep12/Pfurtherecovery.pdf

Liang, S., Chen, H., Zeng, X., Li, Z., Yu, W., Xiao, K., Hu, J., Hou, H., Liu, B., Tao, S., & Yang, J. (2019). A comparison between sulfuric acid and oxalic acid leaching with subsequent purification and precipitation for phosphorus recovery from sewage sludge incineration ash. *Water Research*, *159*, 242–251. https://doi.org/10.1016/j.watres.2019.05.022

Liu, Y., & Qu, H. (2016). Design and optimization of a reactive crystallization process for high purity phosphorus recovery from sewage sludge ash. *Journal of Environmental Chemical Engineering*, *4*(2), 2155–2162. https://doi.org/10.1016/j.jece.2016.03.042

Ly, L. T. T., Vo, P. H., & Doan, V. C. (2009). Hemorrhage disease of cultured tra catfish (Pangasianodon hypophthalmus) in Mekong Delta (Vietnam). *Sraeli Journal of Aquaculture-Bamidgeh*, *61*, 10.

MARA, NY 525-2021 Standard of organic fertilizer. Beijing: Ministry of Agriculture and Rural Affairs of The People's Republic of China (2021). https://www.codeofchina.com/standard/NYT525-2021.html

MARD, QCVN 01-189:2019/BNNPTNT National Technical Regulations on Quality Fertilizers. Ha Noi: Ministry of Agriculture and Rural Development Vietnam (2019).

MARD. (2019b). *QCVN 01-189:2019/BNNPTNT National Technical Regulations on Quality Fertilizers. Ha Noi: Ministry of Agriculture and Rural Development Vietnam*. http://vinacert.vn/pic/files/2-qcvn-01-189_2019-chat-luong-phan-bon-final.pdf

MARD. (2019c). *Report on Results of Production and Business in Agriculture and Rural Development in October and the First 10 Months of 2019* (p. 22). https://mard.gov.vn/ThongKe/Lists/BaoCaoThongKe/Attachments/154/Baocao_T10_2019.pdf

Mêlé, M., C., Paillard, H., Deleris, S., & Bardoux, J. (2014). *Nouveau procédé de recyclage du Phosphore issu des effluents concentrés* (Séminaire Phoph'Or) [Presentation]. Veolia Eau.

Mendes, F. D., & Martins, A. H. (2004). Selective sorption of nickel and cobalt from sulphate solutions using chelating resins. *International Journal of Mineral Processing*, *74*(1–4), 359–371.

Mew, M., Steiner, G., Haneklaus, N., & Geissler, B. (2023). Phosphate price peaks and negotiations – Part 2: The 2008 peak and implications for the future. *Resources Policy*, *83*, 103588. https://doi.org/10.1016/j.resourpol.2023.103588

MINACHEM. (2024). *Industrial chemical price- HNO3*. https://hoachatcongnghe.com/san-pham/1138/nitric-acid-hno3-68.html

Minderhoud, P. S. J., Coumou, L., Erkens, G., Middelkoop, H., & Stouthamer, E. (2019). Mekong delta much lower than previously assumed in sea-level rise impact assessments | Nature Communications. *Nature Communications*, *10*(1), 3874.

MOC, TCXDVN 33:2006 Water supply – Distribution system and facilities design standard. Ha Noi: Ministry of Construction (2006).

Moerman, W., Carballa, M., Vandekerckhove, A., Derycke, D., & Verstraete, W. (2009). Phosphate removal in agro-industry: Pilot- and full-scale operational considerations of struvite crystallization. *Water Research*, *43*(7), 1887–1892. https://doi.org/10.1016/j.watres.2009.02.007

MONRE, QCVN 40:2011/BTNMT National technical regulation on industrial wastewater. Ha Noi: Ministry of Natural Resources and Environment (2011).

Montag, D., & Pinnekamp, J. (2009). The PASH process for P-recovery and overview of the German Funding Programme" Recycling management of plant nutrients, especially phosphorous". *Presentation in BALTIC*, 28–30.

Montag, D., Pinnekamp, J., Dittrich, C., Rath, W., Schmidt, M., Pfennig, A., Seyfried, A., Grömping, M., van Norden, H., & Doetsch, P. (2011). Rückgewinnung von Phosphor aus Klärschlammasche mittels des nasschemischen PASCH-Verfahrens. *Pinnekamp J*. https://phosphorrecycling.de/en/publications/schlusspraesentation/65-/PASCH_Montag%20et%20al.pdf

Morel, F. M., & Hering, J. G. (1993). *Principles and applications of aquatic chemistry*. John Wiley & Sons. https://books.google.com/books?hl=en&lr=&id=lgXpDwAAQBAJ&oi=fnd&pg=PR11&dq=Morel+FMM,+Hering+JG.+Principles+and+applications+of+aquatic+chemistry.+New+York:+John+Wiley+%26+Sons%3B+1993&ots=Xb1Q7L34up&sig=8W7Z220WbfusuByuy82_TXLU7rk

Morin, K. A. (1985). Simplified explanations and examples of computerized methods for calculating chemical equilibrium in water. *Computers & Geosciences*, *11*(4), 409–416.

MOST, TCVN 7957:2008 Drainage and sewerage – External Networks and Facilities – Design Standard. Ha Noi: Ministry of Science and Technology (2008).

Naoum, C., Fatta, D., Haralambous, K. J., & Loizidou, M. (2001). Removal of Heavy Metals from Sewage Sludge by Acid Treatment. *Journal of Environmental Science and Health, Part A*, *36*(5), 873–881. https://doi.org/10.1081/ESE-100103767

Nga, B. T. T., Tran Anh Dao, B., Nguyen Thi, L., Osaki, M., Kawashima, K., Song, D., Salguero, F. J., & Le, V. P. (2020). Clinical and Pathological Study of the First Outbreak Cases of African Swine Fever in Vietnam, 2019. *Frontiers in Veterinary Science*, *7*. https://doi.org/10.3389/fvets.2020.00392

Nguyên P. Q., Bé N. V., & Công N. V. (2014). Quantifying and qualifying sediment load from intensive catfish (Pangasianodon hypophthalmus) ponds and sediment application for vegetable-cultured. *CTU Journal of Science*, *35*, Article 35.

Nicholson, F. A., Chambers, B. J., Williams, J. R., & Unwin, R. J. (1999). Heavy metal contents of livestock feeds and animal manures in England and Wales. *Bioresource Technology*, *70*(1), 23–31. https://doi.org/10.1016/S0960-8524(99)00017-6

Ottosen, L. M., Kirkelund, G. M., & Jensen, P. E. (2013). Extracting phosphorous from incinerated sewage sludge ash rich in iron or aluminum. *Chemosphere*, *91*(7), 963–969. https://doi.org/10.1016/j.chemosphere.2013.01.101

Pengthamkeerati, P., Satapanajaru, T., & Chularuengoaksorn, P. (2008). Chemical modification of coal fly ash for the removal of phosphate from aqueous solution. *Fuel*, *87*(12), 2469–2476. https://doi.org/10.1016/j.fuel.2008.03.013

Petzet, S., Peplinski, B., Bodkhe, S. Y., & Cornel, P. (2011). Recovery of phosphorus and aluminium from sewage sludge ash by a new wet chemical elution process (SESAL-Phos-recovery process). *Water Science and Technology*, *64*(3), 693–699. https://doi.org/10.2166/wst.2011.682

Petzet, S., Peplinski, B., & Cornel, P. (2012). On wet chemical phosphorus recovery from sewage sludge ash by acidic or alkaline leaching and an optimized combination of both. *Water Research*, *46*(12), 3769–3780. https://doi.org/10.1016/j.watres.2012.03.068

Phan, L. T., Bui, T. M., Nguyen, T. T. T., Gooley, G. J., Ingram, B. A., Nguyen, H. V., Nguyen, P. T., & De Silva, S. S. (2009). Current status of farming practices of striped catfish, *Pangasianodon hypophthalmus* in the Mekong Delta, Vietnam. *Aquaculture*, *296*(3), 227–236. https://doi.org/10.1016/j.aquaculture.2009.08.017

Phu T. Q., & Tinh T. K. (2012). Composition of sediment on the intensive catfish farming pond (Pangasianodon hypophthalmus). *CTU Journal of Science*, *22a*, Article 22a.

Pinnekamp, J., Montag, D., Gethke, K., Goebel, S., & Herbst, H. (2007). *Rückgewinnung eines schadstofffreien, mineralischen Kombinationsdüngers Magnesiumammoniumphosphat–MAP aus Abwasser und Klärschlamm* (Forschungsbericht 202 33 308; p. 25). UBA-Texte.

Rietra, R. P. J. J., Hiemstra, T., & Van Riemsdijk, W. H. (2001). Interaction between Calcium and Phosphate Adsorption on Goethite. *Environmental Science & Technology*, *35*(16), 3369–3374. https://doi.org/10.1021/es000210b

Riva Sanseverino, E., Le Thi Thuy, H., Pham, M.-H., Di Silvestre, M. L., Nguyen Quang, N., & Favuzza, S. (2020). Review of Potential and Actual Penetration of Solar Power in Vietnam. *Energies*, *13*(10), Article 10. https://doi.org/10.3390/en13102529

Ruban, V., López-Sánchez, J. F., Pardo, P., Rauret, G., Muntau, H., & Quevauviller, P. (1999). Selection and evaluation of sequential extraction procedures for the

determination of phosphorus forms in lake sediment. *Journal of Environmental Monitoring*, *1*(1), 51–56.

Sarlin, T. H., Priha, O. K., Arnold, M. E., & Kinnunen, P. (2013). Bioleaching of phosphorus from low grade ores and concentrates with acidophilic iron-and sulphur-oxidizing bacteria. *Advanced Materials Research*, *825*, 266–269.

SAWACO. (2024). *Price of water supply for industry*. Title-Page. https://sawaco.com.vn/post-detail/undefined

Schaum, C., Cornel, P., & Jardin, N. (2004). Phosphorus recovery from sewage sludge ash. *Chemical Water and Wastewater Treatment VIII, Proceedings of 11th International Gothenburg Symposium, Gothenburg, Sweden*, 355–363. https://books.google.com/books?hl=en&lr=&id=KLWXI_EePLQC&oi=fnd&pg=PA355&dq=Schaum,+C.,+Cornel,+P.,+Jardin,+N.,+2004.+Phosphorus+recovery+from+sewage+sludge+ash.+In:+Hahn,+H.H.,+Hoffman,+E.,+%C3%98degaard,+H.+(Eds.),+Chemical+Water+and+Wastewater+Treatment+VIII,+IWA+Publishing,+Proceedings+for+the+11th+Gothenburg+Symposium.+8%E2%80%9310+November+2004,+Orlando,+USA.&ots=xEDvDCChCz&sig=REF3iegtbF2pY3kYR9Ng-VR0-xY

Semerci, N., Ahadi, S., & Coşgun, S. (2021). Comparison of dried sludge and sludge ash for phosphorus recovery with acidic and alkaline leaching. *Water and Environment Journal*, *35*(1), 359–370. https://doi.org/10.1111/wej.12633

Shariff, Z. A., Fraikin, L., Bogdan, A., Léonard, A., Meers, E., & Pfennig, A. (2023). PULSE process: Recovery of phosphorus from dried sewage sludge and removal of metals by solvent extraction. *Environmental Technology*, *45*(14), 2820–2832. https://doi.org/10.1080/09593330.2023.2191221

Shiba, N. C., & Ntuli, F. (2017). Extraction and precipitation of phosphorus from sewage sludge. *Waste Management*, *60*, 191–200. https://doi.org/10.1016/j.wasman.2016.07.031

Stark, K., Plaza, E., & Hultman, B. (2006). Phosphorus release from ash, dried sludge and sludge residue from supercritical water oxidation by acid or base. *Chemosphere*, *62*(5), 827–832. https://doi.org/10.1016/j.chemosphere.2005.04.069

Sun, K., Jiang, L., Ye, Q., Wang, Q., Liao, D., Chang, X., Xi, S., & He, R. (2023). Chemical and microbiological characterization of pig manures and digestates. *Environmental Technology*, *44*(13), 1916–1925. https://doi.org/10.1080/09593330.2021.2016993

Tarayre, C., De Clercq, L., Charlier, R., Michels, E., Meers, E., Camargo-Valero, M., & Delvigne, F. (2016). New perspectives for the design of sustainable bioprocesses for phosphorus recovery from waste. *Bioresource Technology*, *206*, 264–274.

Than Thi, H., Khuong Manh, H., Nguyen Chi, T., Xuan Thi Thu, T., & Tran Manh, C. (2020). Land resources and soil fertility in the Southeast region. *Journal of Vietnam Agricultural Science and Technology*, *6*, 9.

Thien Thu, C. T., Cuong, P. H., Hang, L. T., Chao, N. V., Anh, L. X., Trach, N. X., & Sommer, S. G. (2012). Manure management practices on biogas and non-biogas pig farms in developing countries – using livestock farms in Vietnam as an example. *Journal of Cleaner Production*, *27*, 64–71. https://doi.org/10.1016/j.jclepro.2012.01.006

Toor, U. A., Shin, H., & Kim, D.-J. (2019). Mechanistic insights into nature of complexation between aluminum and phosphates in polyaluminum chloride treated sludge for sustainable phosphorus recovery. *Journal of Industrial and Engineering Chemistry*, *71*, 425–434. https://doi.org/10.1016/j.jiec.2018.11.055

Truong, T. V., Tiwari, D., Mok, Y. S., & Kim, D.-J. (2021). Recovery of aluminum from water treatment sludge for phosphorus removal by combined calcination and extraction. *Journal of Industrial and Engineering Chemistry*, *103*, 195–204. https://doi.org/10.1016/j.jiec.2021.07.033

Vietnam Government, 38/2015/ND-CP: Decree on the management of wastes and scraps (2015). https://lic-public.wto.org/en/legislations/2804

Vietnam Rubber Association. (2018). *VIETNAM RUBBER INDUSTRY: CURRENT STATUS AND SUSTAINABLE DEVELOPMENT SOLUTIONS*. https://www.vra.com.vn/thong-tin/vietnam-rubber-industry-current-status-and-sustainable-development-solutions.11616.html

Vietnamese Government. (2020). *Environment Protection Law 2020*. http://vanban.chinhphu.vn/?pageid=27160&docid=202613&classid=1&typegroupid=3

VINACHEM. (2024). *Key products from Vietnam National Chemical group*. https://www.vinachem.com.vn/gioi-thieu/chi-tiet/mot-so-sp-dv-chu-yeu-cua-vinachem.html

Vo Khac, T. (2012). Hydrology and Hydraulic Infrastructure Systems in the Mekong Delta, Vietnam | SpringerLink. In *The Mekong Delta system: Interdisciplinary*

Analyses of a river delta (pp. 49–81). Springer Netherlands. https://link.springer.com/chapter/10.1007/978-94-007-3962-8_3

Vu Hoang Chemicals and Environments. (2024, January 2). Industrial chemical -HCl 37% price. *Công Ty TNHH Công Nghệ Hóa Chất và Môi Trường Vũ Hoàng*. https://vuhoangco.com.vn/gia-axit-clohydric-35-cong-nghiep-moi-nhat/

Withers, P. J., Elser, J. J., Hilton, J., Ohtake, H., Schipper, W. J., & Van Dijk, K. C. (2015). Greening the global phosphorus cycle: How green chemistry can help achieve planetary P sustainability. *Green Chemistry*, *17*(4), 2087–2099.

Yan, J., Kirk, D. W., Jia, C. Q., & Liu, X. (2007). Sorption of aqueous phosphorus onto bituminous and lignitous coal ashes. *Journal of Hazardous Materials*, *148*(1), 395–401. https://doi.org/10.1016/j.jhazmat.2007.02.055

Zhang, H., Li, Q., Han, D., & Liu, R. (2024). Clarifying the Role of Phosphorus Management Strategies in Enhancing the Sustainability of Wastewater Treatment Plants. *Water*, *16*(11), Article 11. https://doi.org/10.3390/w16111539

Zimmermann, J. K. B. (2010). Combination of the microbiological processes bioleaching and acidic phosphorus recovery for the decontamination and nutrient recovery from heavy metal loaded solids. *Technische Hochschule, Aachen*.